National Library of Canada
Bibliothèque nationale du Canada

Canadian Theses Service
Service des thèses canadiennes

Ottawa, Canada
K1A 0N4

NOTICE

The quality of this microform is heavily dependent upon the quality of the original thesis submitted for microfilming. Every effort has been made to ensure the highest quality of reproduction possible.

If pages are missing, contact the university which granted the degree.

Some pages may have indistinct print especially if the original pages were typed with a poor typewriter ribbon or if the university sent us an inferior photocopy.

Previously copyrighted materials (journal articles, published tests, etc.) are not filmed.

Reproduction in full or in part of this microform is governed by the Canadian Copyright Act, R.S.C. 1970, c. C-30.

AVIS

La qualité de cette microforme dépend grandement de la qualité de la thèse soumise au microfilmage. Nous avons tout fait pour assurer une qualité supérieure de reproduction.

S'il manque des pages, veuillez communiquer avec l'université qui a conféré le grade.

La qualité d'impression de certaines pages peut laisser à désirer, surtout si les pages originales ont été dactylographiées à l'aide d'un ruban usé ou si l'université nous a fait parvenir une photocopie de qualité inférieure.

Les documents qui font déjà l'objet d'un droit d'auteur (articles de revue, tests publiés, etc.) ne sont pas microfilmés.

La reproduction, même partielle, de cette microforme est soumise à la Loi canadienne sur le droit d'auteur, SRC 1970, c. C-30.

NL-339 (r. 88/04)

Canada

THE UNIVERSITY OF ALBERTA

ON THE METABOLITES OF *TALAROMYCES FLAVUS*

BY

JULIE SUSANNE RACOK

A THESIS

SUBMITTED TO THE FACULTY OF GRADUATE STUDIES AND RESEARCH

IN PARTIAL FULFILMENT OF THE REQUIREMENTS FOR THE DEGREE

OF DOCTOR OF PHILOSOPHY

DEPARTMENT OF CHEMISTRY

EDMONTON, ALBERTA

FALL 1988

Permission has been granted to the National Library of Canada to microfilm this thesis and to lend or sell copies of the film.

The author (copyright owner) has reserved other publication rights, and neither the thesis nor extensive extracts from it may be printed or otherwise reproduced without his/her written permission.

L'autorisation a été accordée à la Bibliothèque nationale du Canada de microfilmer cette thèse et de prêter ou de vendre des exemplaires du film.

L'auteur (titulaire du droit d'auteur) se réserve les autres droits de publication; ni la thèse ni de longs extraits de celle-ci ne doivent être imprimés ou autrement reproduits sans son autorisation écrite.

ISBN 0-315-45540-3

THE UNIVERSITY OF ALBERTA

RELEASE FORM

NAME OF AUTHOR: JULIE SUSANNE RACOK

TITLE OF THESIS: ON THE METABOLITES OF *TALAROMYCES FLAVUS*

DEGREE FOR WHICH THESIS WAS PRESENTED: DOCTOR OF PHILOSOPHY

YEAR THIS DEGREE GRANTED: 1988

Permission is hereby granted to THE UNIVERSITY OF ALBERTA LIBRARY to reproduce single copies of this thesis and to lend or sell such copies for private, scholarly, or scientific research purposes only.

The author reserves other publication rights and neither the thesis nor extensive extracts from it may be printed or otherwise reproduced without the author's written permission.

Julie S. Racok

(Signature)

6130 Stevens St.

Niagara Falls, Ontario

L2E 3A3

(Permanent address)

Date: October 11, 1988

"We see our cattle fall and our plants wither without being able to render them assistance, lacking as we do understanding of their condition."

- Fabricius (1774)

"Arise, go forth, and conquer..."

- Tennyson

THE UNIVERSITY OF ALBERTA

FACULTY OF GRADUATE STUDIES AND RESEARCH

The undersigned certify that they have read, and recommend to the Faculty of Graduate Studies and Research for acceptance, a thesis entitled ON THE METABOLITES OF *TALAROMYCES FLAVUS* submitted by JULIE SUSANNE RACOK in partial fulfilment of the requirements for the degree of DOCTOR OF PHILOSOPHY.

.....

W.A. Ayer, Supervisor

.....

H.J. Liu

.....

O. Hindsgaul

.....

A. Kalantar

.....

J.P. Tewari

.....

J.W. ApSimon, External Examiner

Date: October 11, 1988

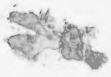

to my parents

ABSTRACT

Studies of the metabolites produced by the soil fungus *Talaromyces flavus* (Klöcker) Stolk and Samson are presented in this thesis. This fungus is an effective biological control agent for Verticillium wilt of eggplant (*Solanum melongena* L.), a disease caused by the fungus *Verticillium dahliae* Kleb.. The first part of this thesis describes the isolation and structure elucidation of the organic soluble metabolites produced when the fungus is grown in liquid still culture. The mycelium extracts afford only the ubiquitous metabolites D-mannitol (**1**), a fatty acid and its methyl ester (**3** and **4**), a di- and triglyceride (**6** and **5**), and ergosterol (**7**). The fungal broth, however, is a source of a number of metabolites of polyketide origin. These include the previously unreported tetraketides, 4,6-dihydroxy-5-methylphthalide (**10**) and 4-carboxy-5-hydroxyphthalaldehydic acid methyl ester (**15**), a hexaketide, 7-hydroxy-2,5-dimethyl-chromone (**13**), and a metabolite whose structure is consistent with that of 3-hydroxymethyl-6,8-dimethoxycoumarin (**17**). 5-Hydroxymethylfurfural (**12**) has also been isolated; however, it is thought to be an artifact in the broth extract. A number of higher order polyketides have been isolated which arise from a heptaketide precursor. These include the known metabolites altenusin (**18**) and its δ-lactone derivative dehydroaltenusin (**19**), and the previously unreported desmethyldehydroaltenusin (**21**). A structurally and biosynthetically interesting spiro metabolite has been obtained, which we have named talaroflavone (**23**), as well as the related compound, deoxytalaroflavone (**27**). D-Glucono-1,4-lactone (**8**) has been isolated from the organic broth extract as well as from the aqueous fungal broth. A clue as to the mechanism of biological control of *V. dahliae* by *T. flavus* rests with metabolite **8**. It is one of two products produced in the oxidation of D-glucose by glucose oxidase, an enzyme whose isolation from *T. flavus* is reported this year. The other product of the enzyme oxidation is hydrogen

peroxide, which is found to inhibit the growth of *V. dahliae*. Results of the study of this antifungal activity and the isolation of other compounds from the *T. flavus* aqueous fungal broth are presented.

Biogenetically, metabolites **10**, **15**, and **23** are formed by a polyketide pathway. [1-^{13}C] Labelled sodium acetate was utilized as a precursor for studying their biosynthetic pathways. The results of these biosynthetic studies are discussed.

ACKNOWLEDGEMENTS

The author wishes to thank:

Dr. William A. Ayer for his time, his energy, and, most of all, his inspiration.

I sincerely thank my friends and colleagues Dr. Francisco X. Talamas, Dr. Barbara S. Migaj, Dr. John B. Macaulay, and Dr. Luis M. Pena-Rodriguez for their friendships and their suggestions from most useful discussions.

Mrs. Anna Szenthe for growing and maintaining the fungal cultures, as well as for her excellent work with the bioassays.

Dr. Lois M. Browne for her advice.

Dr. Tom T. Nakashima and the nuclear magnetic resonance laboratory staff for their help and enthusiasm.

The technical staff of the department of chemistry.

The Natural Sciences and Engineering Research Council (NSERC), as well as the Alberta Heritage Foundation for Medical Research (AHFMR), for financial support.

TABLE OF CONTENTS

CHAPTER		PAGE
PART 1. METABOLITES OF THE ORGANIC EXTRACTS		1
I.	INTRODUCTION	2
II.	RESULTS AND DISCUSSION	7
	Metabolites of the *Talaromyces flavus* Mycelium Extracts	7
	Metabolites of the *Talaromyces flavus* Broth Extract	17
III.	EXPERIMENTAL	77
	Growth of *Talaromyces flavus* and Extraction of the Metabolites	78
	Isolation of the Metabolites	79
PART 2. BIOLOGICAL ACTIVITY OF AND BIOSYNTHETIC STUDIES OF *TALAROMYCES FLAVUS* METABOLITES		105
IV.	INTRODUCTION	106
V.	RESULTS AND DISCUSSION	111
	Biological Activity and the *Talaromyces flavus* Broth	111
	Biosynthetic Studies of *Talaromyces flavus* Metabolites	124
VI.	EXPERIMENTAL	138
	Growth of *Talaromyces flavus* and Isolation of the Aqueous Metabolites	139
	Biosynthetic Studies of Metabolites Produced by *Talaromyces flavus*	143
	[1-^{13}C] Acetate Labelled Metabolites	144

Biological Studies of the Aqueous Broth, Organic Extracts, and Metabolites of *Talaromyces flavus* 145

VII. BIBLIOGRAPHY 149

VIII. APPENDIX 156

LIST OF TABLES

TABLE		PAGE
1	Metabolites isolated from *Talaromyces* species	2
2	^{1}H nmr data for mannitol hexaacetate (**2**)	9
3	Spin decoupling ^{1}H nmr data for the triglyceride (**5**)	12
4	Metabolites from the three broth extracts of *Talaromyces flavus*	18
5	^{1}H and ^{13}C nmr data for D-glucono-1,4-lactone (**8**)	21
6	^{1}H nmr data for D-glucono-1,4-lactone (**8**) and its tetraacetate (**9**) ..	22
7	Spin decoupling ^{1}H nmr data for D-glucono-l,4 lactone tetraacetate (**9**)	23
8	Coupled ^{1}H-^{13}C ^{13}C nmr data with selective ^{1}H-irradiation for the phthalide metabolite (**10**)	26
9	The ^{13}C nmr assignment of 4,6-dihydroxy-5-methylphthalide (**10**) .	28
10	Coupled ^{1}H-^{13}C ^{13}C nmr data with selective ^{1}H-irradiation for 4,6-dimethoxy-5-methylphthalide (**11**)	30
11	^{1}H and ^{13}C nmr data for 4,6-dimethoxy-5-methylphthalide (**11**)	31
12	^{13}C nmr shift differences observed on methylation for compounds **10** and **11**	32
13	NOe results for metabolite **13**	35
14	^{1}H and ^{13}C nmr data for metabolite **15**	42
15	Calculated and observed ^{13}C nmr shifts for 4-carboxy-5-hydroxy-phthalaldehydic acid methyl ester (**15**)	46
16	Nuclear Overhauser enhancement results for metabolite **17**	49
17	Calculated *versus* observed ^{13}C nmr chemical shifts for altenusin ...	51

TABLE		PAGE
18	The ^{1}H nmr data and nOe results for metabolite **23**	62
19	^{13}C nmr data for metabolite **23**	63
20	The ^{13}C nmr chemical shifts of the aromatic portion of 4,6-dihydroxy-5-methylphthalide (**10**), 5,7-dihydroxy-6-methyl-phthalide, and metabolite **23**	64
21	^{13}C nmr assignment of talaroflavone (**23**)	66
22	^{13}C nmr chemical shifts of talaroflavone (**23**) and talaroflavone diacetate (**24**)	68
23	^{13}C nmr data for metabolite **28**	75
24	The ^{13}C nmr assignment of 4,6-dihydroxy-5-methylphthalide (**10**)	125
25	The ^{13}C nmr assignment of 4-carboxy-5-hydroxyphthalaldehydic acid methyl ester (**15**)	132
26	^{13}C nmr assignment of talaroflavone (**23**)	136
27	Bioactivity of crude extracts and metabolites **8** and **10** of *Talaromyces flavus*	148

LIST OF FIGURES

FIGURE		PAGE
1	Metabolites isolated from *Talaromyces* species	3
2	Metabolites isolated from *Penicillium vermiculatum*	5
3	Acyloxy fragmentation of triglyceride **5**	13
4	Acylium type fragmentations and fragment ions of the triglyceride **5**	14
5	Further fragmentation of the triglyceride **5**	14
6	Mass spectral fragmentation of the diglyceride **6**	15
7	The ^{1}H-^{1}H coupling pattern of metabolite **8**	19
8	The ^{1}H-^{1}H COSY spectrum of compound **8**	20
9	Preparation of D-glucono-1,4-lactone (**8**)	19
10	Multiplicity changes in the carbonyl carbon (171.6 ppm) of metabolite **10** with selective ^{1}H-irradiation	26
11	^{1}H and ^{13}C nmr literature data for 5-hydroxymethylfurfural (**12**) .	33
12	The ^{1}H and ^{13}C nmr assignments for 7-hydroxy-2,5-dimethyl-chromone (**13**)	36
13	Acid catalyzed degradation of aloenin	40
14	Formation of monomethyl ether **14**	40
15	Reduction of metabolite **15**	43
16	Reduction of 3,5-dihydroxy-4-methylphthalaldehydic acid methyl ester	43
17	Nuclear Overhauser enhancement results for dehydroaltenusin diacetate (**20**)	56

FIGURE		PAGE
18	The ^{1}H-^{1}H couplings of metabolite **27**	71
19	Metabolites isolated from *Verticillium dahliae*	109
20	The ^{1}H and ^{13}C nmr assignments for hydroxymethylmaltol diacetate (**30**)	115
21	The ^{1}H-^{1}H couplings of acetate **32**	117
22	The ^{1}H and ^{13}C nmr assignments for acetate **32**	118
23	Oxidation of D-glucose by glucose oxidase	120
24	Action of catalase	122
25	The triiodide ion peroxide assay	122
26	Examples of the two regioisomeric phthalide backbones	126
27	Cannizzaro reaction of quadrilineatin	128
28	[1-^{13}C] CH_3CO_2Na labelling study of 4,6-dihydroxy-5-methyl-phthalide (**10**)	129
29	[1-^{13}C] CH_3CO_2Na labelling study of metabolite **15**	133
30	[1-^{13}C] CH_3CO_2Na labelling study of talaroflavone (**23**)	135

LIST OF SCHEMES

SCHEME		PAGE
1	The mannitol cycle	9
2	Base peak formation in the mass spectrum of **3**	11
3	The mass spectral fragmentation of 4,6-dihydroxy-5-methyl-phthalide (**10**)	29
4	Formation of 5-hydroxymethylfurfural (**12**) from D-glucose	34
5	The mass spectral fragmentation of 7-hydroxy-2,5-dimethyl-chromone (**13**)	37
6	Biosynthesis of eugenin	38
7	Proposed biosynthesis of 7-hydroxy-2,5-dimethylchromone (**13**).	39
8	The mass spectral fragmentation of metabolite **15**	45
9	The mass spectral fragmentation of metabolite **17**	48
10	The mass spectral fragmentation of altenusin (**18**)	52
11	The mass spectral fragmentation of dehydroaltenusin diacetate (**20**)	55
12	Mass spectral fragmentation of desmethyldehydroaltenusin triacetate (**22**)	59
13	Biosynthetic pathway to altenusin (**18**), dehydroaltenusin (**19**), and desmethyldehydroaltenusin (**21**)	60
14	The mass spectral fragmentation of deoxytalaroflavone (**27**)	73
15	Formation of deoxytalaroflavone (**27**) from talaroflavone (**23**)	74
16	The mass spectral fragmentation of metabolite **28**	76
17	Extraction of *Talaromyces flavus* broth	80
18	Extraction of *Talaromyces flavus* mycelium	81

SCHEME PAGE

19	Isolation of metabolites from the methanol mycelium extract	82
20	Partition extraction of the ethyl acetate mycelium extract	83
21	Metabolites isolated by chromatography of the hexane portion of the ethyl acetate mycelium extract	84
22	Isolation of metabolites from the partition extracts of the ethyl acetate broth extract	85
23	The mass spectral fragmentation of acetate **32**	116
24	Possible pathway for the formation of compound **31**	118
25	Proposed biosynthetic pathway to the regioisomeric phthalide skeletons	127
26	Proposed biosynthetic pathway to metabolite **15**	131
27	Proposed biosynthetic pathway to talaroflavone (**23**)	137
28	Isolation of metabolites from *Talaromyces flavus* aqueous broth ..	140

LIST OF PLATES

PLATE		PAGE
1	The antifungal bioassay. *Talaromyces flavus versus Verticillium dahliae*	112
2	The effect of hydrogen peroxide on *Verticillium dahliae* microsclerotia production: [H_2O_2] a) 2.7 µL/mL, b) 3.6 µL/mL, c) 7.5 µL/mL; d) *Talaromyces flavus* broth + catalase	121

PART 1. METABOLITES OF THE ORGANIC EXTRACTS

I. INTRODUCTION

The soil fungus *Talaromyces flavus* (Klöcker) Stolk and Samson is the most common species of its genus. This species is an ascomycete and produces its asci in chains.[1,2] *Talaromyces flavus* is frequently isolated from soil, although it may also occur on organic materials undergoing slow decomposition. The species is widespread in its distribution but it is most commonly reported from the warmer regions of the world. *Talaromyces flavus* is the perfect state of the fungus and the imperfect (conidial) state is *Penicillium dangeardii* Pitt. Studies of the metabolites produced by other species of *Talaromyces* have been reported. Table 1 summarizes the metabolites isolated from these species and their structures are illustrated in Figure 1.

Table 1. Metabolites isolated from *Talaromyces* species

species	metabolite
Talaromyces bacillosporus[3]	bacillosporins A, B, and C
	pinselin
T. avellaneus[4]	emodin
	ω-hydroxyemodin
	emodic acid
T. vermiculatus[5]	talaron
T. stipitatus[6]	catenarin
	erythroglaucin
	emodin
T. stipitatus[7,8,9]	talaromycins A, B, C, D, E, and F

As the metabolites listed in Table 1 have a polyketide biogenesis, it was thought that the metabolites produced by *T. flavus* may also be of polyketide origin.

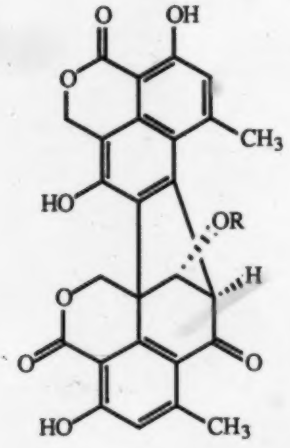

R = OAc, bacillosporin A

R = OH, bacillosporin B

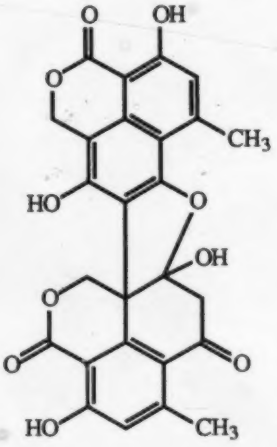

bacillosporin C

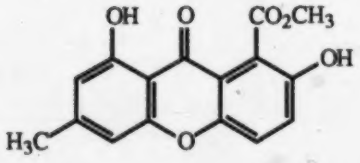

pinselin

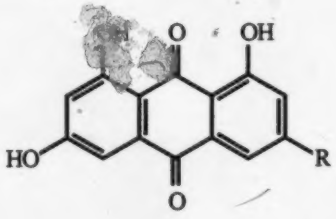

R = CH_3, emodin

R = CH_2OH, ω-hydroxyemodin

R = CO_2H, emodic acid

talaron - a water soluble acidic polysaccharide antifungal antibiotic whose molecular weight is estimated to be 7,000-8,000

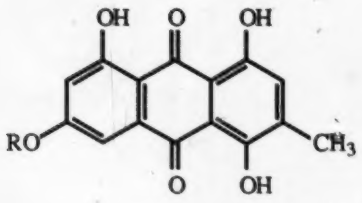

R = H, catenarin

R = CH_3, erythroglaucin

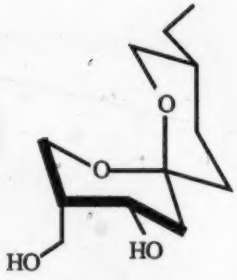

talaromycin A

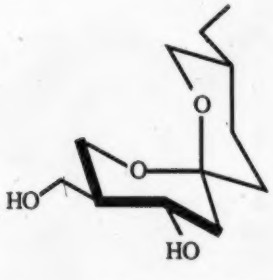

talaromycin B

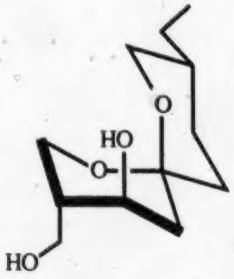

talaromycin C

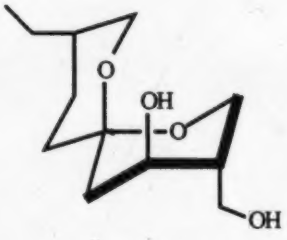

talaromycin D

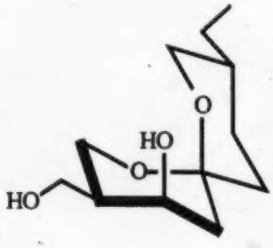

talaromycin E

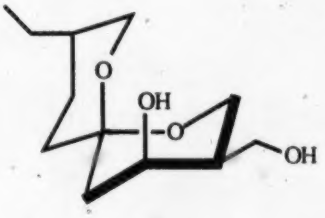

talaromycin F

Figure 1. Metabolites isolated from *Talaromyces* species

The imperfect state of the the fungus, *P. dangeardii* (*T. flavus*), has also been studied. Three metabolites have been isolated and they are all found to possess antibiotic activity.[10-14] These natural products, vermiculine, vermistatin, and vermicillin, are illustrated in Figure 2.

Our interest in studying the metabolites produced by *T. flavus* was instigated with the report of the effectiveness of *T. flavus* as a biological control agent for Verticil-

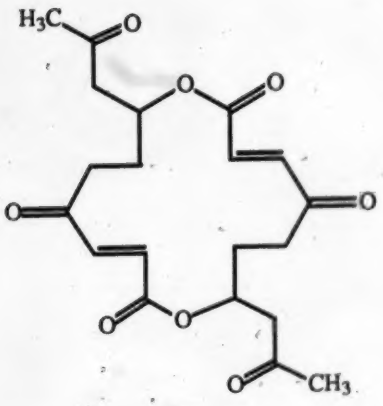

vermiculine

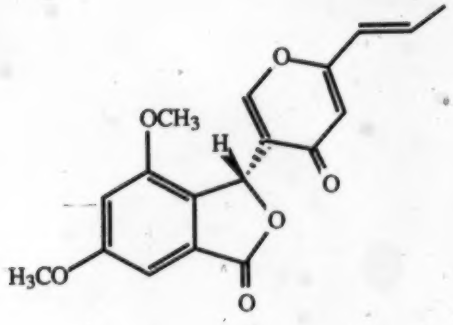

vermistatin

vermicillin (structure not elucidated)

Figure 2. Metabolites isolated from *Penicillium dangeardii*

lium wilt of eggplant (*Solanum melongena* L.), a disease caused by the fungus *Verticillium dahliae* Kleb.[15] The Verticillium wilt organism is a widespread soil inhabitant which infects a wide range of herbaceous and woody plants. Further details regarding this biological control and the nature of the wilting disease will be discussed in Part 2 of this thesis.

Talaromyces flavus has been reported to show biological activity not only towards *V. dahliae* but also towards the plant pathogens *Sclerotinia sclerotiorum* (Lib.) de Bary,[16] *Rhizoctonia solani* Kühn,[17] and *V. albo-atrum* Reinke and Berth..[18] In this regard, *T. flavus* may act as an antagonist or an hyperparasite. In the former, a plug to plug bioassay displays a zone of inhibition and a chemical toxin is implicated but with the latter, such a compound is not necessarily involved as the destruction may result by direct disruption through parasitism.[19] *Talaromyces flavus* is known to be a destructive hyperparasite of *S. sclerotiorum*, the cause of the serious disease Sclerotinia wilt of sunflower. *Talaromyces flavus* is destructive to the hyphae of *S. sclerotiorum*. This mode of action is similar to that of *T. flavus* on *R. solani*.[17] It has been suggested that

the mode of parasitism of *V. albo-atrum* by *T. flavus* in controlling Verticillium wilt of tomato involves antibiosis and competition.[18]

It is often assumed that for a biological control agent to suppress root diseases it must be able to compete effectively with the natural soil biota in order to become established in the rhizosphere of the host. It is only then that the organism can interact with the pathogen to reduce disease. One method by which this may occur is for the control agent to reduce the activity of the pathogen. It is known that *T. flavus* reduces the ability of microsclerotia of *V. dahliae* to germinate. Although there is no clear correlation between microsclerotia survival and the proportion of the microsclerotia colonized by *T. flavus*, the fact that colonization did occur indicates that parasitism or antibiosis may have taken place.[20] *Talaromyces flavus* is also able to occupy the rhizosphere of potato and of cotton, suggesting that it may suppress Verticillium wilt of these two plants.[20,21] The widespread adoption of a biological control agent for a soilborne disease will depend on the ability of the organism to establish itself in different soils. Studies of the edaphic parameters associated with the establishment of *T. flavus* as a biological control suggest that it may be suitable for widespread use.[22,23]

Studies in our laboratories indicated that *T. flavus* grows best on a malt extract medium (compared to a potato dextrose broth and Czapek medium). Thus, this medium was used throughout the study. It is found that the mycelium possesses no biological activity. The fungal broth exhibits antibacterial activity against *Pseudomonas aeruginosa*, *Staphylococcus aureus*, and *Streptococcus pyogenes* and antifungal activity towards *V. dahliae*. Extraction of the broth with ethyl acetate removes the antibacterial activity; however, the antifungal activity remains in the aqueous broth. In isolating and determining the structures of organic and water soluble metabolites from *T. flavus* we had hoped that some would display the biological activities noted above.

II. RESULTS AND DISCUSSION

Metabolites of the *Talaromyces flavus* Mycelium Extracts

Talaromyces flavus was grown on a sterile malt extract medium for four weeks. The mycelium was subjected to extraction with ethyl acetate and methanol. Methanol was added to the two extracts and an insoluble white solid was filtered off. Recrystallization from methanol afforded a white, granular compound (**1**). Compound **1**, melting point 170-172°C, shows a ratio of 1:1:1:4 hydrogens in the ^1H nuclear magnetic resonance (nmr) spectrum (DMSO-d_6). Although a good high resolution mass spectrum (hrms) of this compound could not be obtained, the chemical ionization mass spectrum (cims) shows ions at 183 ($M^+ + 1$, 63) and 200 ($M^+ + 18$, 100). A molecular formula consistent with a molecular weight of 182 is $C_6H_{14}O_6$. As the ^1H nmr spectrum shows that the relative number of hydrogens is 1:1:1:4, the actual ratio of hydrogens must be 2:2:2:8 to account for the fourteen hydrogens in the molecule. The element of symmetry in metabolite **1** is reflected in the ^{13}C nmr spectrum as only three signals are observed, rather than six, at 71.3 (d), 69.7 (d), and 63.8 (t) ppm. The infrared (ir) spectrum shows a broad hydroxyl absorption at 3318 cm^{-1} and C-O stretches at 1081 and 1019 cm^{-1}. The hydroxyl hydrogens are seen in the ^1H nmr spectrum at 4.40 (2H, d, J = 6.0 Hz), 4.31 (2H, t, J = 6.0 Hz), and 4.12 (2H, d, J = 7.5 Hz) ppm. Addition of D_2O greatly reduces the intensity of these signals. The remaining eight carbinolic hydrogens are seen as a multiplet between 3.63 and 3.35 ppm. A polyhydroxy metabolite consistent with these data is D-mannitol (**1**). Each of the four chiral centers is of S-configuration. D-mannitol (**1**) possesses a C_2 axis of symmetry, resulting in three pairs of equivalent carbons. An authentic sample of D-mannitol (**1**) was obtained[24] whose physical and spectral data compare well with that of the metabolite isolated.

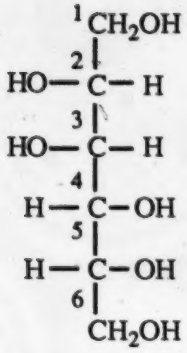

D-mannitol **1**

Reaction of D-mannitol (**1**) with acetic anhydride and pyridine at room temperature overnight affords the hexaacetate of compound **1**, melting point 123-125°C.

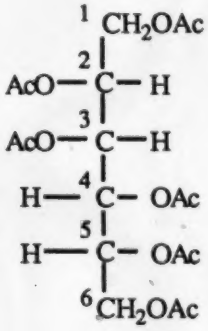

D-mannitol hexaacetate **2**

The cims shows a peak at 452 ($M^+ + 18$, 100) which gives 434 as the molecular weight for the hexaacetate **2**, consistent with the molecular formula $C_{18}H_{26}O_{12}$. The ir spectrum shows no hydroxyl absorption but does possess a carbonyl absorption at 1743 cm^{-1} and C-O bands at 1226 and 1033 cm^{-1}. The ^1H nmr spectrum shows acetate methyl groups at 2.03, 2.05, and 2.07 ppm (6H each, s), consistent with the symmetry of this metabolite. The ^1H nmr data for D-mannitol hexaacetate (**2**) are consistent with those expected and are summarized in Table 2.

Table 2. ^1H nmr data for mannitol hexaacetate (**2**)

	chemical shift (ppm)
H-3, H-4	5.43 (2H, d, J = 9.0 Hz)
H-2, H-5	5.05 (2H, ddd, J = 2.5, 5.0, 9.0 Hz)
H-1, H-6	4.20 (2H, dd, J = 2.5, 12.5 Hz)
H-1', H-6'	4.05 (2H, dd, J = 5.0, 12.5 Hz)
$OCOCH_3$	2.07 (6H, s)
$OCOCH_3$	2.05 (6H, s)
$OCOCH_3$	2.03 (6H, s)

Further confirmation of the identity of D-mannitol (**1**) is the optical rotation of the hexaacetate **2** which, found to be +22.4° (c 6.2, $CHCl_3$), closely agrees with that reported in the literature (+25.0° ($CHCl_3$)).[25]

The "mannitol cycle" (Scheme 1) functions as an important NADPH regenerating system.[26] The enzymes involved in this process have been found in several genera of Fungi Imperfecti. In view of the widespread occurrence of D-mannitol (**1**) in fungi, the possibility exists that the cycle operates in a large number of species.

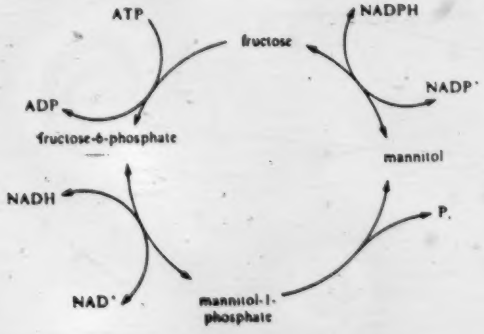

Scheme 1. The mannitol cycle

The methanol soluble portion of the methanol Soxhlet extract was subjected to flash chromatography, eluting with benzene followed by benzene-ether (9:1). The least polar metabolite (**3**) was obtained as a clear colorless oil, having a molecular formula of $C_{19}H_{34}O_2$ (294), as determined by hrms and confirmed by cims (312, $M^+ + 18$, 100). The ir spectrum shows an ester carbonyl at 1745 cm^{-1}. The molecule possesses three sites of unsaturation, one of which is the carbonyl. Infrared absorptions at 3000 and 720 cm^{-1} and a four-hydrogen multiplet from 5.43 to 5.28 ppm in the ^1H nmr spectrum suggest that the other two sites of unsaturation are *cis* double bonds. A three-hydrogen singlet at 3.66 ppm, two-hydrogen triplets at 2.77 and 2.30 ppm, and a four-hydrogen multiplet from 2.08 to 1.77 ppm suggest the partial structures shown below.

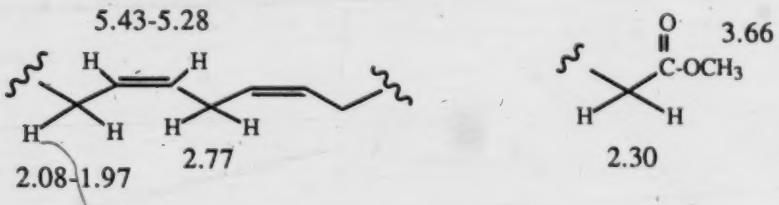

Together with the remaining signals in the ^1H nmr spectrum, these data are consistent with that of methyl linoleate (**3**).

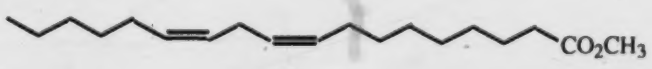

methyl linoleate **3**

The base peak in the hrms at m/z 74 arises from the McLafferty rearrangement of the methyl ester (Scheme 2). Although the possibility exists that this methyl ester (**3**) forms during the Soxhlet extraction of the mycelium with methanol, it has also been detected by thin layer chromatography (tlc) in the ethyl acetate mycelium extract where no methanol was utilized.

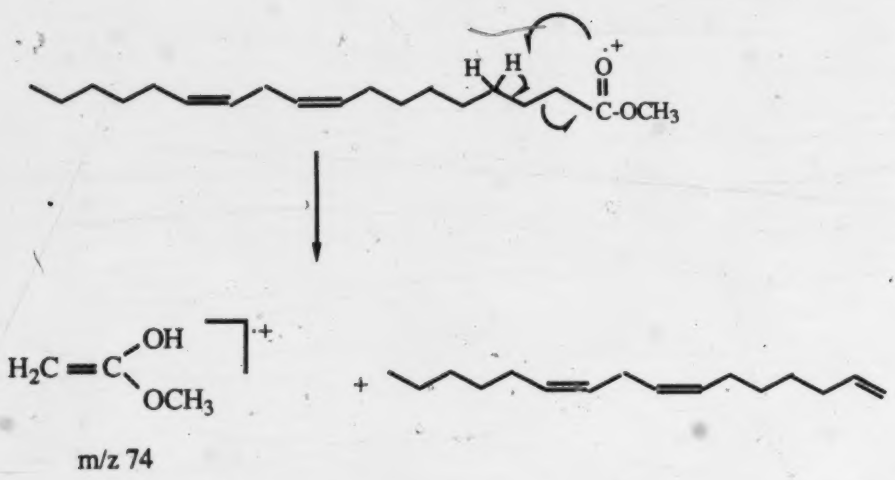

m/z 74

Scheme 2. Base peak formation in the mass spectrum of **3**.

Linoleic acid (**4**) was isolated from the methanol mycelium extract by flash chromatography, eluting with dichloromethane-ethyl acetate (9:1). This clear, colorless oil shows a broad hydroxyl absorption in its ir spectrum from 3460 to 2400 cm^{-1}. The molecular formula of $C_{18}H_{32}O_2$ (280), as determined by hrms, is consistent with that of the acid **4** and is confirmed by cims (298, $M^+ + 18$, 71). The ^1H nmr spectrum is very similar to that of its methyl ester (**3**), although the acid **4** lacks the three hydrogen methoxyl singlet of the ester **3**.

linoleic acid **4**

From three different sources, the ethyl acetate and methanol mycelium extracts, as well as the Skellysolve B portion of the ethyl acetate broth extract, a clear, colorless oil (metabolite **5**) was isolated whose ir spectrum shows an ester carbonyl at 1746 cm^{-1}. The appearance in the ^1H nmr spectrum of doublet of doublets at 4.29 (2H, J = 5.0, 12.0 Hz) and 4.14 (2H, J = 6.0, 12.0 Hz) ppm is indicative of the hydrogens at C-1 and C-3 of a triglyceride. A one hydrogen multiplet at 5.25 ppm was shown to be that

hydrogen attached to C-2 of the triglyceride backbone by a spin decoupling experiment (Table 3). Irradiation of the signal at 5.25 ppm caused the collapse of the signal at 4.29 ppm to a doublet (J = 12.0 Hz) and that at 4.14 ppm to a doublet (J = 12.0 Hz). Hydrogen signals at 5.35, 2.77, 2.31, and 2.04 ppm suggested that at least one of the fatty acid residues of the triglyceride (**5**) was a linoleyl one, as these resonances were seen in the spectra of metabolites **3** and **4**. That the resonances at 5.35, 2.77, and 2.04 ppm are coupled to one another was shown by spin decoupling experiments. Irradiation of one of the signals caused a change in the appearance of the other two in all three cases. These results are summarized in Table 3.

Table 3. Spin decoupling ^1H nmr data for the triglyceride (**5**)

signal irradiated (ppm)	observed change
5.35	2.77 (br s)
	2.04 (br t)
5.25	4.29 (dd $\longrightarrow$ d (J = 12.0 Hz)
	4.14 (dd $\longrightarrow$ d. (J = 12.0 Hz)
2.77	5.35 (m)
	2.04 (br t)
2.04	5.35 (m)
	2.77 (br d)

Identification of the fatty acid residues comprising the triglyceride (**5**) was done by analysis of its high and low resolution mass spectra.[27] The low resolution mass spectrum (lrms) shows a peak at m/z 856, consistent with the molecular formula $C_{55}H_{100}O_6$. Three fragment ions arising from loss of one of the fatty acid residues in

the high resolution mass spectrum are seen at m/z 601 (14), 577 (36), and 575 (26) (Figure 3).

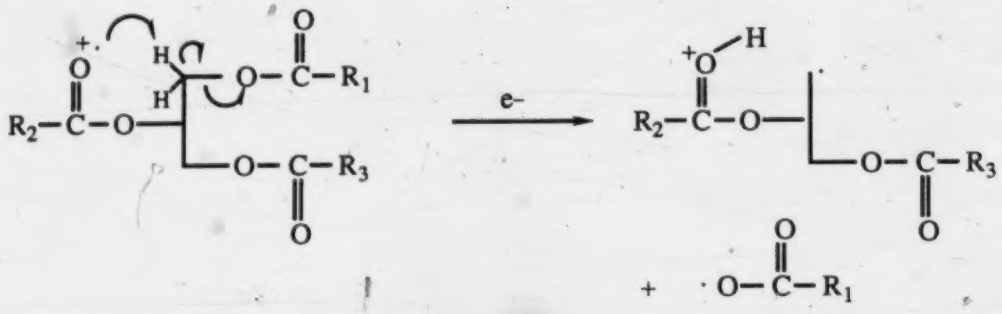

Figure 3. Acyloxy fragmentation of triglyceride **5**

Analysis of this type of fragmentation reveals the identity of the different acyl residues present in the triglyceride. Usually, the least abundant fragment corresponds to the loss of the acyloxy residue at C-2. In this case, that peak occurs at m/z 601 which corresponds to the fragment containing linoleic and linolenic acid residues. The other two ions at m/z 577 and 575 correspond to those of linoleic and palmitic acids and linolenic and palmitic acids, respectively. Fragments formed by cleavage of the ester bond give rise to the acylium ions at m/z 264 (19), 262 (69), and 239 (14). There are two possible fragmentation mechanisms for this cleavage as illustrated in Figure 4. The first fragmentation is favored for the acyl residues at C-1 and C-3 of the trigylceride since two carbinolic hydrogens are available for the fragmentation. Steric hindrance is not a major problem. The second fragmentation illustrated is favored at C-2. This supports the proposal that the palmitoyl residue is at C-2. Further support for the occurrence of the palmitoyl residue at C-2 is seen in the ion at m/z 313, which, it is suggested, arises from loss of the acyl residues at C-1 and C-3 (Figure 5). If R_2 is palmitoyl, this four membered ring fragment ion is observed at m/z 313. These data are consistent with a triglyceride (**5**) composed of the three fatty acid residues linoleic, linolenic, and palmitic.

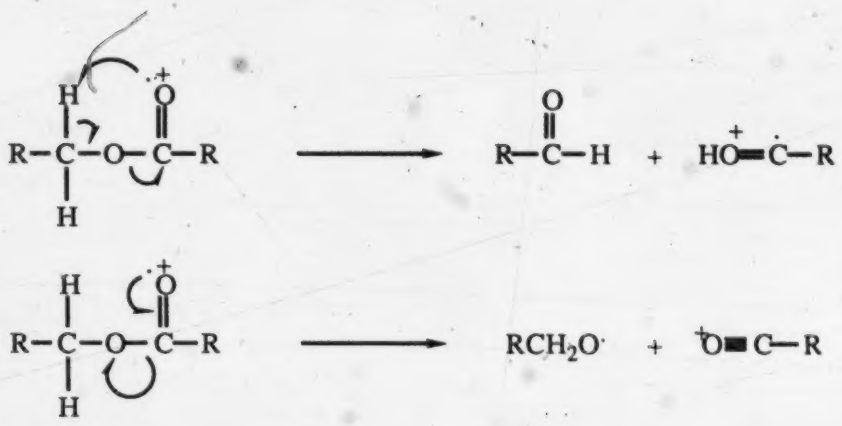

m/z 264 $HO^{+}{=}\dot{C}-(CH_2)_7(CH{=}CH-CH_2)_2(CH_2)_3CH_3$

262 $HO^{+}{=}\dot{C}-(CH_2)_7(CH{=}CH-CH_2)_3CH_3$

239 $O^{+}{\equiv}C-(CH_2)_{14}CH_3$

Figure 4. Acylium type fragmentations and fragment ions of the triglyceride **5**

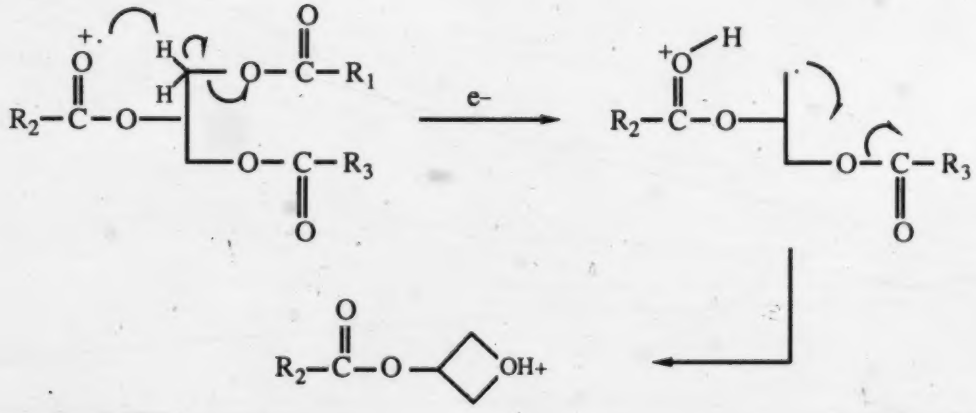

m/z 313 if R_2 = palmitoyl

Figure 5. Further fragmentation of the triglyceride **5**

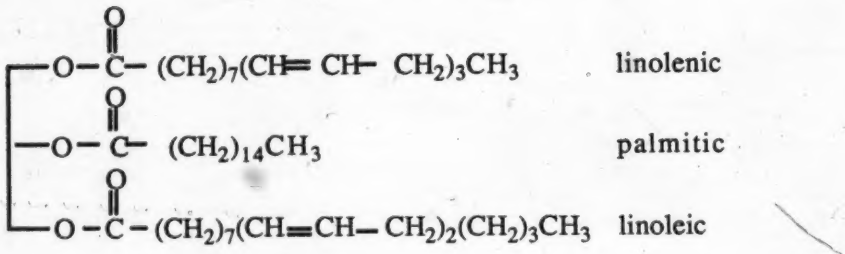

triglyceride **5**

In addition to the triglyceride (**5**), a diglyceride (**6**) was isolated from the ethyl acetate mycelium extract. The ir spectrum of this clear, colorless oil is similar to that of the triglyceride (**5**); however, it shows an additional broad hydroxyl absorption at 3460 cm^{-1}. The signals in the ^1H nmr spectrum are also similar. The low resolution mass spectrum shows an ion at m/z 577, which is assigned to the fragment illustrated (Figure 6).

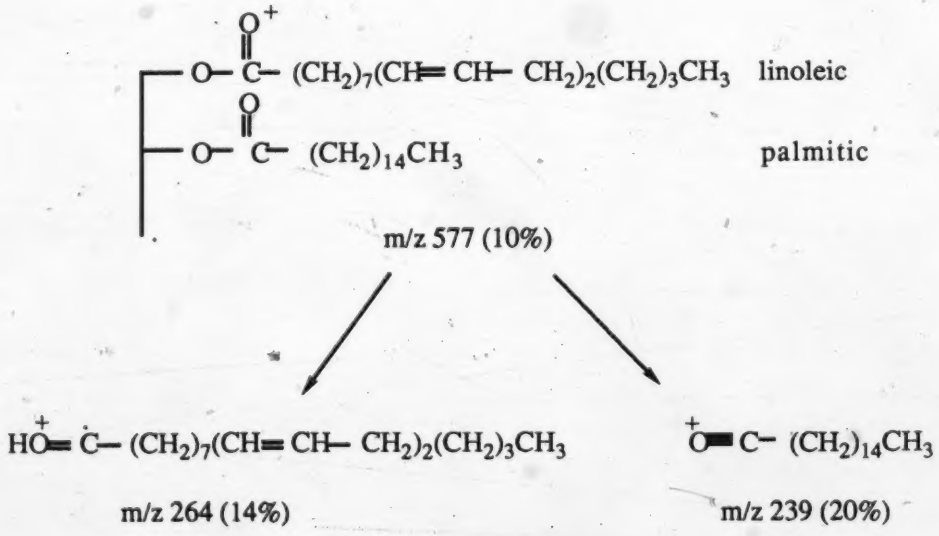

Figure 6. Mass spectral fragmentation pattern of the diglyceride **6**

This ion then fragments to give the ions at m/z 264 and 239. An additional ion is seen at m/z 313 (28), as for the triglyceride (**5**), suggesting that the palmitoyl residue is again at

C-2. The acylium ion of this residue is found at m/z 239 and the ion at m/z 264 corresponds to that of linoleic acid. Thus, the fatty acids of this diglyceride (**6**), also found in the triglyceride (**5**), are linoleic and palmitic.

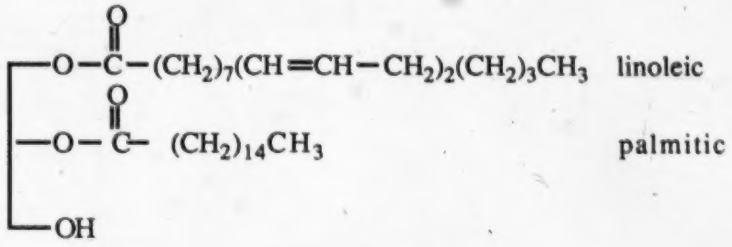

diglyceride **6**

The final metabolite isolated from the methanol and ethyl acetate mycelium extracts was obtained as a cream colored solid. Recrystallization from 95% ethanol gave white plates having a melting point 163-165°C. The molecular formula of metabolite **7** is $C_{28}H_{44}O$ (396) as determined from its high resolution mass spectrum and confirmed by chemical ionization (379, $M^+ + 1 - H_2O$, 100). It displays a broad hydroxyl absorption in the ir spectrum at 3390 cm^{-1}. The ultraviolet (uv) spectrum shows maxima at 262, 271, 281, and 293 nm. The band at 271 nm is consistent with that of an homoannular diene.[28] The ^1H nmr spectrum shows vinylic hydrogens at 5.57, 5.38, and 5.20 ppm and a carbinolic hydrogen at 3.65 ppm. The remaining signals are representative of aliphatic hydrogens, including six methyl groups (4 x d, 2 x s). These data are consistent with that of ergosterol (**7**). A comparison of these data with those of an authentic sample of ergosterol (**7**) confirms its identity.

In summary, the mycelium of *T. flavus* contains primarily ubiquitous non-polar metabolites. In the partition extraction of the ethyl acetate Soxhlet extract, 85% of the material is found in the hexane extract with the remaining 15% distributed evenly between the dichloromethane and ethyl acetate extracts. The hexane extract contains

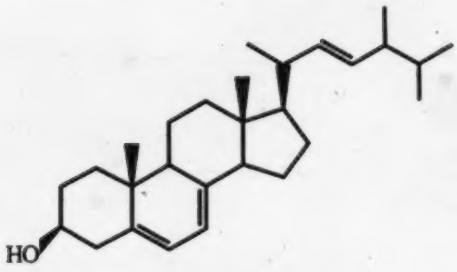

ergosterol **7**

mostly triglyceride (**5**, 65%), ergosterol (**7**, 8%), and diglyceride (**6**, 1%), together with linoleic acid (**4**) and methyl linoleate (**3**).

Metabolites of the *Talaromyces flavus* Broth Extract

The liquid culture of *T. flavus* was extracted with ethyl acetate. The concentrated extract was dissolved in a water-methanol solution and extracted with Skellysolve B, dichloromethane, and ethyl acetate. A blank malt extract medium was extracted in the same way in order to compare the metabolites produced by the fungus with the compounds from the medium itself. The three crude extracts were examined by thin layer chromatography. The dichloromethane extract appeared to contain more components than the other extracts. The metabolites of each crude extract were separated by chromatography. The pure compounds isolated from each of these three broth extracts are listed in Table 4.

A metabolite isolated from the polar ethyl acetate extract, which accounts for 50% of the weight of this fraction, was obtained as a white solid. Recrystallization from acetic acid gave a white powder, melting point 127-129°C. The parent ion in the high resolution mass spectrum was not detected. The chemical ionization mass spectrum shows an ion at 196 ($M^+ + 18$, 100) which indicates a molecular weight of 178 and

Table 4. Metabolites from the three broth extracts of *Talaromyces flavus*

extract	metabolite
Skellysolve B	**5**
Dichloromethane	**10, 12, 13, 15, 17, 18, 19, 21, 23, 27, 28**
Ethyl acetate	**8**

suggests a molecular formula of $C_6H_{10}O_6$ for metabolite **8**. The highest mass peak in the hrms is seen at m/z 160, corresponding to the loss of water from the parent ion. The ir spectrum displays a broad hydroxyl absorption at 3300 cm^{-1} and a carbonyl band at 1776 cm^{-1}, consistent with that of a γ-lactone.[29] The ^1H nmr spectrum (methanol-d_4) shows six carbinolic hydrogens. Since there are ten hydrogens in the metabolite (**8**), four of them must be exchangeable. The coupling pattern among the six hydrogens is illustrated in Figure 7 and was determined by spin decoupling and ^1H-^1H correlated spectroscopy (COSY) experiments.[30,31] In the ^1H-^1H COSY spectrum (Figure 8), one observes, in addition to the couplings observed in the one dimensional spectrum, a weak correlation in the cross peak between H-2 and H-4. The γ-lactone carbonyl carbon is seen at 177.5 ppm in the ^{13}C nmr spectrum. Doublet carbons, at 81.0, 74.4, 74.2, and 71.4 ppm, and a triplet carbon at 63.8 ppm, comprise the remainder of the spectrum. These data suggest that metabolite **8** is D-glucono-1,4-lactone.

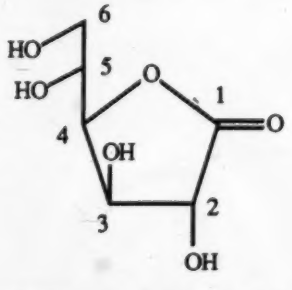

D-glucono-1,4-lactone **8**

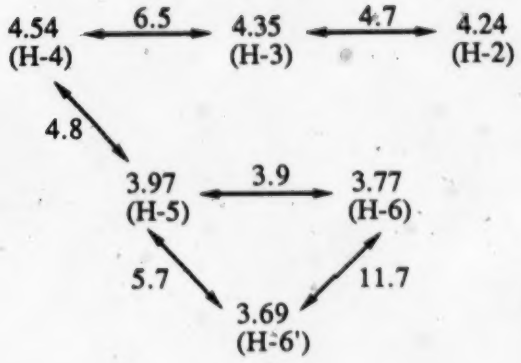

Figure 7. The ^{1}H-^{1}H coupling pattern of metabolite **8**

Although this is the first report of the isolation of this metabolite from a fungus, it is well known in carbohydrate chemistry. A comparison of the ^{1}H and ^{13}C nmr data reported [32,33] for D-glucono-1,4-lactone (**8**) with those obtained for the metabolite agree well (Table 5). To confirm the identity of D-glucono-1,4-lactone (**8**), a synthetic sample was prepared by refluxing a solution of D-glucono-1,5-lactone[34] in acetic acid for one hour[35] (Figure 9). After cooling to room temperature, the solution was seeded with the γ-lactone

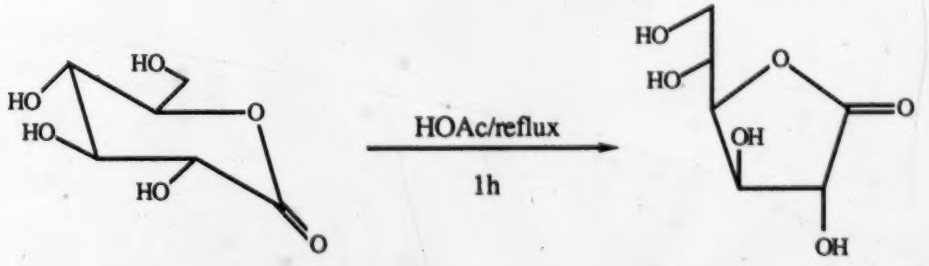

D-glucono-1,5-lactone D-glucono-1,4-lactone **8**

Figure 9. Preparation of D-glucono-1,4-lactone **8**

(**8**). This afforded compound **8** in 30% yield. The equilibrium ratio of γ- to δ-lactone is 2:1, favoring the five-membered ring lactone.[36] The half-life for the hydrolysis of the δ-lactone is two hours. It is reasonable, then, that the γ-lactone be produced in less than

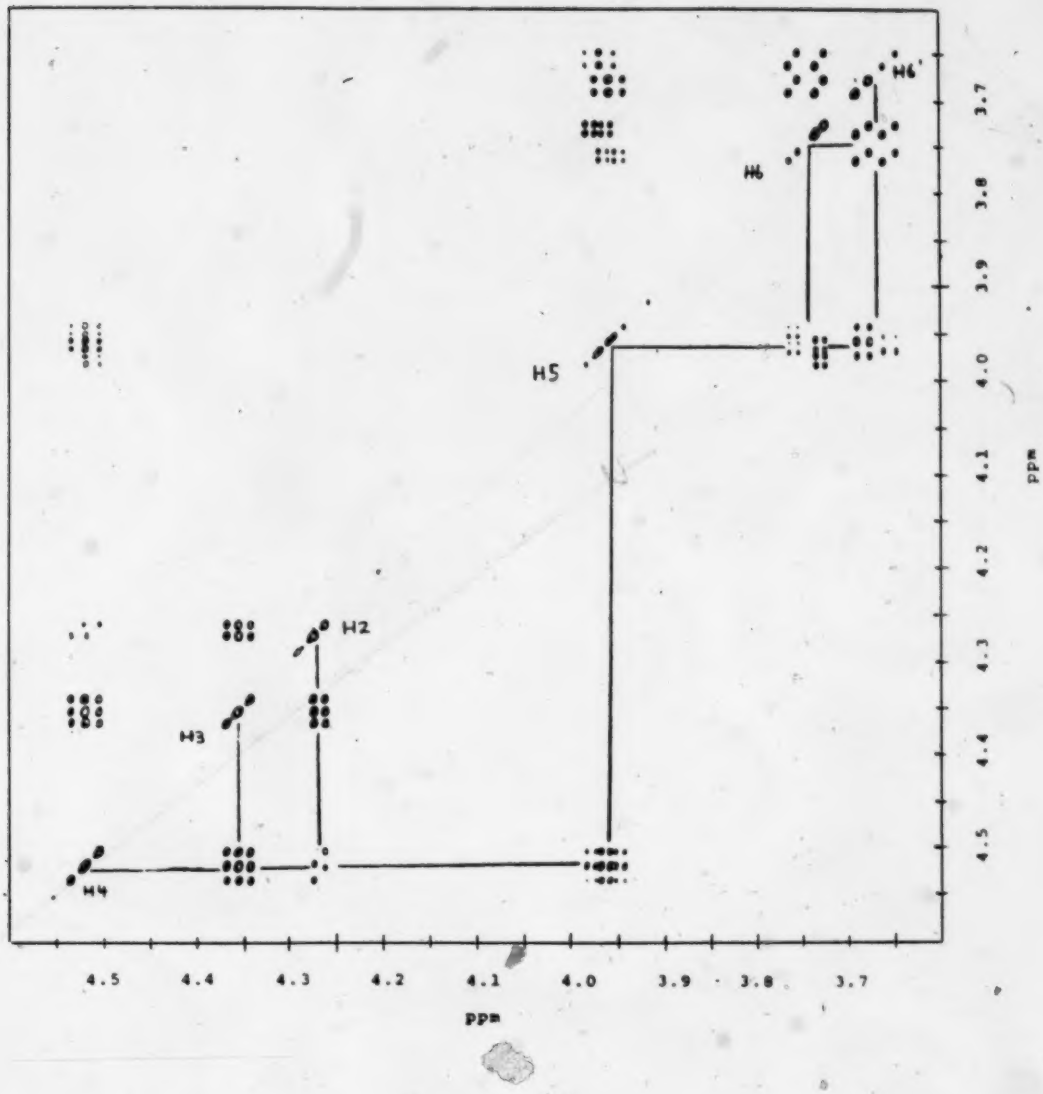

Figure 8. The ^{1}H-^{1}H COSY spectrum of compound **8** (CD_3OD/D_2O 1:1, 400 MHz, COSY 45, contour plot)

Table 5. ^{1}H and ^{13}C nmr data for D-glucono-1,4-lactone (8)

	^{1}H (ppm)			^{13}C (ppm)	
	found	literature[32]		found	literature[33]
H-2	4.24	4.27	C-1	177.5	177.9
H-3	4.35	4.37	C-2	74.2[a]	73.4[b]
H-4	4.54	4.56	C-3	74.4[a]	73.8[b]
H-5	3.97	4.00	C-4	81.0	80.5
H-6	3.77	3.78	C-5	71.4[a]	71.2[b]
H-6'	3.69	3.70	C-6	63.8	63.2

a,b - assignments may be interchanged

50% yield as the reaction was run for only one hour. Attempted base catalyzed (CD_3OD/CD_3ONa) isomerization of the γ- to δ-lactone in an nmr tube failed to produce the δ-lactone cleanly. This is not surprising as the γ-lactone is the more stable of the two. The spectral data for the synthetic sample of compound **8** agree well with that of the natural product. A mixed melting point of synthetic and natural lactones showed no depression. The fact that the parent ion is not observed in the hrms of metabolite **8** may be accounted for by the facile β-elimination of water from the γ-lactone, affording the ion at m/z 160.

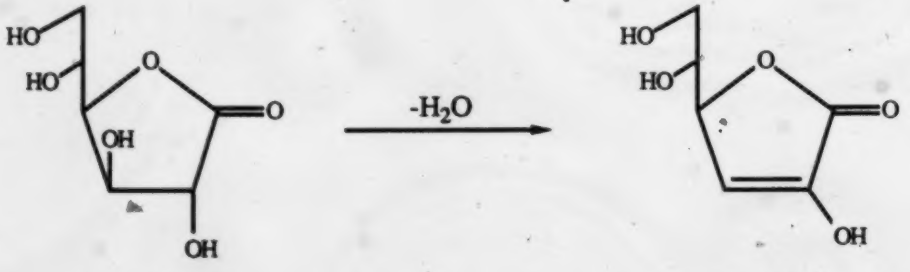

m/z 178 m/z 160

Reaction of D-glucono-1,4-lactone (**8**) with acetic anhydride and pyridine affords the tetraacetate **9** as white needles, melting point 101-102°C. Although the hrms does not show the parent ion, cims reveals an ion at 364 (M^+ + 18, 100). This corresponds to a molecular weight of 346 and a molecular formula of $C_{14}H_{18}O_{10}$ for the tetraacetate **9**.

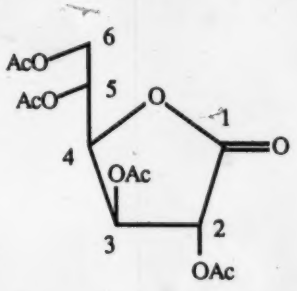

D-glucono-1,4-lactone tetraacetate **9**

The ir spectrum shows the γ-lactone carbonyl at 1806 cm^{-1} and the acetate carbonyl at 1751 cm^{-1}. Acetate methyl groups are seen in the ^1H nmr spectrum (Table 6) at 2.19, 2.12, 2.10, and 2.05 ppm. The hydrogens of the secondary alcohols (H-2, H-3, and H-5) shift downfield more than 1.0 ppm on acetylation, consistent with that expected.[37]

Table 6. ^1H nmr data for D-glucono-1,4-lactone (**8**) and its tetraacetate (**9**) (δ (ppm))

	alcohol (**8**) (CD_3OD/D_2O)	acetate (**9**) ($CDCl_3$)	$\delta_{OAc} - \delta_{OH}$
H-4	4.54 (dd, J = 4.8, 6.5 Hz)	4.96 (dd, J = 5.5, 8.0 Hz)	0.42
H-3	4.35 (dd, J = 4.7, 6.5 Hz)	5.62 (dd, J = 3.0, 5.5 Hz)	1.27
H-2	4.24 (d, J = 4.7 Hz)	5.23 (d, J = 3.0 Hz)	0.99
H-5	3.97 (ddd, J = 3.9, 4.8, 5.7 Hz)	5.35 (ddd, J = 3.0, 5.0, 8.0 Hz)	1.38
H-6	3.77 (dd, J = 3.9, 11.7 Hz)	4.58 (dd, J = 3.0, 12.0 Hz)	0.81
H-6'	3.69 (dd, J = 5.7, 11.7 Hz)	4.15 (dd, J = 5.0, 12.0 Hz)	0.46

The hydrogens of the primary alcohol (H-6, H-6') shift downfield an average of 0.5 ppm on acetylation, also in agreement with that expected for a primary alcohol.[37] Confirmation of the hydrogen assignments for the acetate **9** was achieved by spin decoupling experiments (Table 7). The ^{13}C nmr spectrum shows carbonyl signals

Table 7. Spin decoupling ^{1}H nmr data for D-glucono-1,4-lactone tetraacetate (**9**)

signal irradiated (ppm)	observed change
5.62	5.23 (d ⟶ s)
	4.96 (dd ⟶ d (J = 8.0 Hz))
5.35	4.96 (dd ⟶ d (J = 5.5 Hz))
	4.58 (dd ⟶ d (J = 12.0 Hz))
	4.15 (dd ⟶ d (J = 12.0 Hz))
4.96	5.62 (dd ⟶ d)
	5.35 (ddd ⟶ dd)

(lactone plus four acetates) at 170.3, 169.3, 169.1, 169.0, and 168.7 ppm and acetate methyl groups at 20.6 (2 x C), 20.4, and 20.2 ppm. The optical rotation of the acetate **9** was found to be +59° (c 1.0, acetone), in good agreement with that reported (+60.3° (acetone)).[38] The tetraacetate **9** of synthetic D-glucono-1,4-lactone (**8**) was prepared in the same manner as described for the natural product. The physical and spectral data compare well between the synthetic and natural samples.

D-Glucono-1,4-lactone (**8**) is one of the three most abundant metabolites produced by *T. flavus* in still culture, other than D-mannitol (**1**) and the triglyceride (**5**). It is at least twenty-five times more abundant than any other metabolite isolated from this fungus. D-Glucono-1,4-lactone (**8**) is also found in the aqueous broth of *T. flavus*.

Details of its biological activity and role in the biological control of *V. dahliae* by *T. flavus* are discussed in the second part of this thesis.

One of the first metabolites isolated from *T. flavus* precipitated from the chromatography solvent as long, slender colorless needles, having a melting point 240-241°C. From hrms, the molecular formula of compound **10** is $C_9H_8O_4$ (180). This is confirmed by cims which shows an ion at 198 (M^+ + 18, 100). The ir spectrum displays a broad hydroxyl absorption at 3360 cm^{-1} and a carbonyl band at 1730 cm^{-1}. The uv spectrum displays absorptions at 213, 259, and 306 nm, which shift bathochromically *ca.* 20 nm each on addition of base (232, 278, 328 nm). Neutralization with acid gives back the original spectrum (212, 259, 307 nm), suggesting a phenolic chromophore.[39] The ^1H nmr spectrum of metabolite **10** consists of five singlets. Broad downfield singlets at 8.92 and 8.64 ppm are exchangeable on addition of D_2O and, thus, may be ascribed to the phenolic hydrogens. A one hydrogen aromatic singlet at 6.84 ppm, a two hydrogen singlet at 5.19 ppm, and a three hydrogen aromatic methyl singlet at 2.18 ppm comprise the remainder of the spectrum. The ^{13}C nmr spectrum consists of a carbonyl carbon at 171.6 ppm, phenolic carbons at 158.5 and 151.2 ppm, aromatic carbons at 126.1, 125.2, and 119.3 ppm, an aromatic methine carbon at 102.6 ppm, an oxygenated methylene carbon at 68.5 ppm, and an aromatic methyl quartet carbon at 9.2 ppm. These data, along with the six sites of unsaturation present in this metabolite, suggest a phthalide ring system having two hydroxyl and one methyl substituents.

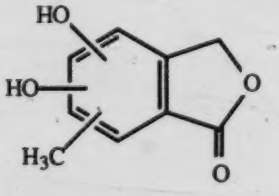

There are twelve possible structures for this system. In an attempt to determine the relative orientation of the substituents on the ring, a nuclear Overhauser enhancement (nOe) experiment was performed. Presaturation of the methyl, methylene, or methine singlets showed no nuclear Overhauser enhancements. In spin decoupling experiments, the half widths ($w_{1/2}$)[40] of each of the singlets failed to show any narrowing. These data are most consistent with the two structures shown below.

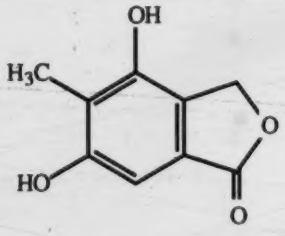

4,6-dihydroxy-5-methylphthalide

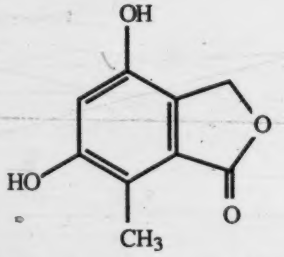

4,6-dihydroxy-7-methylphthalide

The carbons bearing hydrogen atoms are of significant distance apart that no nuclear Overhauser enhancements nor ^{1}H-^{1}H couplings are expected. In addition, the *meta*-arrangement of hydroxyl groups favors a polyketide biogenesis, as expected for this metabolite (**10**). Distinguishing between the two isomers is possible by observation of the long range ^{1}H-^{13}C coupling constants in the ^{13}C nmr spectrum. Table 8 shows these data and how the multiplicities change with irradiation of the different hydrogens. Most worthy of note is the change in the multiplicity of the carbonyl carbon at 171.6 ppm (Figure 10). In the fully coupled spectrum, acquired with gated decoupling, this signal consists of four lines with 2 and 3 Hz coupling constants. Irradiation of the aromatic hydrogen (6.84 ppm) simplifies the signal to a triplet with a 2 Hz coupling constant. This represents the three bond coupling ($^{3}J_{CH}$) of the carbonyl carbon with the two methylene hydrogens (5.19 ppm). With long range ^{1}H-^{13}C coupling constants, it is found that $^{3}J_{CH} > {}^{2}J_{CH} > {}^{4}J_{CH}$.[41,42] From the standpoint of stereochemical effects, it is

Table 8. Coupled ^{1}H-^{13}C ^{13}C nmr data with selective ^{1}H-irradiation for the phthalide metabolite (**10**) (δ (ppm))

		^{1}H-irradiated (ppm)			
δ_C	gated decoupling	6.84	5.19	2.18	5.19 + 2.18
9.2	q (J = 130 Hz)				
68.5	t (J = 155 Hz)				
102.6	d (J = 165 Hz)				
119.3	t (J = 5,7 Hz)	q (J = 6 Hz)	m	d (J = 5.5 Hz)	q (J = 6 Hz)
125.2	s	s	s	s	s
126.1	q (J = 5,6 Hz)	t (J = 3.5,5.5 Hz)	d (J = 6 Hz)	m	t (J = 3,4 Hz)
151.2	m	m	q (J = 3,4 Hz)	s	q (J = 4 Hz)
158.5	m	q (J = 4 Hz)	m	br d (J = 1.5 Hz)	q (J = 4 Hz)
171.6	q (J = 2,3 Hz)	t (J = 2 Hz)	d (J = 3 Hz)	q (J = 2,3 Hz)	s

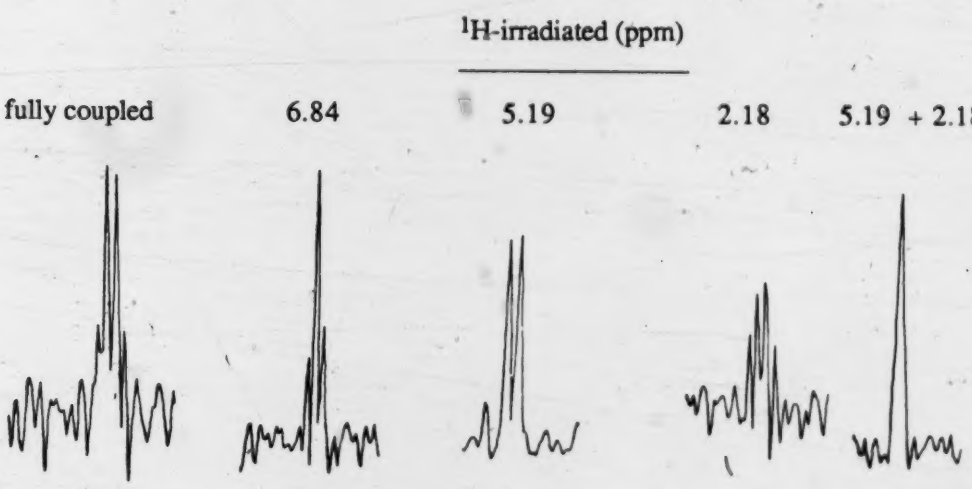

Figure 10. Multiplicity changes in the carbonyl carbon (171.6 ppm) of metabolite **10** with selective ^{1}H-irradiation

found that spin-spin interactions between ^{13}C and ^{1}H nuclei separated by three bonds show much of the character of ^{1}H-^{1}H couplings.[41] When the methylene hydrogens at 5.19 ppm are irradiated, the signal for the carbonyl carbon becomes a doublet. This must arise from the three bond coupling ($^{3}J_{CH}$) of this carbon with the aromatic hydrogen. This observation confirms the structure of metabolite **10** as 4,6-dihydroxy-5-methylphthalide, in which the aromatic hydrogen is *peri-* to the carbonyl. This three bond coupling would not be observed in 4,6-dihydroxy-7-methylphthalide. Furthermore, irradiation of the methyl signal has no effect on the signal multiplicity of the carbonyl carbon and irradiation of the methylene and aromatic hydrogens simultaneously removes all coupling with this carbon, giving a singlet. A further look at the multiplicity changes of the other carbons provides the complete carbon assignment of this metabolite (**10**). Irradiation of the aromatic hydrogen (6.84 ppm) simplifies the phenolic carbon at 158.5 ppm to a quartet (J = 4 Hz) so that this carbon must be the C-6 phenol. The carbon at 119.3 ppm is also simplified to a quartet and is assigned as C-5. Saturation of the methylene hydrogens (5.19 ppm) eliminates their coupling with the C-4 phenolic carbon (151.2 ppm). The signal at 126.1 ppm becomes a doublet (J = 6 Hz), indicative of a three bond coupling ($^{3}J_{CH}$) with the aromatic hydrogen (H-7) and, thus, is assigned as C-3a. The signal at 125.2 ppm shows no coupling and is assigned as C-7a. This lack of long range coupling is also found for this carbon in 3-Q-ethyl-cyclopolic acid.[43]

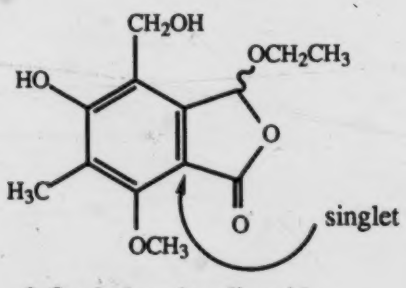

3-Q-ethyl-cyclopolic acid

The ^{13}C nmr assignment for 4,6-dihydroxy-5-methylphthalide (**10**) is shown in Table 9.

Table 9. The ^{13}C nmr assignment of 4,6-dihydroxy-5-methylphthalide (**10**)

	δ_C (ppm, acetone-d_6)
C-1	171.6
C-3	68.5
C-3a	126.1
C-4	151.2
C-5	119.3
C-6	158.5
C-7	102.6
C-7a	125.2
C-5 $\underline{C}H_3$	9.2

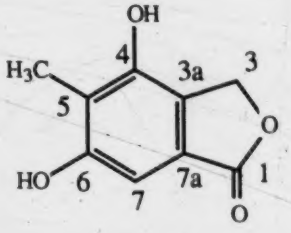

10

In the high resolution mass spectrum (Scheme 3), compound **10** loses an hydrogen atom to give a stable radical ion at m/z 179 and then carbon monoxide to afford the base peak at m/z 151. This is followed by loss of another molecule of carbon monoxide (m/z 123) from one of the phenolic carbons.[44] This is illustrated in Scheme 3. One of the noteworthy features in the ir spectrum of metabolite **10** is the carbonyl absorption at 1730 cm^{-1}. This absorption is at low frequency for a γ-lactone. This is the same

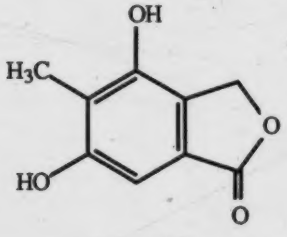

10

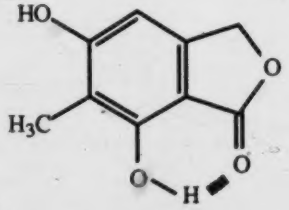

5,7-dihydroxy-6-methylphthalide

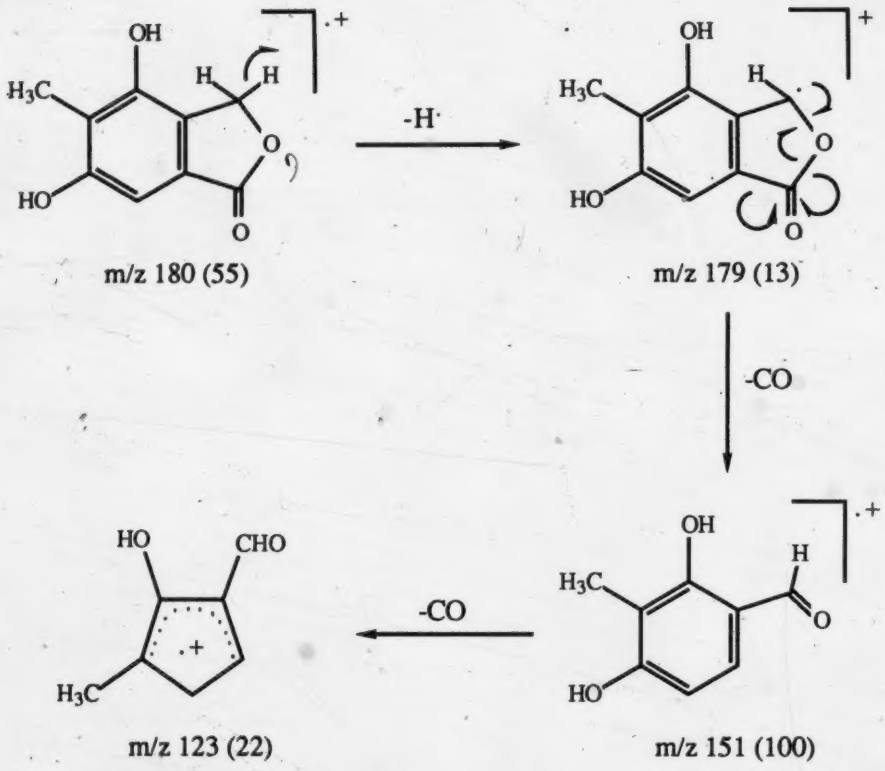

Scheme 3. The mass spectral fragmentation of 4,6-dihydroxy-5-methylphthalide (**10**)

frequency reported[45] for its regioisomer, 5,7-dihydroxy-6-methylphthalide, where intramolecular hydrogen bonding is presumably responsible for the lower frequency absorption. The cause of the shift to lower frequency in metabolite **10** may result from intermolecular hydrogen bonding as the ir spectrum was recorded as an acetone cast.

4,6-Dihydroxy-5-methylphthalide (**10**) is a new natural product. It has been prepared synthetically[45] and our physical and spectral data agree well with a synthetic sample of this phthalide.[46] A number of phthalide metabolites have been isolated from nature, including many isomeric ones, and their biosynthesis is interesting. The second part of the thesis discusses some of these metabolites, in relation to their biosyntheses, along with the results of sodium [1-^{13}C] acetate labelling studies pertaining to the biosynthesis of 4,6-dihydroxy-5-methylphthalide (**10**).

Reaction of 4,6-dihydroxy-5-methylphthalide (**10**) with potassium carbonate and methyl iodide in refluxing acetone for 2.5 hours affords white flakes of compound **11**, melting point 162-162.5°C. This compound lacks an hydroxyl absorption in the ir spectrum; however, it does show a lactone carbonyl at 1765 cm^{-1}. The uv spectrum displays absorptions at 214, 255, and 304 nm, which show no bathochromic shift on addition of base. A molecular ion is seen in the hrms at m/z 208, consistent with the formula $C_{11}H_{12}O_4$. Peaks in the cims at 209 ($M^+ + 1$, 100) and 226 ($M^+ + 18$, 68) confirm this. The base peak in the hrms at m/z 179 corresponds to the loss of an hydrogen atom and carbon monoxide, as for the dihydroxy metabolite **10**. The ^1H nmr spectrum shows methoxy singlets at 3.93 and 3.96 ppm. The carbons of these methyl groups are seen in the ^{13}C nmr spectrum at 56.6 and 59.4 ppm. These data correspond well with those obtained from an authentic sample of 4,6-dimethoxy-5-methylphthalide (**11**)[46] as well as with those reported[47] for the natural product **11**. It has been isolated from *Aspergillus silvaticus* and is given the name Q-methylsilvaticol. The long range ^1H-^{13}C coupling constants in the ^{13}C nmr spectrum of the dimethoxy derivative **11** were studied in the same manner as outlined for the dihydroxy metabolite **10** (Table 10).

Table 10. Coupled ^1H-^{13}C ^{13}C nmr data with selective ^1H-irradiation for 4,6-dimethoxy-5-methylphthalide (**11**)

δ_C (ppm)	^{13}C-^1H fully coupled	irradiate 5.51 (CH_2) ppm
124.8	s	s
126.1	m	q (J = 6 Hz)
128.9	m	d (J = 6 Hz)

Although most of the carbons are readily assigned for the dimethoxy derivative **11** (Table 11), the long range ^1H-^{13}C coupling of three carbons (124.8, 126.1, and 128.9

ppm) was examined to confirm their assignments. The carbon at 124.8 ppm is a singlet and is assigned as C-7a by analogy with C-7a of the dihydroxy metabolite **10**. The carbons at 126.1 and 128.9 ppm are multiplets in the fully coupled spectrum; however, irradiation of the methylene hydrogens (5.51 ppm) simplifies the former to a quartet (J = 6 Hz) and the latter to a doublet (J = 6 Hz). This doublet is characteristic of the multiplicity of C-3a in the dihydroxy metabolite **10** and, thus, the signal at 128.9 ppm is

Table 11. ^{1}H and ^{13}C nmr data for 4,6-dimethoxy-5-methylphthalide (**11**)

	^{1}H (ppm)		^{13}C (ppm)
H-7	7.02 (1H, s)	C-1	171.1
H-3	5.51 (2H, s)	C-3	68.9
OCH_3	3.96 (3H, s)	C-3a	128.9
OCH_3	3.93 (3H, s)	C-4	154.0
C-5 CH_3	2.14 (3H, s)	C-5	126.1
		C-6	160.8
		C-7	100.9
		C-7a	124.8
		C-5 CH_3	9.6
		C-4 OCH_3	59.4
		C-6 OCH_3	56.6

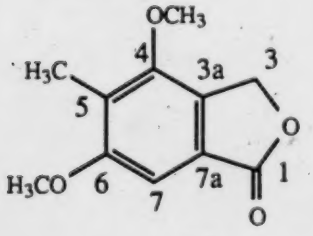

11

that of C-3a. The signal at 126.1 ppm (C-5) shows coupling with the C-5 methyl hydrogens. This ^{13}C nmr assignment differs from that proposed by Achenbach[45] and from that reported[47] for the natural product; but, it is consistent with the change in chemical shifts expected on O-methylation[47] (Table 12). It is found that methylation of a

Table 12. ^{13}C nmr shift differences observed on methylation for compounds **10** and **11**.

	δ_{OH} (ppm) **10**	δ_{OCH_3} (ppm) **11**	$\delta_{OCH_3} - \delta_{OH}$ (ppm)
C-3a	126.1	128.9	+2.8 (*ortho-para*)
C-4	151.2	154.0	+2.8 (*ipso*)
C-5	119.3	126.1	+6.8 (*ortho*)
C-6	158.5	160.8	+2.3 (*ipso*)
C-7	102.6	100.9	-1.7 (*ortho-para*)
C-7a	125.2	124.8	-0.4 (*meta*)

phenolic hydroxyl group gives rise to downfield shifts (from +0.4 to +3.4 ppm; mean +1.8 ppm) for *ipso*- carbons, downfield shifts (from +4.5 to +6.1 ppm; mean +5.2 ppm) for *ortho*- carbons, and, also, downfield shifts (from +3.5 to +5.5 ppm; mean +4.6 ppm) for the *para*- carbons. The *meta*- carbons are not greatly affected by O-methylation. The shift ranges from -0.6 to +0.4 ppm (mean -0.2 ppm). The data in Table 12 agree well with these findings, lending support to the ^{13}C nmr assignments reported.

Another of the lower molecular weight compounds from *T. flavus* is isolated as a yellow oil. The hrms of compound **12** provides the formula $C_6H_6O_3$ (126), which is confirmed by chemical ionization (144, $M^+ + 18$, 100). The loss of an hydrogen atom and carbon monoxide in the mass spectrum to give the base peak at m/z 97, absorption bands at 2840 and 2700 (w) cm^{-1} in the ir spectrum, and a singlet in the ^1H nmr spectrum at 9.58 ppm that does not exchange on addition of D_2O, suggest that compound **12** is an aldehyde. In addition to the aldehyde hydrogen, the ^1H nmr spectrum contains doublets at 7.19 and 6.50 ppm, each with a coupling constant of 3.5 Hz. A two hydrogen singlet is seen at 4.70 ppm and a D_2O exchangeable broad singlet

is found at 1.62 ppm. The uv spectrum displays absorptions at 221 and 281 nm, consistent with that of a furfural.[48] The ^{13}C nmr spectrum consists of a methylene carbon at 57.6 ppm, methine carbons at 110.2, 123.3, and 178.1 ppm, and quaternary carbons at 153.7 and 163.0 ppm. These data suggest the compound 5-hydroxymethyl-furfural (**12**), whose reported[49,50] nmr assignments, shown in Figure 11, agree well with those found for this aldehyde.

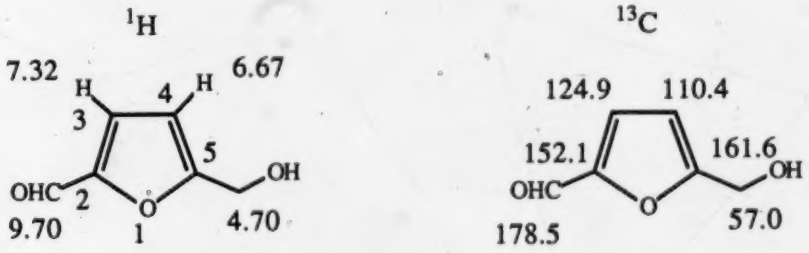

Figure 11. ^{1}H and ^{13}C nmr literature data for 5-hydroxymethylfurfural (**12**)

5-Hydroxymethylfurfural (**12**) is probably an artifact in the broth extract. It is thought to arise from D-glucose as illustrated in Scheme 4.[51] Dehydration of D-glucose leads to the enol shown, which, from its tautomeric 3-deoxyosone form, loses another molecule of water. Cyclization of the alcohol on to the carbonyl carbon generates the five-membered ring, followed by dehydration to afford the furfural **12**. This process is accelerated with heating. When D-glucose was added to the fungal medium after autoclaving, the amount of 5-hydroxymethylfurfural (**12**) found in the broth extract is reduced by *ca.* 90%.

Another metabolite found in the dichloromethane portion of the ethyl acetate broth extract is isolated as white flakes. This solid sublimes at 200°C. From hrms, its molecular formula is $C_{11}H_{10}O_3$ (190), which is confirmed by chemical ionization (191, $M^+ + 1$, 100). This metabolite (**13**) is phenolic as its uv spectrum (241, 249, and 288

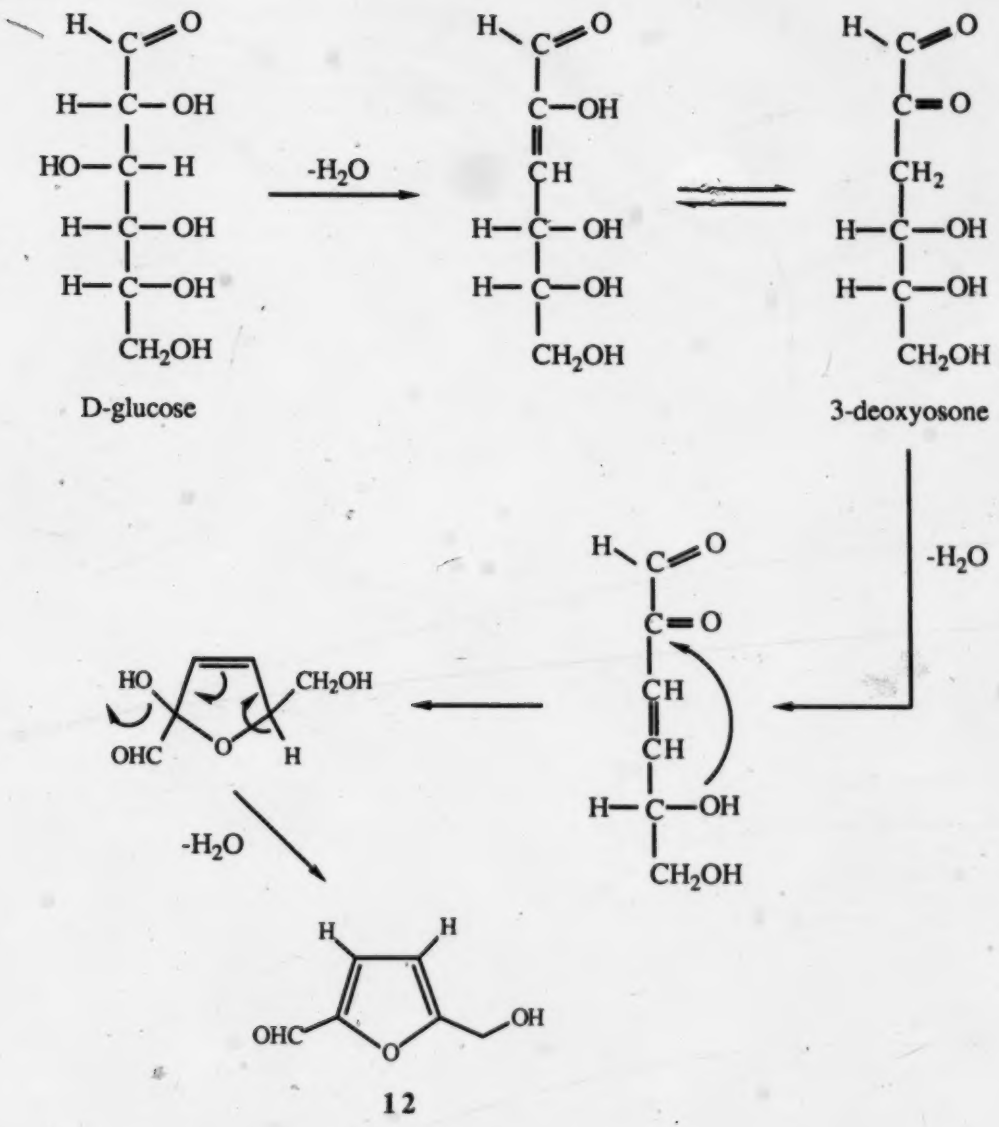

Scheme 4. Formation of 5-hydroxymethylfurfural (**12**) from D-glucose[1]

nm) displays a bathochromic shift on addition of base (254, 325 nm), which reverts to the original spectrum on neutralization with acid (241, 249, 288 nm). The ir spectrum displays a broad hydroxyl absorption at 3400-3000 cm^{-1}, consistent with the phenolic nature of compound **13**. It also shows absorptions at 1649, 1618, and 1557 cm^{-1},

consistent with that of a γ-pyrone.[52] The ^1H nmr spectrum (methanol-d_4) consists of *meta*- related aromatic hydrogens at 6.64 (d, J = 2.5 Hz) and 6.62 (dq, J = 2.5, 1.0 Hz) ppm. This latter hydrogen has been shown by spin decoupling experiments to be coupled to a methyl group at 2.70 (3H, bs) ppm. Irradiation of the aromatic hydrogen causes a sharpening of the methyl signal. This methyl group is shifted downfield *ca.* 0.5 ppm from where an aromatic methyl is expected to resonate, suggesting that it may be *peri*- to a carbonyl group. In addition, a vinylic hydrogen at 6.00 ppm (q, J = 1.0 Hz) has been shown to be coupled to a methyl group at 2.31 ppm (d, J = 1.0 Hz). Furthermore, nuclear Overhauser enhancement studies reveal the enhancements indicated in Table 13.

Table 13. NOe results for metabolite **13**

^1H presaturated (ppm)	nOe enhancement ppm (%)
6.62	2.70 (4)
6.00	2.31 (2)
2.70	6.62 (32)
2.31	6.00 (12)

Two partial structures for this metabolite include a *meta*- substituted aromatic ring and a methyl substituted double bond.

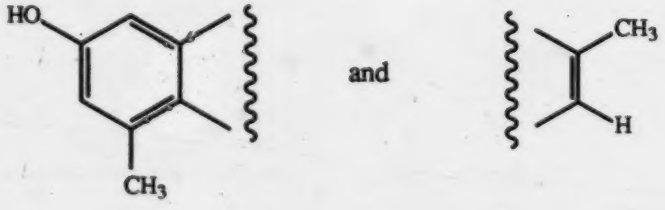

The ^{13}C nmr spectrum shows a signal at 182.0 ppm, consistent with that of a chromone carbonyl. Downfield carbons at 166.6 (s), 163.1 (s), and 161.5 (s) ppm, together with the remaining signals at 143.7 (s), 118.0 (d), 115.7 (s), 111.4 (d), 101.7 (d), 23.0 (q), and 19.8 (q) ppm, suggest the structure 7-hydroxy-2,5-dimethylchromone (**13**).

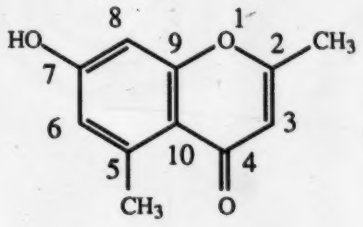

13

Metabolite **13** is known in nature and has been isolated from the roots of *Polygonum cuspidatum*, a plant used in Chinese and Japanese traditional medicine.[53] It has also been isolated from a rhubarb, *Rhei rhizoma*.[54] The physical and spectral data for metabolite **13** are in good agreement with those reported in the literature.[53,54] The ^{1}H and ^{13}C nmr assignments are shown in Figure 12.

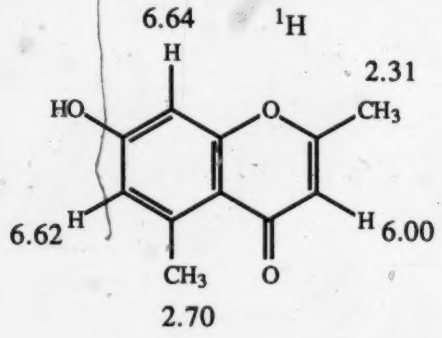

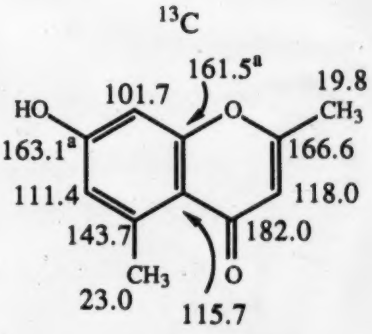

[a]assignments may be interchanged

Figure 12. The ^{1}H and ^{13}C nmr assignments for 7-hydroxy-2,5-dimethylchromone(**13**)

The mass spectral fragmentation is outlined in Scheme 5. The base peak in the mass spectrum of **13** is also the parent ion at m/z 190. This is a common occurrence for chromones as they do not possess sites of facile bond rupture, and this is reflected in the

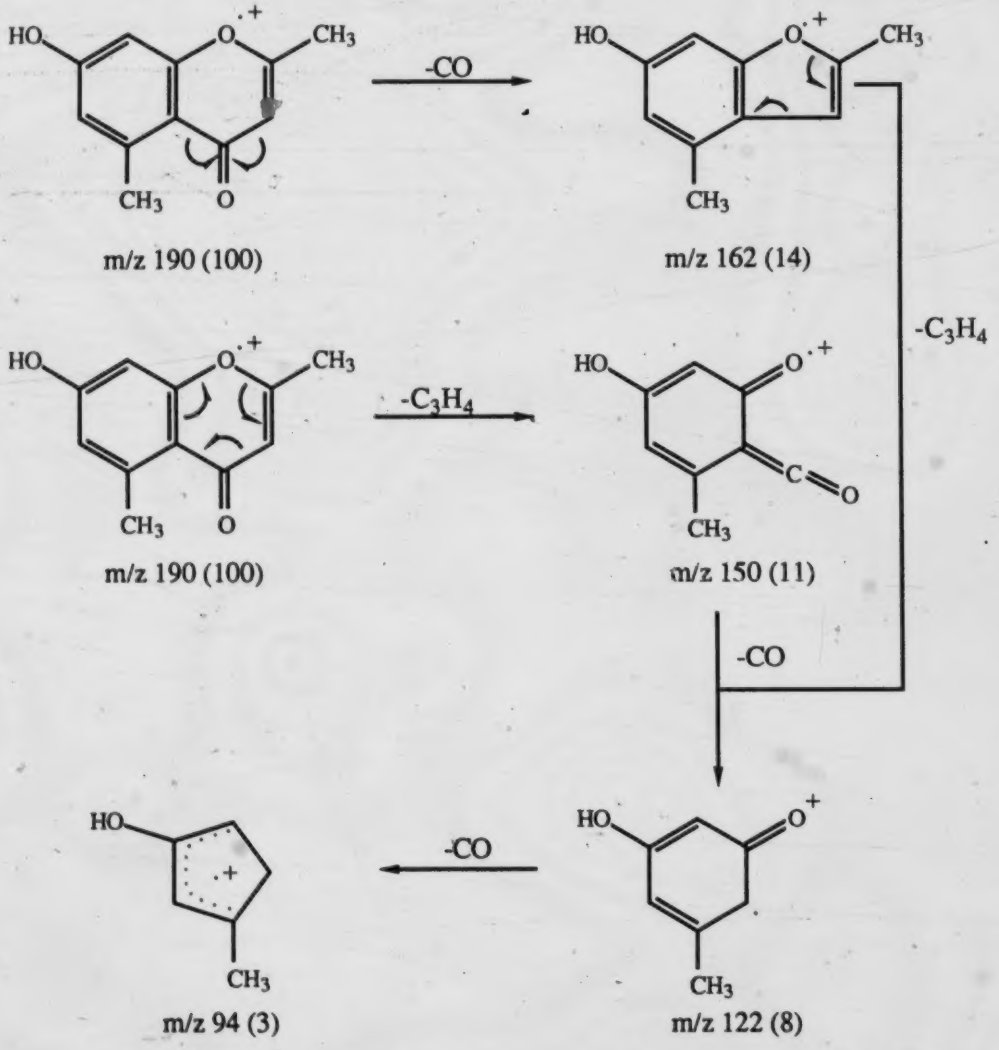

Scheme 5. The mass spectral fragmentation of 7-hydroxy-2,5-dimethylchromone (**13**)

great abundance of the molecular ion. Loss of propyne in a reverse Diels-Alder manner and expulsion of carbon monoxide are common fragmentations of chromones.[55] The

biosynthesis of metabolite **13** is interesting as it does not seem to follow the pattern of most chromones, such as eugenin, which arise from a pentaketide precursor (Scheme 6).

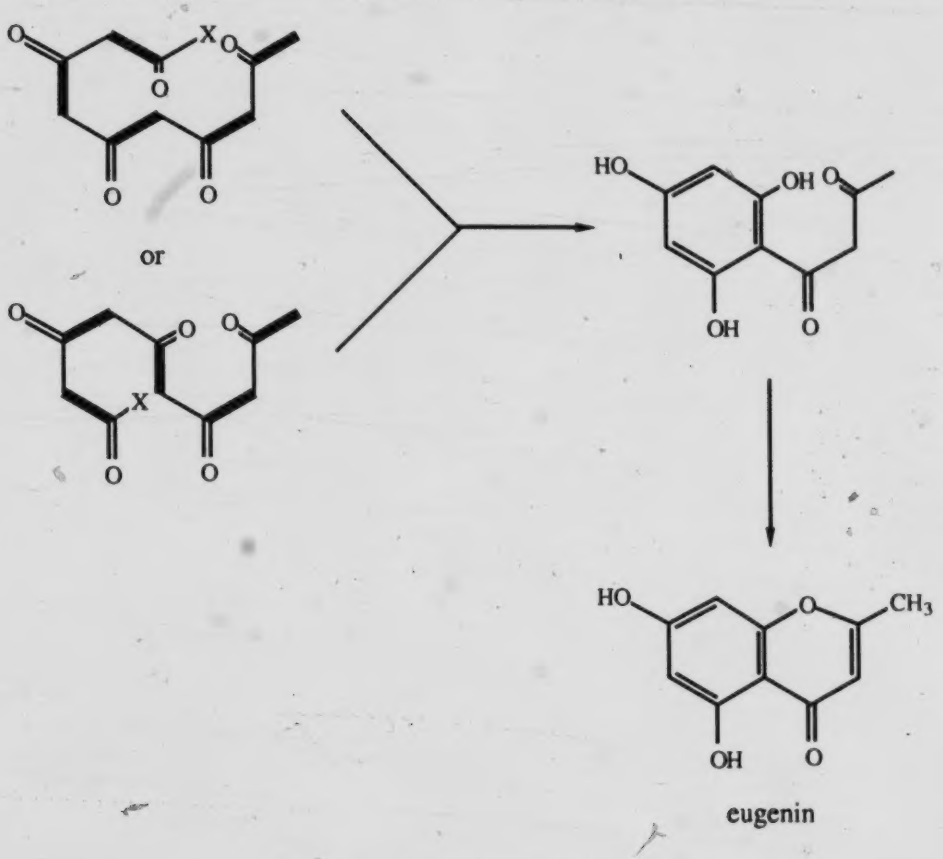

Scheme 6. Biosynthesis of eugenin

The most probable biosynthesis (Scheme 7) of 7-hydroxy-2,5-dimethylchromone (**13**) appears to originate with a hexaketide precursor which cyclizes to form the aromatic ring, followed by hydrolysis of the thioester, and decarboxylation. Ring closure and dehydration afford the natural product **13**. Although the biosynthesis of metabolite **13** has not been studied, it is known to be a degradation product of aloenin, a metabolite found in *Aloe arborescens* var. *natalensis* (Figure 13). The plant is frequently used in folk remedies. Aloenin was found to be biosynthesized *via* the acetate-malonate pathway

by feeding ^{14}C and ^{3}H labelled acetate and measuring the specific activity of the degradation products, one of which is the chromone **13**.[56]

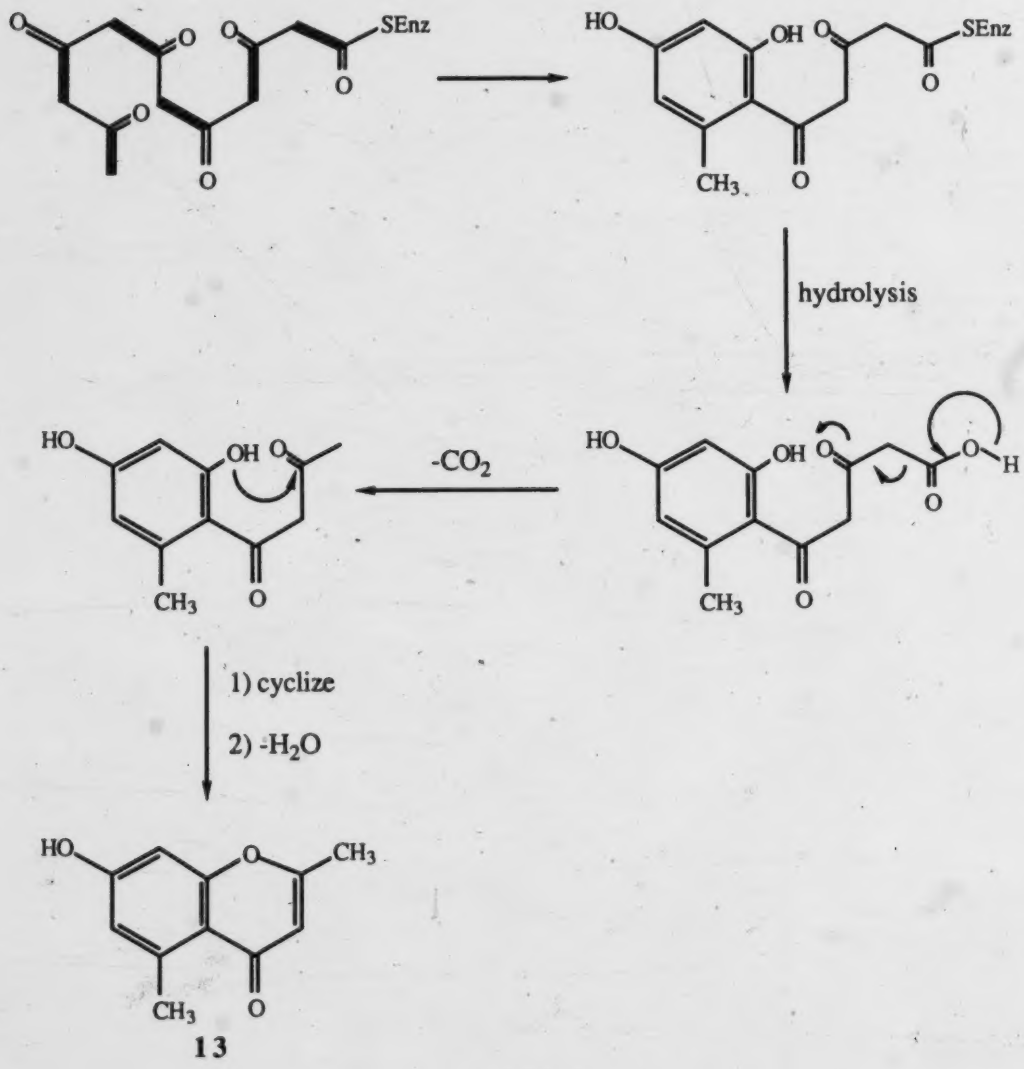

13

Scheme 7. Proposed biosynthesis of 7-hydroxy-2,5-dimethylchromone (**13**)

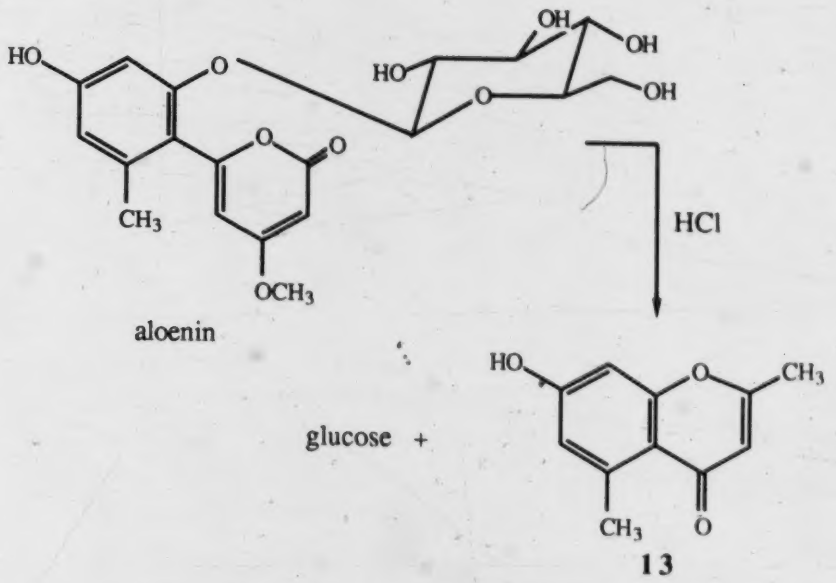

Figure 13. Acid catalyzed degradation of aloenin.

Treatment of 7-hydroxy-2,5-dimethylchromone (**13**) with diazomethane affords a monomethyl ether (**14**) (Figure 14). The ether **14** melts at 115-117°C. Its molecular

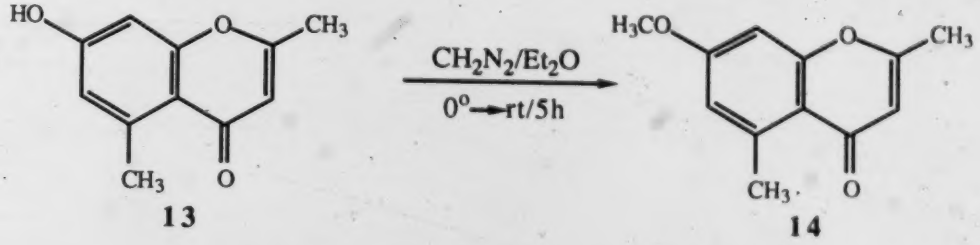

Figure 14. Formation of monomethyl ether **14**.

formula of $C_{12}H_{12}O_3$ (204), obtained from hrms, is consistent with that of the monomethyl ether of **13**. The cims confirms the molecular weight with an ion at 205 ($M^+ + 1$, 100). The ir spectrum shows no hydroxyl absorption and the uv spectrum (248, 280 nm) displays no bathochromic shift on addition of base. The ^1H nmr spectrum of **14** shows a methoxy singlet at 3.86 ppm (3H, s) and the carbon atom resonates at 55.6 ppm. The two aromatic hydrogens appear as a broadened singlet at

6.66 ppm. As observed for the hydroxyl compound **13**, in the mass spectrum of **14** the base peak is also the parent ion at m/z 204. Loss of propyne (m/z 164, 5) and carbon monoxide (m/z 176, 6) are again the major fragmentations observed. The physical and spectral data for compound **14** agree with those reported.[57,58]

The most colorful metabolite isolated from *T. flavus* is a granular yellow solid, compound **15**, which decomposes on melting at 190°C. Its molecular formula, as determined by hrms, is $C_{10}H_8O_6$ (224). This is confirmed by chemical ionization (225, $M^+ + 1$, 100; 242, $M^+ + 18$, 32). The ir spectrum shows a broad hydroxyl absorption from 3560 to 2400 cm^{-1}, a medium intensity band at 1757 cm^{-1}, and strong absorptions at 1655 and 1635 cm^{-1}. The uv spectrum of compound **15** consists of maxima at 225, 293, and a long wavelength absorption at 428 nm. On addition of base, only the 293 nm band shifts bathochromically (229, 305, 426 nm). Neutralization with acid gives back the original spectrum (226, 293, 427 nm). The hrms shows major fragmentation ions at m/z 193 (M^+ - OCH_3, 95), 192 (193 - H, 86), 164 (192 - CO, 100), 136 (164 - CO, 22), and 108 (136 - CO, 13). The ^1H nmr spectrum (acetone-d_6) consists of four singlets (Table 14): a one hydrogen singlet at 10.46 ppm, which does not exchange on addition of D_2O, one hydrogen resonances at 6.79 and 6.45 ppm, and a three hydrogen methoxy group at 3.53 ppm. A ^{13}C nmr signal at 196.6 ppm (d), and the ^1H nmr resonance at 10.46 ppm, together with the loss of an hydrogen atom and carbon monoxide from the ion at m/z 193 in the mass spectrum (m/z 192 and 164), suggest that metabolite **15** possesses an aldehyde functionality. A broad hydroxyl absorption in the ir spectrum and a ^{13}C nmr signal at 169.4 ppm (s) suggest a carboxylic acid moiety. A ^1H nmr absorption at 3.53 ppm and ^{13}C nmr signals at 160.1 (s) and 56.4 ppm (q), together with the loss of a methoxy group (m/z 193) in the high resolution mass spectrum, are consistent with that of a methyl ester. These three functional groups account for three of the seven sites of unsaturation in compound **15**. The other four

Table 14. ^{1}H and ^{13}C nmr data for metabolite **15**

^{1}H (ppm)	^{13}C (ppm)
10.46 (1H, s)	196.6 (d)
6.79 (1H, s)	169.4 (s)
6.45 (1H, s)	166.3 (s)
3.53 (3H, s)	160.1 (s)
	136.8 (s)
	122.7 (s)
	114.6 (s)
	103.9 (d)
	102.4 (d)
	56.4 (q)

sites may be accounted for by a benzene ring. One hydrogen singlets in the ^{1}H nmr spectrum at 6.79 and 6.45 ppm may be hydrogens in a *para*- relationship on the aromatic ring. These account for $C_{10}H_7O_5$ of a molecular formula of $C_{10}H_8O_6$. There remains only an hydroxyl group not accounted for and the ^{13}C nmr signal at 166.3 ppm (s) is reasonable for that of a phenolic carbon. The partial structures shown below may be drawn for metabolite **15**.

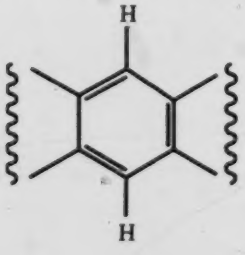

-CHO

-COOH

-$COOCH_3$

-OH

A clue as to the relative orientation of the four substituents on the aromatic ring is found in the reduction of metabolite **15** with sodium borohydride. After the reaction proceeds for fifteen seconds, the bright yellow color of the solution fades and, after ten minutes, the starting material is converted to a more polar compound as seen by tlc. The ir spectrum of the reduction product **16** possesses a broad hydroxyl absorption at 3240 cm^{-1} and a carbonyl band at 1755 cm^{-1}. The aldehyde signal has disappeared from the ^1H nmr spectrum, as well as the ester methoxyl group. These are replaced by a two hydrogen singlet at 5.01 ppm. Since esters are reduced much more slowly than aldehydes in a sodium borohydride reduction,[59] there must be a secondary reaction in which the alkoxide ion formed in the reduction attacks the ester carbonyl and displaces the methoxy group (Figure 15).

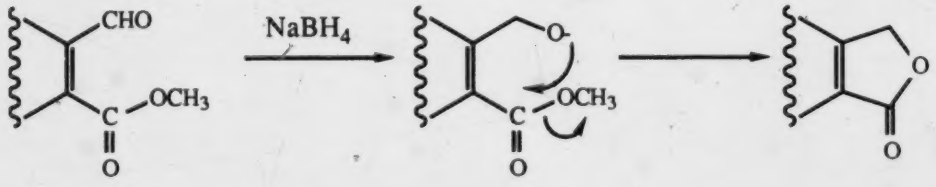

Figure 15. Reduction of metabolite **15**

This has been observed in the sodium borohydride reduction of 3,5-dihydroxy-4-methylphthalaldehydic acid methyl ester[60] (Figure 16). This compound is the methyl

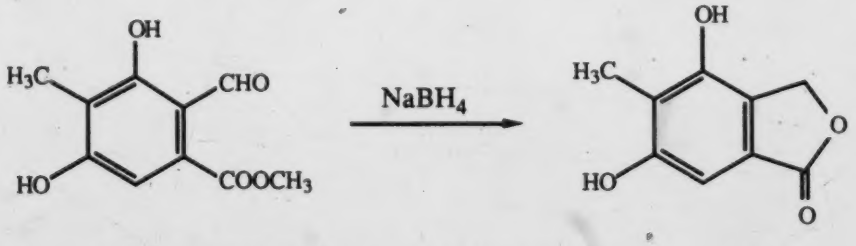

3,5-dihydroxy-4-methylphthalaldehydic acid methyl ester **10**

Figure 16. Reduction of 3,5-dihydroxy-4-methylphthalaldehydic acid methyl ester

ester derivative of 3,5-dihydroxy-4-methylphthalaldehydic acid, a natural product isolated from a *Penicillium* species. Reduction of the ester is reported to afford metabolite **10**, 4,6-dihydroxy-5-methylphthalide. This suggests that metabolite **15** may be a derivative of a precursor to the natural product **10**. The presence of a γ-lactone ring in compound **16** is supported by the carbonyl band at 1755 cm^{-1} in the ir spectrum and by the two hydrogen singlet at 5.01 ppm in the ^1H nmr spectrum. With this result from the reduction reaction, the aldehyde and ester groups must be *ortho-* to one another on the aromatic ring, narrowing the proposed structures of metabolite **15** to two. Both structures are consistent with the nOe results. Presaturation of the methoxy singlet at 3.53 ppm results in an enhancement of 7% in the signal at 6.45 ppm. The methyl signal is enhanced 2% when this aromatic hydrogen is irradiated. The mass spectral fragmentation pattern is also consistent with both structures (Scheme 8). Loss of the methoxy group from the methyl ester affords the acylium ion at m/z 193. Loss of an hydrogen atom from the aldehyde gives the peak at m/z 192 and expulsion of the ester

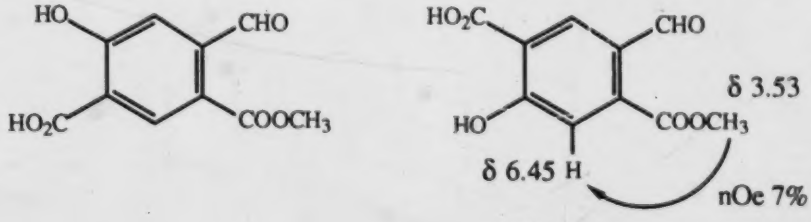

4-carboxy-5-hydroxyphthalaldehydic acid methyl ester (**15**)

carbonyl as carbon monoxide provides the base peak at m/z 164. Further loss of the aldehyde carbonyl as carbon monoxide (m/z 136) and expulsion of the phenolic carbon as carbon monoxide gives the fragment ion at m/z 108. Table 15 shows the calculated[61] and observed ^{13}C nmr shifts for metabolite **15**. The differences in observed *versus* calculated shifts for three carbons (C-2, C-3, and C-6) are significant; however, it has

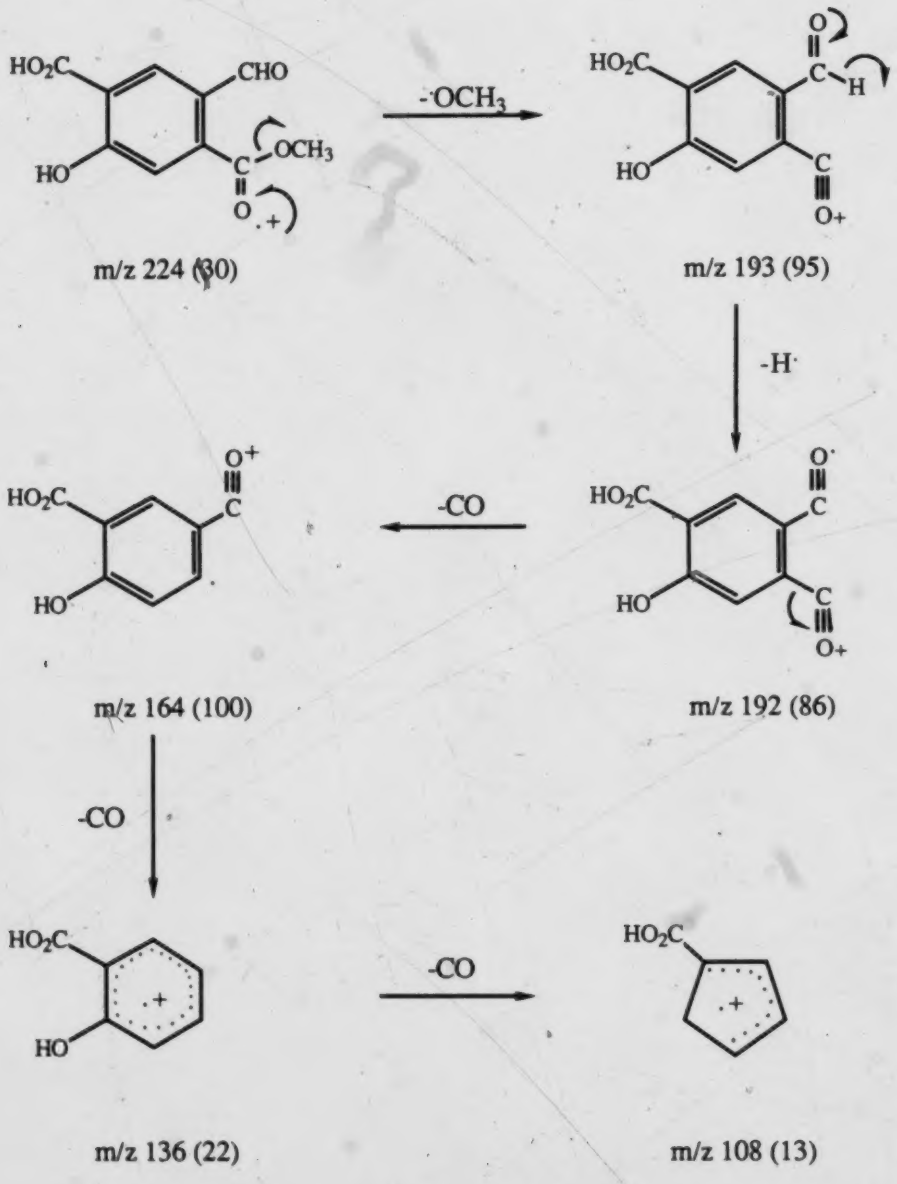

Scheme 8. The mass spectral fragmentation of metabolite **15**

been difficult to obtain more data for metabolite **15** as it is somewhat unstable. It seems to oxidize readily to the acid as the ^{1}H nmr spectrum of compound **15** a few weeks after its isolation shows that the three singlets are doubled and the intensity of the aldehyde

Table 15. Calculated and observed ^{13}C nmr shifts for 4-carboxy-5-hydroxyphthalaldehydic acid methyl ester (**15**)

	observed (ppm)	calculated[61] (ppm)
C-1	136.8	138.4
C-2	114.6	130.9
C-3	103.9	132.8
C-4	122.7	123.0
C-5	166.3	162.5
C-6	102.4	117.5

signal is greatly reduced. In addition, metabolite **15** appears to decompose readily as polar baseline material is observed in tlc shortly after its isolation. Attempts to make the acetate or to methylate compound **15** have failed. These difficulties, together with the paucity in which metabolite **15** is produced, have made the structure elucidation of this metabolite troublesome. From results of feeding [1-^{13}C] labelled sodium acetate to the fungus, the most probable structure of metabolite **15** is 4-carboxy-5-hydroxyphthalaldehydic acid methyl ester. The results of this labelling study, along with a proposed biosynthesis of metabolite **15**, are discussed in the second part of this thesis.

Another of the metabolites isolated from *T. flavus* in small amount has a molecular formula of $C_{12}H_{12}O_5$ (236), as determined by hrms. Chemical ionization confirms the molecular weight with ions at 237 ($M^+ + 1$, 100) and 254 ($M^+ + 18$, 84). The ir spectrum shows an hydroxyl absorption at 3360 cm^{-1}, carbonyl bands at 1760 (sh) and 1711 cm^{-1}, and double bond absorptions at 1657 and 1592 cm^{-1}. The uv spectrum displays maxima at 256 and 286 nm, which do not shift on addition of base, suggesting that the hydroxyl group in this metabolite (**17**) is not phenolic. The ^1H nmr

spectrum ($CDCl_3$-CD_3OD 1:1) shows *meta*- related aromatic hydrogens at 6.65 (d, J = 2.6 Hz) and 6.48 (d, J = 2.6 Hz) ppm. A triplet (1H, J = 1.4 Hz) at 7.70 ppm is coupled to a doublet at 4.55 ppm (2H, J = 1.4 Hz). Methoxy groups resonate at 3.90 and 3.81 ppm (each 3H, s). These data suggest two partial structures, one aromatic ring having *meta*- related methoxy groups, and the other an hydroxymethyl substituted double

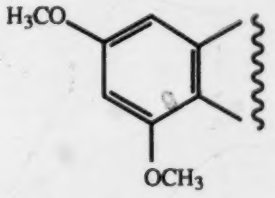

and

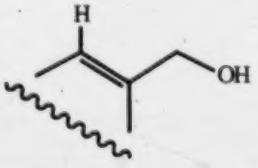

bond. The downfield hydrogen at 7.70 ppm is consistent with that of a coumarin hydrogen on the β-carbon of the double bond.[62] The ir absorptions at 1711, 1657, and 1592 cm^{-1} also support the coumarin skeleton.[52] Two possible structures for metabolite **17** are 3-hydroxymethyl-5,7-dimethoxycoumarin and 3-hydroxymethyl-6,8-dimethoxy-coumarin. Although ^{13}C nmr would allow the two metabolites to be easily distinguished,

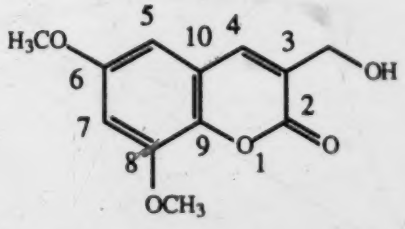

3-hydroxymethyl-6,8-dimethoxycoumarin

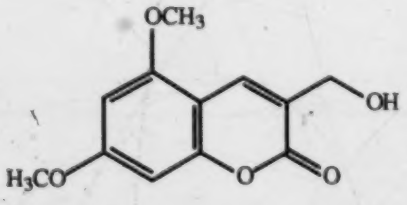

3-hydroxymethyl-5,7-dimethoxycoumarin

compound **17** was never isolated in quantities large enough to acquire the twelve carbon signals. The signals that are observed are consistent with both structures: (55.8 and 56.3 ppm (2 x OCH_3), 61.3 ppm (CH_2OH), 101.2 and 103.0 ppm (aromatic methines), 128.6 ppm (s), 138.7 ppm (vinylic methine), and 148.1 ppm (s)). The mass spectrum of coumarin **17** shows few fragment ions (Scheme 9). This metabolite, like the

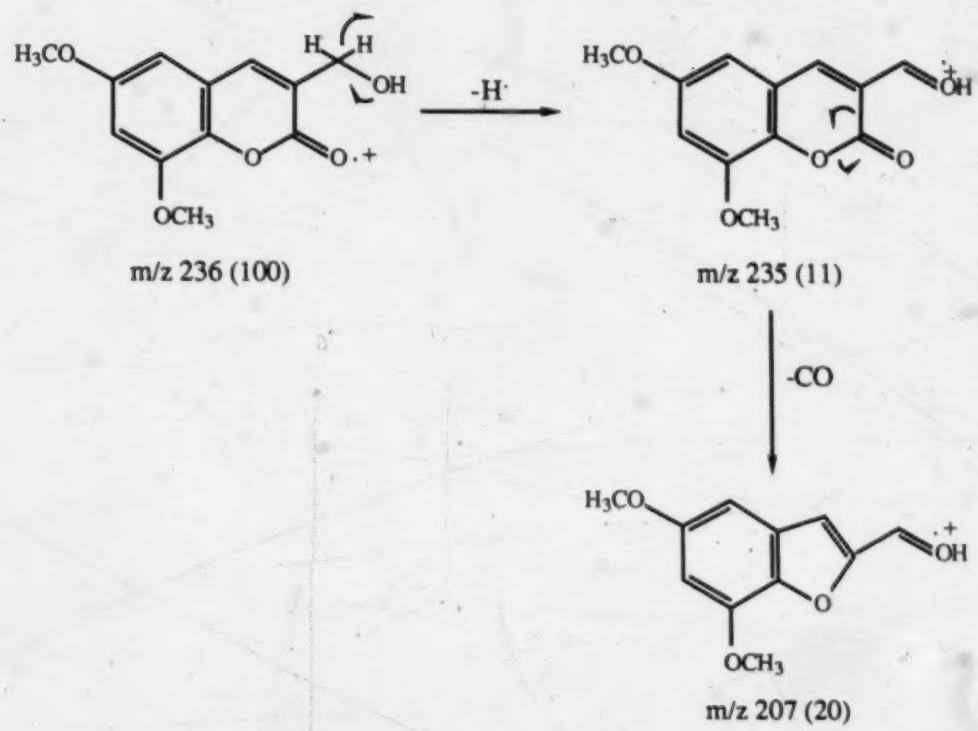

Scheme 9. The mass spectral fragmentation of metabolite **17**

chromone **13**, lacks sites of facile bond rupture. The parent ion of coumarin **17** at m/z 236 is also the base peak. Loss of one of the methylene hydrogens of the primary alcohol affords the stable radical ion at m/z 235. Loss of the lactone carbonyl as carbon monoxide, a common extrusion fragment of coumarins,[63] provides the substituted benzofuran fragment at m/z 207. NOe experimental results are summarized in Table 16. Of greatest significance is the nOe to the aromatic hydrogen at 6.48 ppm when the vinylic hydrogen at 7.70 ppm is presaturated, and *vice versa*, suggesting that these two hydrogens are *peri-* to one another. The unusual observation is that the methoxy group at 3.81 ppm shows a nOe to only one aromatic hydrogen at 6.48 ppm and not to the one at 6.65 ppm, although the *meta-* orientation of hydrogens is strongly supported by their

Table 16. Nuclear Overhauser enhancement results for metabolite **17**

presaturate (ppm)	nOe enhancement (ppm, %)
7.70	6.48
6.65	3.90
6.48	7.70, 3.81
4.55	7.70
3.90	6.65 (35%)
3.81	6.48 (18%)

coupling constant of 2.6 Hz. On the basis of the data available, the most reasonable structure for metabolite **17** is 3-hydroxymethyl-6,8-dimethoxycoumarin. It has not been reported in the literature, either synthetically or from nature.

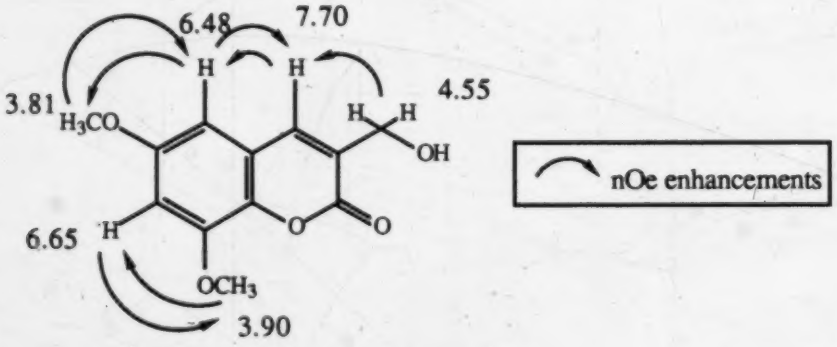

3-hydroxymethyl-6,8-dimethoxycoumarin (**17**)

A number of higher order polyketides arising from cyclization of a heptaketide precursor have been isolated from *T. flavus*. The first of these metabolites crystallizes from the solvent as white flakes, having a melting point 194-196°C. Its hrms gives the molecular formula $C_{15}H_{14}O_6$ (290). The peak of highest m/z in the cims is at 247, which may be accounted for by the facile loss of carbon dioxide ($M^+ - CO_2 + 1$, 93).

This metabolite (**18**) shows a broad hydroxyl absorption in the ir spectrum from 3600 to 2800 cm^{-1}, characteristic of a carboxylic acid. A weak band is seen at 1645 cm^{-1} and a more intense one at 1610 cm^{-1}. The ^1H nmr spectrum ($CDCl_3$-CD_3OD 1:1) shows aromatic singlet hydrogens at 6.47 and 6.40 ppm and *meta*- related aromatic hydrogens at 6.27 and 6.04 ppm (each a doublet, J = 2.6 Hz). A methoxy signal is seen at 3.65 ppm (3H, s) and an aromatic methyl group at 1.77 ppm (3H, s). These account for ten of the fourteen hydrogens in the molecule; thus, there are four exchangeable hydrogens. Having two *para*- and two *meta*- related aromatic hydrogens suggests that there are two benzene rings in the molecule. The melting point, ^1H nmr, and ir data reported[64] for a known metabolite, altenusin, whose structure is shown below, are similar to these data.

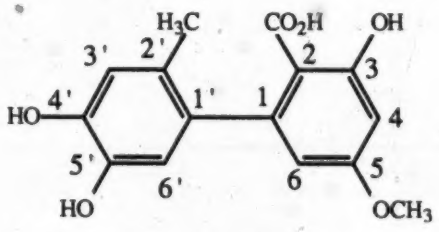

altenusin

Table 17 shows that the ^{13}C nmr data for metabolite **18** compare well with the values calculated for altenusin using the empirical parameters for the calculation of chemical shifts in substituted benzenes.[61] Altenusin (**18**) was first reported from *Alternaria tenuis* in 1957;[65] however, a structure for the metabolite was not proposed until 1970.[64] It has since been isolated from *A. kikuchiana* and is used as a herbicide.[66] The mass spectral fragmentation is explained in Scheme 10. Loss of water from the parent ion (m/z 290) *via* the six membered transition state shown with half arrows affords the resonance stabilized ion at m/z 272, which loses carbon monoxide to give the peak at m/z 244. The base peak in the mass spectrum at m/z 246 arises from the loss of the carboxylic acid functionality as carbon dioxide. The methyl group at 1.77 ppm is at higher field than

Table 17. Calculated[61] *versus* observed ^{13}C nmr chemical shifts for altenusin (δ(ppm))

	found for metabolite **18**	calculated for altenusin
$\underline{C}H_3$	18.5	
$O\underline{C}H_3$	55.0	
C-4	99.5	100.3
C-2	105.9	109.2
C-6	110.1	105.8
C-3'	115.2[a]	116.2
C-6'	115.9[a]	118.4
C-2'	126.6	130.9
C-1'	133.9	136.4
C-5'	141.3[b]	140.2
C-4'	143.0[b]	142.7
C-1	146.2	145.4
C-3	163.1[c]	158.3
C-5	164.1[c]	166.4
$\underline{C}O_2H$	172.8	

a, b, c, - assignments may be interchanged

expected for an aromatic methyl group. The favored conformation of this biphenyl metabolite (**18**) is probably a twisted one. In this case, the methyl group is shielded, resulting from the diamagnetic anisotropy[67] of the other benzene ring.

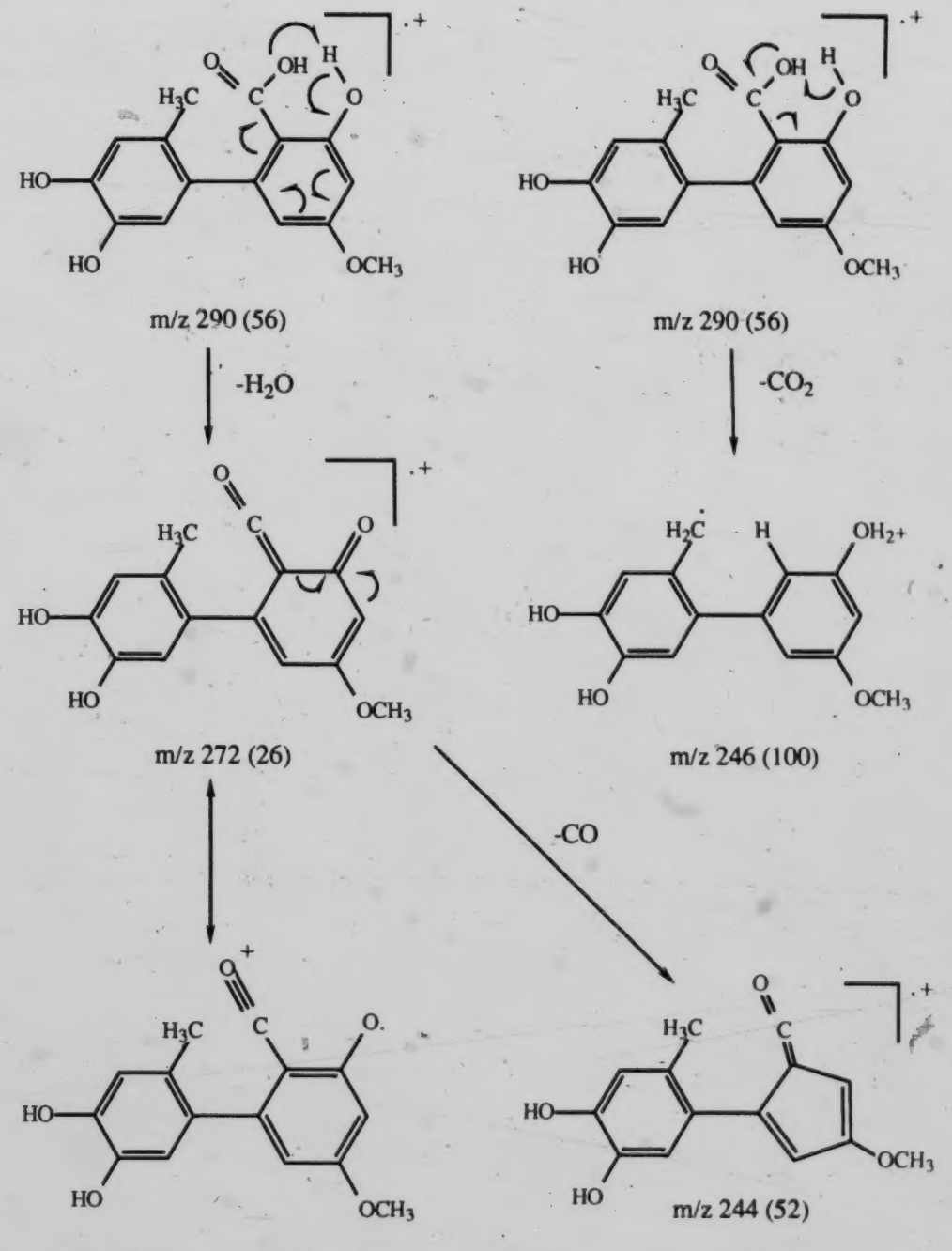

Scheme 10. The mass spectral fragmentation of altenusin (**18**)

Two metabolites closely related to altenusin (**18**) have been obtained from the fungus. These metabolites were isolated as their acetates since they were difficult to purify as the free alcohols. The ^1H nmr spectrum of a reasonably pure sample of the first of these alcohols (compound **19**) provided a clue as to its identity. A strongly hydrogen bonded hydroxyl hydrogen resonates at 11.30 ppm. *Meta*- coupled aromatic hydrogens at 6.73 and 6.63 ppm (each a doublet, J = 2.3 Hz) and a methoxy signal at 3.91 ppm suggest that an aromatic ring similar to that in altenusin (**18**) is present in metabolite **19**. The remaining signals consist of downfield singlets at 6.69 and 6.28 ppm and a methyl singlet at 1.73 ppm. These data agree well with those reported in an article which describes the crystal structure of (±)-dehydroaltenusin.[68] The structure of

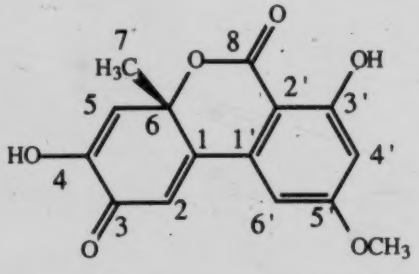

dehydroaltenusin (**19**)

dehydroaltenusin was initially misassigned and it was reported that the triacetate shown below had been formed.[64]

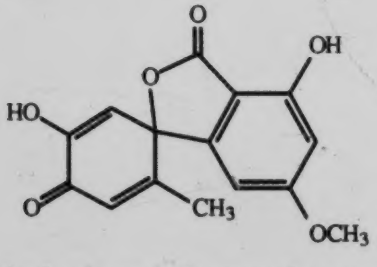

dehydroaltenusin (proposed structure)

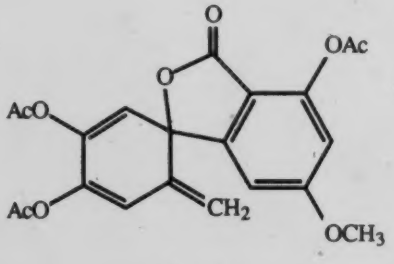

triacetate

In our hands, acetylation of dehydroaltenusin (**19**) affords a diacetate, the properties of which are consistent with the structure **20**. The melting point agrees with that reported.[64] The molecular formula of diacetate **20** is $C_{19}H_{16}O_8$ as determined from its hrms and confirmed by chemical ionization (390, $M^+ + 18$, 100). The ir spectrum shows no hydroxyl absorption but carbonyl bands for aromatic (1776 cm^{-1}) and aliphatic (1732 cm^{-1}) acetates are seen. Absorptions at 1688 and 1664 cm^{-1} are consistent with those expected for the unsaturated ketone moiety.[69] The ^1H nmr spectrum shows *meta*-coupled aromatic hydrogens at 6.77 and 6.60 ppm (each a doublet, J = 1.9 Hz) and a methoxyl group at 3.86 ppm, consistent with the aromatic ring found in dehydroaltenusin (**19**) and altenusin (**18**). A one hydrogen singlet resonates at 6.36 ppm. The diacetate **20** reveals a coupling of 1.4 Hz between the vinylic hydrogen at 6.30 ppm and the methyl group at 1.73 ppm. In the alcohol **19** no four bond coupling is seen. This vinylic hydrogen has also been shifted upfield 0.4 ppm on acetylation. An aromatic acetoxyl methyl at 2.42 ppm and an aliphatic methyl at 2.29 ppm complete the spectrum. The mass spectral fragmentation pattern of **20** (Scheme 11) resembles that of its biogenetic biphenyl precursor, altenusin (**18**), in that it shows the loss of water, carbon monoxide, and carbon dioxide, although in a different fashion. Loss of the two acetate moieties as ketene occurs first to give the fragment ions at m/z 330 and 288. This latter ion corresponds to the molecular weight (288) and molecular formula ($C_{15}H_{12}O_6$) of dehydroaltenusin (**19**) itself. Loss of water and carbon monoxide are possible from one resonance form of the parent ion to give fragment ions at m/z 270 and 260, respectively. Elimination of carbon monoxide from the ion at m/z 260 gives the ion at m/z 232. Loss of carbon dioxide from the other resonance form at m/z 288 affords the m/z 244 ion. NOe experiments show a 22% enhancement of the vinylic hydrogen signal at 6.30 ppm when the methyl group at 1.73 ppm is presaturated. A small enhancement of the methyl signal is seen when the vinylic hydrogen is presaturated. Presaturation of

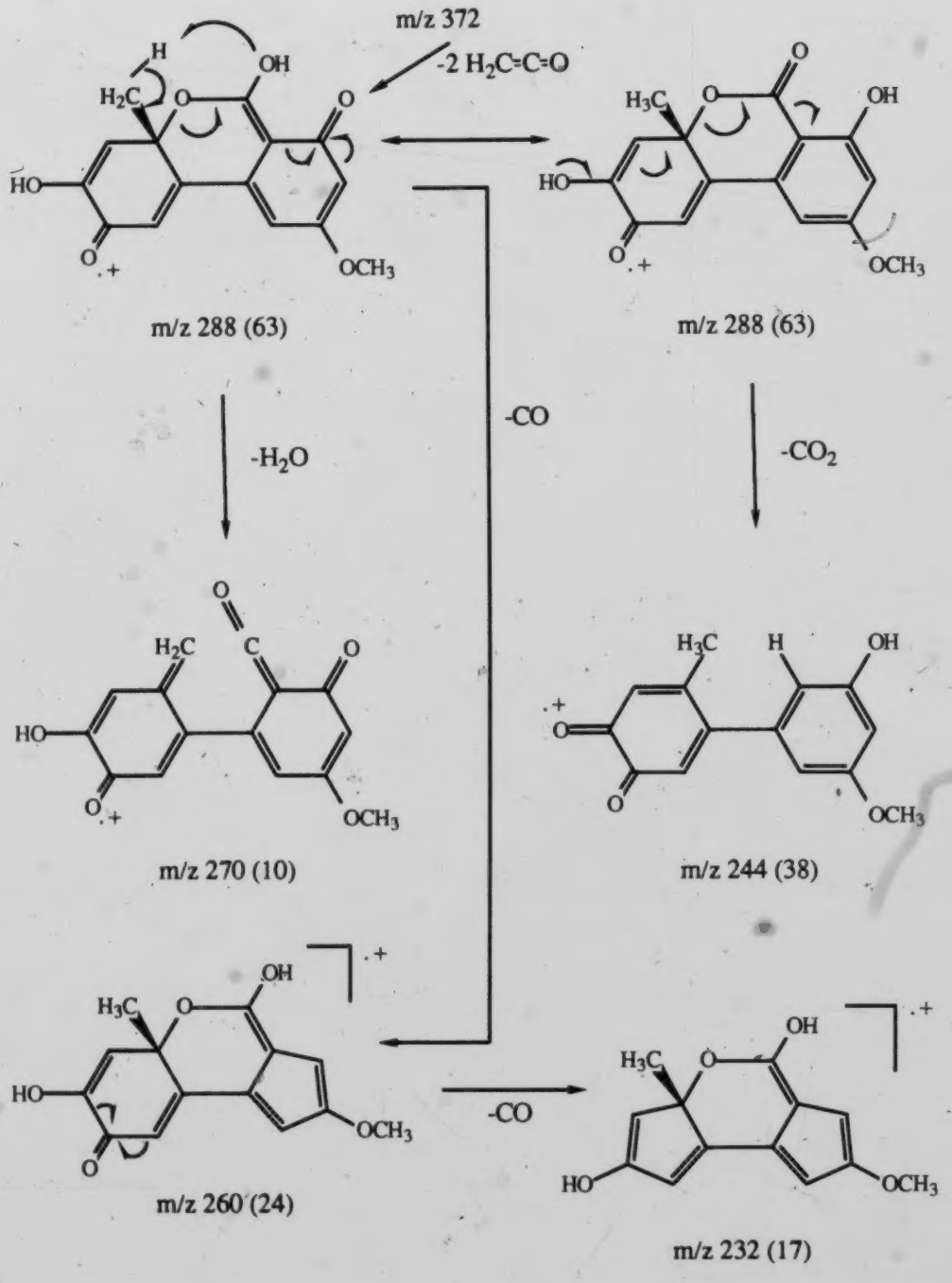

Scheme 11. The mass spectral fragmentation of dehydroaltenusin diacetate (**20**)

the methoxy group at 3.86 ppm results in a 24% enhancement of the signal at 6.77 ppm and a 17% enhancement of the signal at 6.60 ppm. Presaturation of this latter aromatic hydrogen shows enhancement, not only of the methoxy signal, but also of the vinylic hydrogen at 6.36 ppm. These data are summarized in Figure 17. Dehydroaltenusin (**19**), like altenusin (**18**), has been isolated from *Alternaria tenuis* and *A. kikuchiana*.[66]

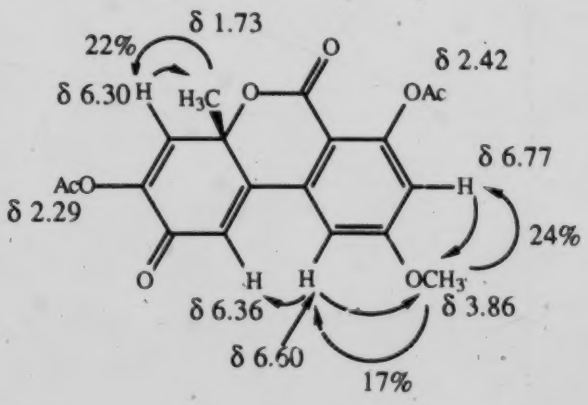

Figure 17. Nuclear Overhauser enhancement results for dehydroaltenusin diacetate (**20**)

Due to the small amount of this metabolite isolated, no attempt was made to determine if compound **19** was optically active or racemic. Our requests for a comparison sample have not been answered.

The second metabolite (**21**) isolated as its acetate (**22**) is structurally very closely related to dehydroaltenusin (**19**). It is a triacetate as evidenced by the sequential loss of three molecules of ketene from the parent ion in the mass spectrum (m/z 400 ($C_{20}H_{16}O_9$, 3), 358 (100), 316 (63), and 274 (89)). This latter ion corresponds to a molecular formula of $C_{14}H_{10}O_6$, differing from dehydroaltenusin (**19**) by a methylene (CH_2) unit. The ^1H nmr spectrum of the triacetate **22** is very similar to that of dehydroaltenusin diacetate (**20**). *Meta*- coupled aromatic hydrogens are seen at 7.10 and 6.97 ppm (each a doublet, J = 1.7 Hz) and a four bond coupling of 1.5 Hz is found between the vinylic

hydrogen at 6.31 ppm and the methyl signal at 1.74 ppm. A one hydrogen singlet resonates at 6.37 ppm. Acetyl methyl signals are seen at 2.43, 2.31, and 2.29 ppm. The methoxy signal present in the ^1H nmr spectrum of the diacetate **20** is absent in the triacetate **22**. Since the molecular formula of the triacetate **22** is a methylene unit less than that of the diacetate **20**, it is reasonable that this metabolite (**21**) is desmethyldehydroaltenusin. The molecular weight and formula of the triacetate **22** (400,

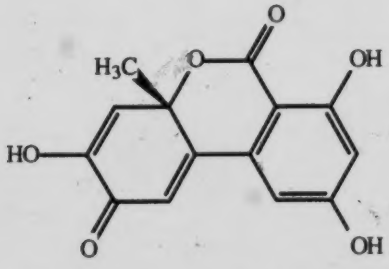

desmethyldehydroaltenusin (**21**)

$C_{20}H_{16}O_9$), as determined by hrms, is confirmed by chemical ionization, which shows an ion at 418 (M^+ + 18, 100). The ir spectrum shows an intense and rather broad absorption at 1777 cm^{-1} for the aromatic acetate carbonyls and much less intense absorption bands at 1680, 1660, and 1610 cm^{-1}. The chemical shifts of the ^1H nmr signals closely match with those found for the diacetate **20**. The only significant difference is that the shifts of the aromatic hydrogens in the triacetate **22** are *ca.* 0.35 ppm further downfield than in the diacetate **20**, as would be expected for substitution of acetoxy for methoxy. Desmethyldehydroaltenusin triacetate (**22**) fragments, after loss of the three acetate units as ketene, in the same manner as dehydroaltenusin diacetate (**20**). The fragment ions are consistently found fourteen mass units lower (Scheme 12). As for dehydroaltenusin (**19**), no attempt was made to measure the optical rotation of this metabolite (**21**).

Formation of the two known metabolites, altenusin (**18**) and dehydroaltenusin (**19**), and the previously unreported desmethyldehydroaltenusin (**21**), may be envisaged as proceeding by cyclization of a heptaketide precursor to give the biphenyl derivative shown in Scheme 13. An oxidation and reduction sequence, and methylation of the phenol indicated, afford the biphenyl metabolite altenusin (**18**). Its δ-lactone derivative, dehydroaltenusin (**19**), forms by oxidative cyclization of **18**. The chemical interconversion of these two metabolites, **18** and **19**, has been achieved:[64,66] oxidation of **18** to **19** with ferric chloride and reduction of **19** to **18** with sodium dithionate. Desmethyldehydroaltenusin (**21**) may be formed by the same oxidation-reduction sequence of the biphenyl intermediate where the phenol is not methylated.

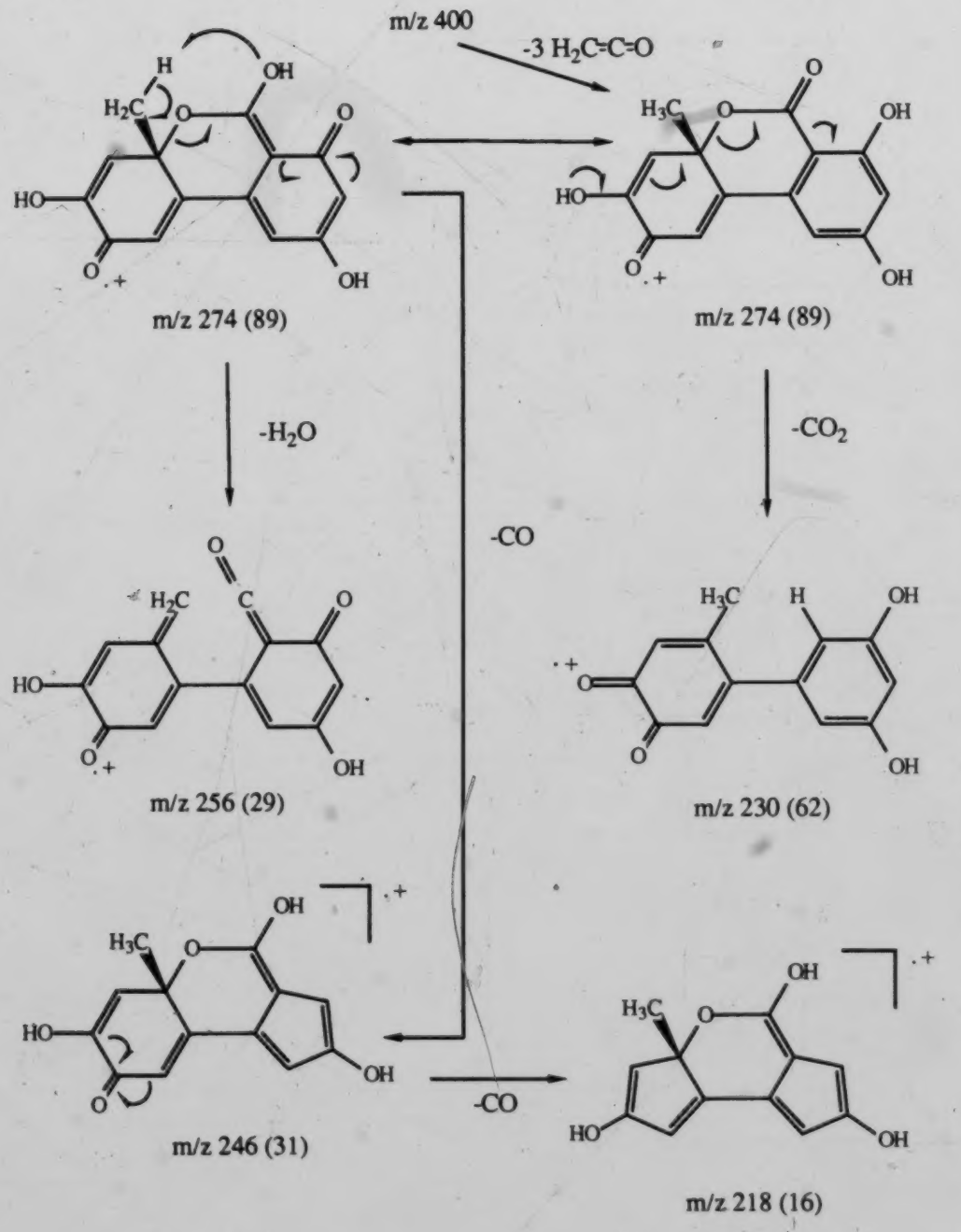

Scheme 12. Mass spectral fragmentation of desmethyldehydroaltenusin triacetate (**22**)

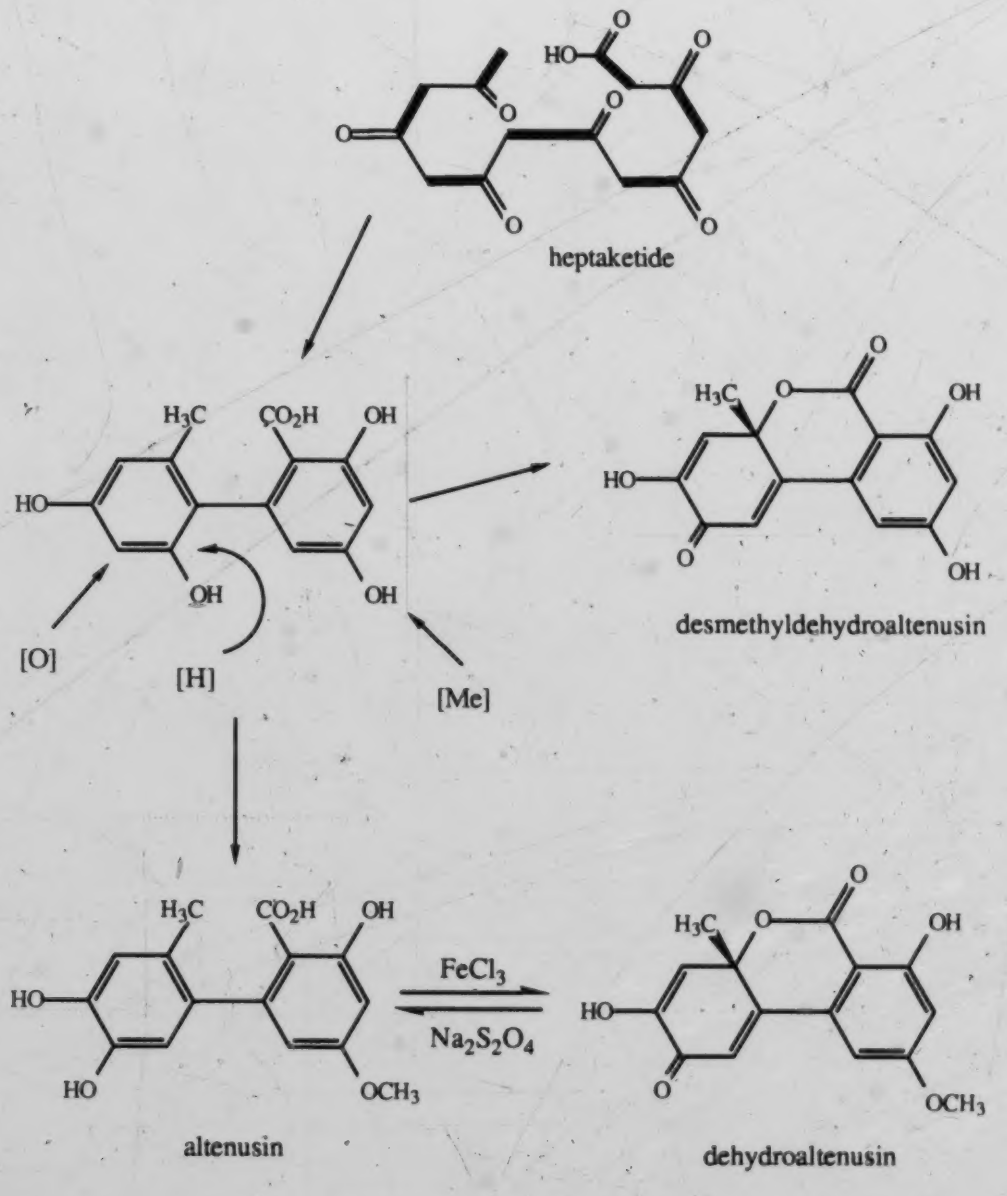

Scheme 13. Biosynthetic pathway to altenusin (**18**), dehydroaltenusin (**19**), and desmethyldehydroaltenusin (**21**)

Another structurally and biosynthetically interesting metabolite isolated from *T. flavus* seems to arise from the same heptaketide biphenyl intermediate. This white solid (compound **23**) decomposes on melting at 230°C. Its molecular formula is $C_{14}H_{12}O_6$ (276), as determined by hrms. Its cims shows ions at 277 ($M^+ + 1$, 44) and 294 ($M^+ + 18$, 76), which confirm the molecular weight. The ir spectrum displays a broad hydroxyl absorption at 3240 cm^{-1}, carbonyl bands at 1748 and 1723 cm^{-1}, and a double bond absorption at 1617 cm^{-1}. The uv spectrum shows absorptions at 217, 257, and 296 nm, which shift bathochromically on addition of base (228, 256, and 325 nm). Neutralization with acid gives back the original spectrum (216, 257, and 295 nm), suggesting a phenolic chromophore.[39] The ^1H nmr spectrum (methanol-d_4) shows *meta*- related aromatic hydrogens at 6.44 and 6.05 ppm (each a doublet, J = 2.0 Hz), both of which show a nuclear Overhauser enhancement of 6% and 8%, respectively, when the methoxy signal at 3.80 ppm is irradiated. This evidence of a *meta*- substituted aromatic ring resembles the data for this partial structure in the three metabolites (**18**, **19**, and **21**) previously discussed. The carbinolic hydrogen of a secondary alcohol is seen at 4.74 ppm and an allylic coupling, as well as a 6% nOe, is observed between the methyl signal at 1.86 ppm and the vinylic hydrogen at 6.34 ppm. These ^1H nmr data are summarized in Table 18. The ^{13}C nmr data are shown in Table 19. These data lead to the three partial structures shown below. These structures account for eleven of the

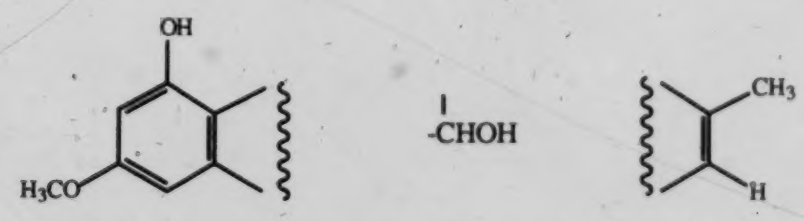

fourteen carbons, all of the hydrogens, and three of the six oxygen atoms of metabolite **23**, as well as five of the nine sites of unsaturation. Four more sites of unsaturation

Table 18. The ^1H nmr data and nOe results for metabolite **23**

^1H (ppm)		
6.44 (1H, d, J = 2.0 Hz)	←	6%
6.34 (1H, q, J = 1.5 Hz)	←	6%
6.05 (1H, d, J = 2.0 Hz)	←	8%
4.74 (1H, s)		
3.80 (3H, s)	—	nOe
1.86 (3H, d, J = 1.5 Hz)	—	nOe

need to be accounted for. Considering the number of downfield carbon signals (Table 19), one or more of them should be attributable to carbonyl groups and the remaining sites of unsaturation to the rings formed by joining these partial structures. The longer wavelength absorption bands (257 and 296 nm) in the uv spectrum suggest that there is a carbonyl group attached to the aromatic ring. The uv spectrum of metabolite **23** corresponds to that reported for the methoxyphthalide shown below.[70] A comparison of

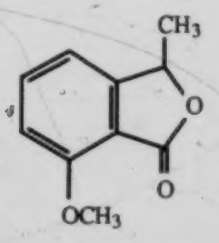

λ_{max} 247, 290 nm

the ^{13}C nmr data for the benzene ring of 4,6-dihydroxy-5-methylphthalide (**10**), its regioisomer, 5,7-dihydroxy-6-methylphthalide,[45] and metabolite **23** are shown in Table 20. The chemical shifts of the carbons at the ring junctions (C-3a and C-7a) change considerably, depending on whether the carbonyl group is *peri*- to the aromatic hydrogen or *peri*- to the hydroxyl group. When the carbonyl is *peri*- to the hydrogen, the chemical

Table 19. ^{13}C nmr data for metabolite **23**

δ (ppm, multiplicity)
202.0 (s)
171.4 (s)
170.2 (s)
168.5 (s)
159.9 (s)
150.8 (s)
131.4 (d)
106.5 (s)
103.5 (d)
101.0 (d)
94.2 (s)
79.7 (d)
56.5 (q)
13.4 (q)

shifts of these two carbons are similar (125.2 and 126.1 ppm), as in metabolite **10**; however, when the carbonyl moiety is *peri*- to the hydroxyl substituent, the carbons shift further apart (103.8 and 147.4 ppm), as in 5,7-dihydroxy-6-methylphthalide. The ^{13}C nmr data for the aromatic portion of metabolite **23** agrees well with the latter phthalide, a regioisomer of that isolated from *T. flavus* (metabolite **10**). A five-membered ring α,β-unsaturated ketone with a methyl substituent on the β-carbon of the double bond is suggested by the uv absorption at 217 nm.[71] Signals in the ^{13}C nmr spectrum at 202.0,

Table 20. The ^{13}C nmr chemical shifts of the aromatic portion of 4,6-dihydroxy-5-methylphthalide (**10**), 5,7-dihydroxy-6-methyl-phthalide, and metabolite **23**

	^{13}C chemical shift (ppm)		
	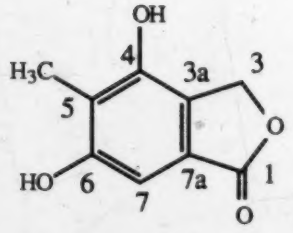	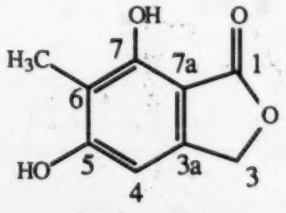	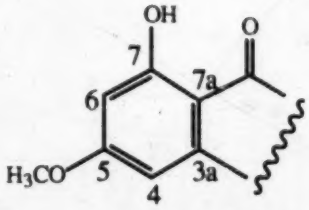
	10	5,7-dihydroxy-6-methylphthalide	**23**
	(acetone-d_6)	(acetone-d_6)	(methanol-d_4)
C-3a	126.1	147.4	150.8
C-4	151.2	101.4	103.5
C-5	119.3	164.0	168.5
C-6	158.5	not reported	101.0
C-7	102.6	156.2	159.9
C-7a	125.2	103.8	106.5

171.4, and 131.4 ppm[72] and ^1H nmr signals at 1.86 ppm, for the methyl group, and 6.34 ppm for the vinylic hydrogen,[62] are consistent with a β-methyl substituent on the double bond. This partial structure accounts for two of the three remaining unsaturation sites. A carbon signal at 170.2 ppm may be ascribed to the carbonyl bonded to the aromatic ring if this is an ester carbonyl. This then accounts for all six oxygen atoms of metabolite **23**. All that remains to be accounted for is one quaternary carbon atom at 94.2 ppm. A third ring joining the aromatic and enone portions of metabolite **23** and

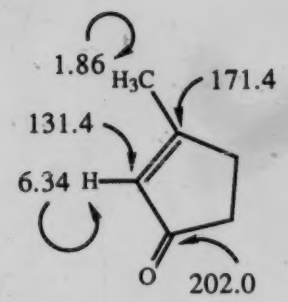

incorporating this quaternary carbon fulfills the final site of unsaturation required. These data lead to the structurally interesting spiro metabolite **23**, which we have named talaroflavone. This structure is consistent with the ir absorptions at 1748 (γ-lactone),[29]

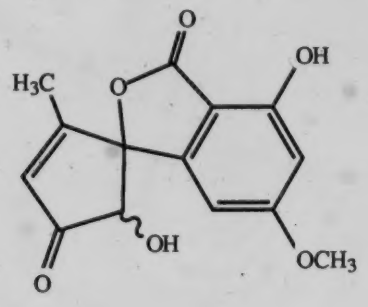

talaroflavone (**23**)

1723, and 1617 (α,β-unsaturated cyclopentenone) cm^{-1}.[73] The ^{13}C nmr assignments are summarized in Table 21. The parent ion (m/z 276 (100)) in the mass spectrum of talaroflavone (**23**) is also the base peak, suggesting that the molecule does not contain sites of facile bond rupture. Fragment ions arise from the loss of water and three molecules of carbon monoxide (from the phenol, the ester carbonyl, and the ketone). Talaroflavone (**23**) is optically active, $[\alpha]_D = +181^o$ (c 0.74, methanol). Attempting to discern the stereochemistry at the spiro center (C-3) and of the C-5' hydroxyl of talaroflavone (**23**) has proved troublesome; however, data obtained from the diacetate

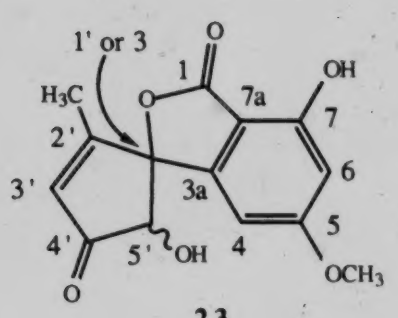

23

Table 21. ^{13}C nmr assignment of talaroflavone (**23**)

	chemical shift (ppm, multiplicity)
C-1	170.2[a] (s)
C-3 (C-1')	94.2 (s)
C-3a	150.8 (s)
C-4	103.5[b] (d)
C-5	168.5[a] (s)
C-6	101.0[b] (d)
C-7	159.9 (s)
C-7a	106.5 (s)
C-2'	171.4[a] (s)
C-3'	131.4 (d)
C-4'	202.0 (s)
C-5'	79.7 (d)
$\underline{C}H_3$	13.4 (q)
$O\underline{C}H_3$	56.5 (q)

a,b - assignments may be interchanged

(**24**) of this spiro metabolite **23** have provided answers for the latter. The diacetate **24** has a molecular formula of $C_{18}H_{16}O_8$ (360), as determined by hrms. Loss of each acetate as ketene affords the ions at m/z 318 (100) and 276 (97). The ir spectrum shows no hydroxyl absorption; however, there is a carbonyl absorption at 1777 cm^{-1} (aromatic acetoxyl) and 1732 cm^{-1} (acetoxyl and cyclopentenone), together with a double bond absorption at 1621 cm^{-1}. The ^1H nmr spectrum shows aromatic hydrogens at 6.93 and 6.61 ppm, downfield *ca.* 0.5 ppm from their resonances in the dihydroxy form. This is consistent with the acetylation of an *ortho-* or *para-* phenolic hydroxyl.[74] One aromatic acetate methyl group is seen at 2.35 ppm and one aliphatic acetate methyl at 1.82 ppm, upfield from its expected position by *ca.* 0.3 ppm.[75] The hydrogen at 4.74 ppm in the alcohol **23** is shifted downfield 1.07 ppm on acetylation to 5.81 ppm, consistent with that expected for acetylation of a secondary alcohol.[37] The ^{13}C nmr spectrum of **24** shows two new signals for acetate carbonyl carbons in the region 165-170 ppm and methyl carbons at 20.4 and 19.8 ppm. The ketone carbonyl is shifted upfield from 202.0 to 197.1 ppm, suggesting the loss of hydrogen bonding. The ^{13}C nmr assignments for the alcohol **23** and the acetate **24** are summarized in Table 22. The changes in chemical shift of the aromatic carbons of **23** on acetylation are shown in Table 22 and are consistent with those expected.[76] It is found that the signal due to the carbon bearing the hydroxyl group shifts upfield -6.6 to -15.6 ppm on acetylation. In talaroflavone (**23**), C-7 shifts upfield -10.4 ppm. The signals for the *ortho-* and *para-* carbon atoms are found to shift downfield +4.1 to +12.1 ppm and +2.0 to +7.9 ppm, respectively. The *ortho-* carbons of **23**, C-6 and C-7a, shift to lower field +11.1 and +5.9 ppm, respectively, while the *para-* carbon, C-4, is found downfield +3.2 ppm. The *meta-* carbon signals are only shifted slightly on acetylation (+0.9 ppm to -4.3 ppm), as C-3a shifts downfield +0.7 ppm and C-5 shifts upfield -1.3 ppm in the acetate **24**.

Table 22. ^{13}C nmr chemical shifts of talaroflavone (**23**) and talaroflavone diacetate (**24**) (ppm)

	talaroflavone (**23**)	talaroflavone diacetate (**24**)	$\delta_{OAc} - \delta_{OH}$
C-1	170.2[a] (s)	168.1[c] (s)	
C-3 (C-1')	94.2 (s)	92.7 (s)	
C-3a	150.8 (s)	151.5 (s)	+0.7 (*meta*)
C-4	103.5[b] (d)	106.7[d] (d)	+3.2 (*para*)
C-5	168.5[a] (s)	167.2[c] (s)	-1.3 (*meta*)
C-6	101.0[b] (d)	112.1[d] (d)	+11.1 (*ortho*)
C-7	159.9 (s)	149.5 (s)	-10.4 (*ipso*)
C-7a	106.5 (s)	112.4 (s)	+5.9 (*ortho*)
C-2'	171.4[a] (s)	172.0[c] (s)	
C-3'	131.4 (d)	133.2 (d)	
C-4'	202.0 (s)	197.1 (s)	
C-5'	79.7 (d)	78.1 (d)	
C-2' $\underline{C}H_3$	13.4 (q)	13.3 (q)	
$O\underline{C}H_3$	56.5 (q)	57.2 (q)	
C-7 OAc	-	170.8[c] (s), 20.4 (q)	
C-5' OAc	-	170.0[c] (s), 19.8 (q)	

a, b, c, d - assignments may be interchanged

The upfield shift of the aliphatic methyl acetate in the ^1H nmr spectrum of **24** provides a clue as to the stereochemistry at C-5'. If the configuration at this center is as shown on the left, then, in the acetate **24**, the aliphatic methyl group lies inside the shielding cone

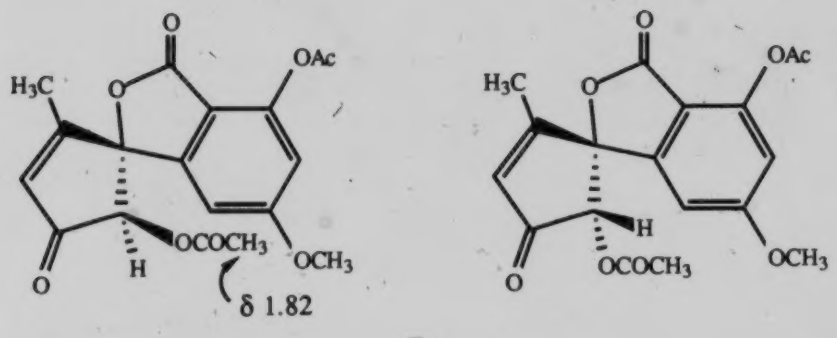

of the benzene ring. In the diastereoisomer having the opposite configuration, the acetate methyl lies well away from the aromatic ring and should exhibit a more characteristic chemical shift (*ca.* 2.1 ppm). This notable upfield shift of the C-5' acetate methyl group, ascribed to the diamagnetic anisotropy of the benzene ring,[67] leads to the proposal that the configuration at C-5' of talaroflavone (**23**) is as shown on the left. The optical rotary dispersion (ord) spectrum of the acetate **24** is a positive plain curve and the circular dichroic (cd) spectrum shows a positive Cotton effect. Attempts to crystallize talaroflavone diacetate (**24**) failed to give crystals suitable for X-ray analysis. The *mono*- and *di-p*-nitrobenzoates (**25** and **26**, respectively) of talaroflavone (**23**) were prepared (see Experimental section); however, very poor yields were obtained in both cases, presumably due to the bulkiness of the substituents. Only 0.8 mg (13%) of talaroflavone *mono-p*-nitrobenzoate (**25**) and 0.5 mg (5%) of talaroflavone *di-p*-nitrobenzoate (**26**) were obtained, from which suitable crystals could not be obtained. Talaroflavone (**23**) is structurally similar to griseofulvin, a commercially important antifungal antibiotic isolated

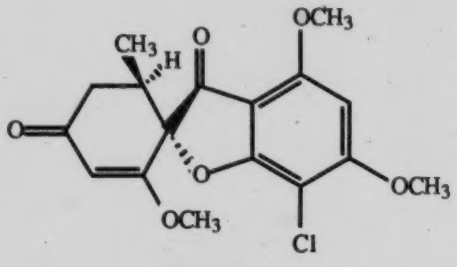

griseofulvin

from *Penicillium griseofulvum*.[77,78] It would be interesting to test talaroflavone (**23**) to see if it displays biological activity in this regard.

The biosynthesis of the spiro metabolite (**23**) is interesting. Results of labelling studies on talaroflavone (**23**), feeding [1-^{13}C] labelled sodium acetate to *T. flavus*, and a discussion of the biosynthetic pathway leading to this metabolite (**23**), are presented in the second part of this thesis.

A metabolite believed to be closely related to talaroflavone (**23**), whose melting point is 178-180°C, has a molecular formula of $C_{14}H_{12}O_5$ (260), as determined from its hrms. This is confirmed by chemical ionization (261 (M^+ + 1, 17); 278 (M^+ + 18, 100)). The ir spectrum shows an hydroxyl absorption from 3400 to 2800 cm^{-1}, together with bands at 1713, 1679, 1610, and 1565 cm^{-1}. The ^{1}H nmr spectrum shows a downfield hydroxyl hydrogen at 11.35 ppm, *meta*- related aromatic hydrogens at 6.70 and 6.69 ppm (each a doublet, J = 2.3 Hz), and a methoxy group at 3.94 ppm (3H, s). These ^{1}H nmr data resemble that found for the aromatic portion of talaroflavone (**23**) and the other heptaketide metabolites (**18**, **19**, and **21**). Compound **27**, however, shows an

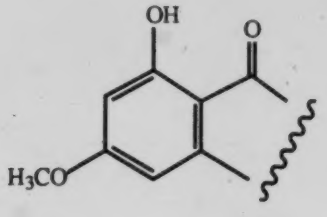

additional saturated spin system, outlined in Figure 18. An hydrogen resonating at 3.43 ppm is coupled to a methyl group at 1.46 ppm (d, J = 6.9 Hz) and to two methylene hydrogens (2.95 ppm (dd, J = 6.6, 19.0 Hz) and 2.31 ppm (dd, J = 1.3, 19.0 Hz)). These methylene hydrogens show a -19.0 Hz coupling constant between one another.

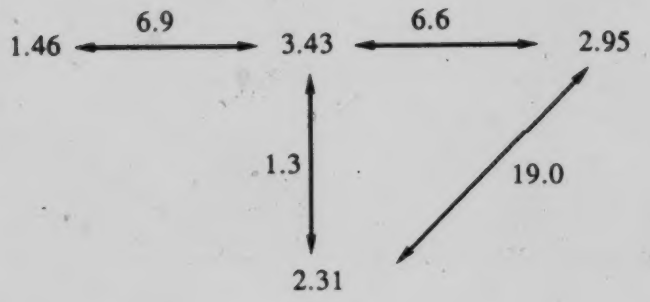

Figure 18. The ^{1}H-^{1}H couplings of metabolite **27**

The two partial structures shown below may be drawn from these data. These account

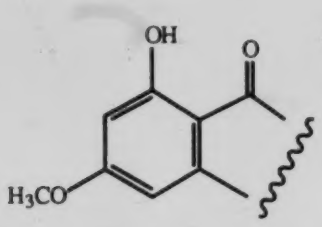

and

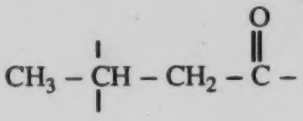

for $C_{12}H_{12}O_4$ of the molecular formula of $C_{14}H_{12}O_5$ and six of the nine sites of unsaturation in metabolite **27**. The saturated chain of metabolite **27** may arise by reduction of the cyclopentenone ring of talaroflavone (**23**). Only eight of the fourteen

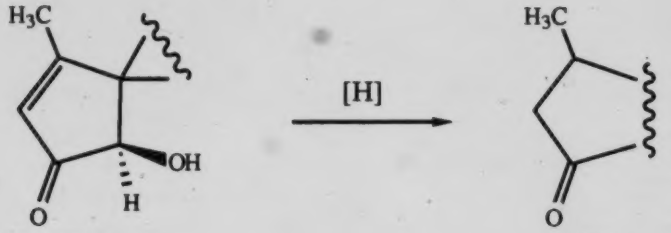

23 **27**

carbons of metabolite **27** are visible in the ^{13}C nmr spectrum, due to the small amount of material available. These carbons resonate at 21.1 (q), 28.4 (d), 42.9 (t), 56.1 (q), 103.1 (d), 103.3 (d), 115.3 (s), and 134.6 (s) ppm. The protonated carbon assignments are shown below. A structure consistent with these data is one we have named deoxy-

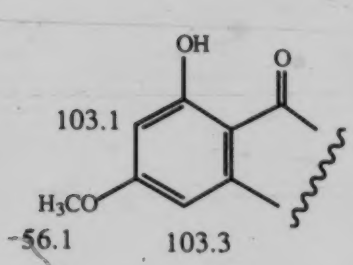

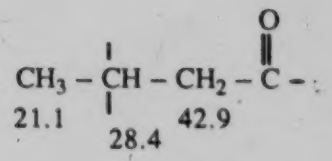

talaroflavone (**27**). The ir bands at 1713, 1679, 1610, and 1565 cm^{-1} are consistent with those expected for the α-pyrone and α,β-unsaturated ketone moieties.[79]

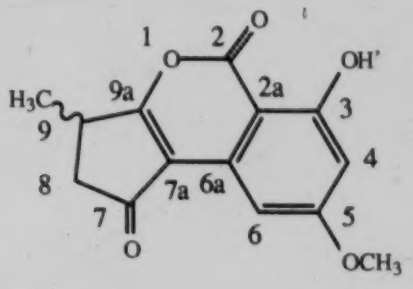

deoxytalaroflavone **27**

The mass spectral fragmentation pattern is outlined in Scheme 14. Metabolite **27** loses two molecules of carbon monoxide and one methyl group by three different pathways to give the fragment ion at m/z 189. Further loss of carbon monoxide affords the ion at m/z 161. Loss of the methyl group may occur from the methoxy ether, followed by loss of carbon monoxide,[80] or from the methyl group at C-9. Expulsion of the α-pyrone carbonyl and the ketone carbonyl as carbon monoxide account for the other two molecules of carbon monoxide lost. If the methyl group at C-9 is lost (rather than that from the methoxy group), loss of the other molecule of carbon monoxide may be accounted for in the expulsion of the C-3 phenol. One of the aromatic hydrogens is significantly further downfield in metabolite **27**, compared to its chemical shift in **23** (6.69 *versus* 6.05 ppm). Other than the small solvent effect, the proximity of H-6 to the ketone carbonyl in **27** may account for this noticeable deshielding. The hydrogen at C-9

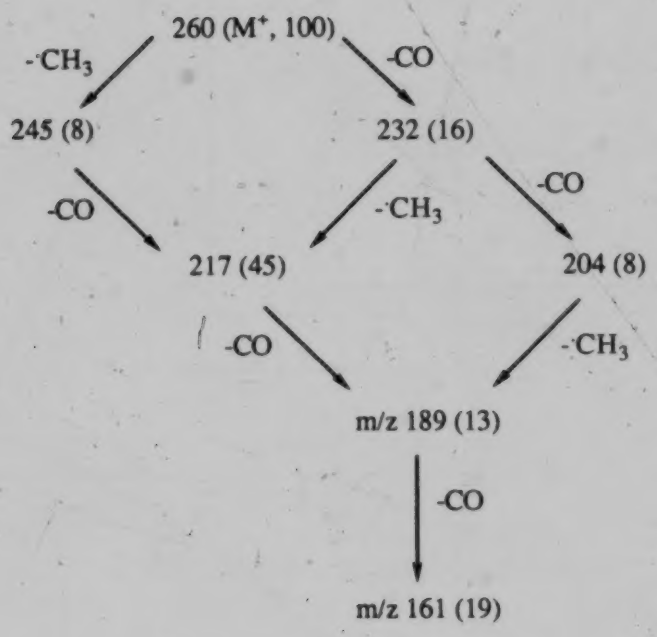

Scheme 14. The mass spectral fragmentation of deoxytalaroflavone (**27**)

is found at 3.43 ppm. This downfield shift may be due to its vinylogous location with respect to the conjugated aromatic system. Metabolite **27**, having a molecular formula $C_{14}H_{12}O_5$, differs from that of talaroflavone (**23**), $C_{14}H_{12}O_6$, by only one oxygen atom. Its formation from talaroflavone (**23**) may be envisaged in three steps as shown in Scheme 15. Reduction of the double bond may occur in talaroflavone (**23**), or possibly earlier along the pathway, as this reduction is difficult chemically. Reduction from the least hindered side of talaroflavone (**23**) should favor formation of the isomer shown at C-9 in **27**. Ring opening at the spiro center may occur as shown to form the six-six-five-membered ring system, followed by loss of an hydrogen atom α- to the ketone carbonyl. Overall, addition of hydrogen to the double bond, loss of water, and bond migration in metabolite **23**, afford the related natural product **27**, deoxytalaroflavone.

The last of the polyketide metabolites isolated arising from a heptaketide precursor, has a molecular formula of $C_{15}H_{12}O_7$ (304), as determined by hrms. This

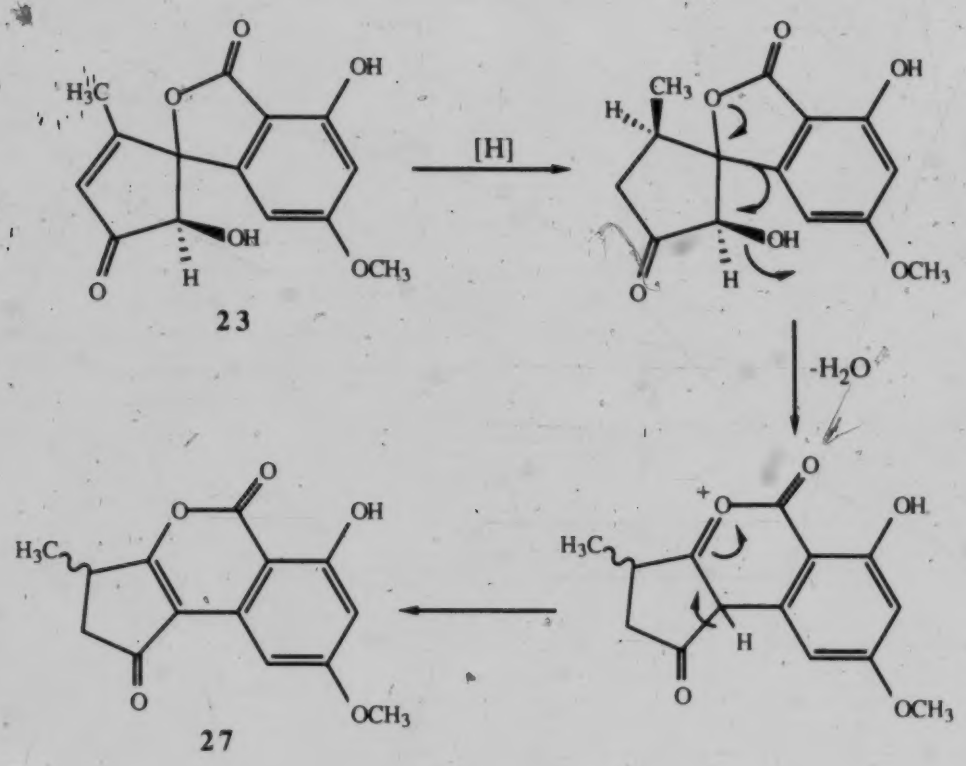

Scheme 15. Formation of deoxytalaroflavone (**27**) from talaroflavone (**23**)

metabolite (**28**) has one more oxygen atom than four of those previously discussed (**18**, **19**, **21**, and **23**), suggesting that it has been oxidized. The ir spectrum shows a broad hydroxyl absorption from 3600 to 2800 cm^{-1}, a weak band at 1710 cm^{-1}, and stronger absorptions at 1648 and 1612 cm^{-1}. A noticeable difference in the ^1H nmr spectrum (methanol-d_4) of this metabolite (**28**), compared with those heptaketide metabolites previously discussed, is the absence of the *meta-* coupling between the aromatic hydrogens. There are one hydrogen signals at 7.04, 6.66, and 6.38 ppm, all of which are singlets. A methoxy signal resonates at 3.85 ppm and an aromatic methyl group is seen at 2.36 ppm. These account for nine of the twelve hydrogens; thus, there are three

exchangeable ones. The ^{13}C nmr data are summarized in Table 23. The mass spectral fragmentation is outlined in Scheme 16.

Table 23. ^{13}C nmr data for metabolite **28**

chemical shift (ppm)	multiplicity
173.7	s
169.1	s
165.6	s
162.4	s
136.3	s
133.0	s
128.7	s
125.3	d
124.0	s
113.2	s
97.2	d
94.3	d
92.5	s
55.7	q
17.5	q

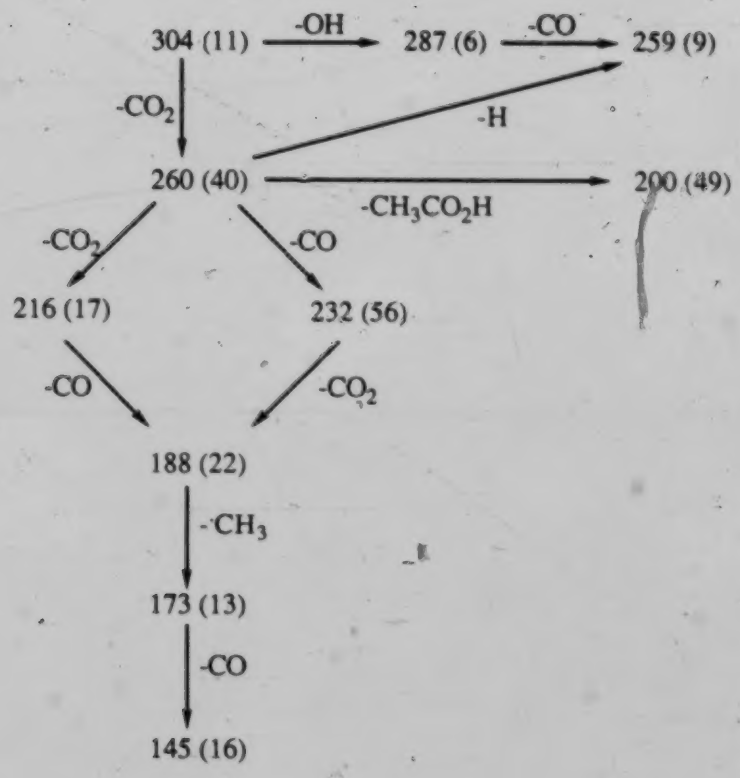

Scheme 16. The mass spectral fragmentation of metabolite **28**

III. EXPERIMENTAL

Unless otherwise stated the following particulars apply. All solvents except diethyl ether and n-hexane were distilled prior to use. Skellysolve B refers to Skelly Oil Company light petroleum, bp 62-70°C. Pyridine was distilled from CaH_2 and stored over KOH. Analytical thin layer chromatography (tlc) was carried out on aluminum sheets precoated (0.2 mm) with silica gel 60 F-254 (E. Merck, Darmstadt). Materials were detected by visualization under an ultraviolet (uv) lamp (254 or 350 nm), or by spraying with a solution of phosphomolybdic acid (5%) containing a trace of ceric sulfate in aqueous sulfuric acid (5%, v/v), or a solution of anisaldehyde (2%) in aqueous sulfuric acid (10%, v/v), followed by charring on a hot plate. Flash column chromatography[81] was performed with Merck Silica Gel 60 (40 - 63 μm). High resolution mass spectra (hrms) were recorded on an A.E.I. MS-50 mass spectrometer coupled to a Data General Nova 4 computer. Low resolution mass spectra (lrms) were recorded on an A.E.I. MS-12 mass spectrometer. Chemical ionization mass spectra (cims) were recorded on an A.E.I. MS-12 mass spectrometer. Ammonia was used as the reagent gas. Data are reported as m/z (relative intensity). Unless diagnostically significant, peaks with intensities less than 10% of the base peak are omitted. Fourier transform infrared (ftir) spectra were recorded as $CHCl_3$, CH_2Cl_2, CH_3COCH_3, or CH_3OH casts on a Nicolet 7199 FT interferometer. Ultraviolet (uv) spectra were obtained on a Hewlett Packard 8450A Diode Array spectrophotometer. Optical rotations were measured on a Perkin Elmer 241 polarimeter. Circular dichroic (cd)-optical rotary dispersion (ord) spectra were measured on a Jasco Model SS20 cd-ord spectrometer. ^1H nuclear magnetic resonance (^1H nmr) spectra were measured on a Bruker WH-200, WH-360, WH-400, AM-300, or AM-400 spectrometer with an Aspect 2000 or 3000 computer system. Residual $C\underline{H}Cl_3$ in $CDCl_3$, $C\underline{H}D_2OD$ in CD_3OD, $C\underline{H}D_2COCD_3$ in

CD_3COCD_3, or CHD_2SOCD_3 in CD_3SOCD_3 was employed as the internal standard (assigned as 7.26, 3.30, 2.04, and 2.49 ppm, respectively, downfield from tetramethylsilane (TMS)). Measurements are reported in ppm downfield from TMS (δ). ^{13}C nuclear magnetic resonance (^{13}C nmr) spectra were measured on a Bruker AM-300, WH-400, or AM-400 spectrometer. $CDCl_3$, CD_3OD, or CD_3COCD_3 was employed as the internal standard (assigned as 77.0, 49.0, or 29.8 ppm, respectively, downfield from TMS (δ)). Melting points were recorded on a Fisher-Johns or Leitz-Wetzlar melting point apparatus and are uncorrected.

Growth of *Talaromyces flavus* and Extraction of the Metabolites

The strain (ATCC 52201; UAMH 4890) of *T. flavus* used in this study was obtained from the American Type Culture Collection, Rockville, Maryland. It was isolated from sclerotia of *Sclerotina minor* buried in soil at Beltsville, Maryland. The strains (UAMH 5360, 5366) of *V. dahliae* used in this study were obtained from D.R. Fravel, Soilborne Diseases Laboratory, Beltsville, Maryland. Stock cultures of *T. flavus* were maintained at 4°C in slant tubes containing Difco potato dextrose agar. To initiate liquid still cultures of the fungus, an aqueous spore suspension of *T. flavus* was used to inoculate two agar plates (10% filtered V-8 juice (Campbell Soup Company Ltd.), 1% glucose, 2% agar). After incubation for two weeks, the plate cultures were blended in a Waring blender with *ca.* 200 mL of sterile water and 20 mL aliquots were inoculated into each of 10 - 2.8 L Fernbach flasks charged with 1 L of sterile malt extract medium (2% (w/v) glucose, 2% (w/v) malt extract, and 0.1% (w/v) peptone). The culture was kept at room temperature for four weeks. The culture broth was decanted from the mycelium by filtration through cheesecloth, concentrated *in vacuo* to *ca.* one litre, and continuously extracted with ethyl acetate for 48 hours. The organic extract was dried and concentrated

to give an oil (*ca.* 1g) which was then dissolved in a water-methanol solution (85:15, 100 mL) and extracted with n-hexane (3 x 100 mL), dichloromethane (3 x 100 mL), and ethyl acetate (3 x 100 mL) (Scheme 17). The organic extracts were dried and concentrated to give oils which were separated as described below (Scheme 22). The mycelium was washed with methanol, air dried, and then subjected to continuous extraction in a Soxhlet extractor with ethyl acetate for 6 hours or with methanol for 24 hours (Scheme 18). The organic extract was dried, concentrated, and separated as described below (Schemes 19, 20, and 21).

Isolation of the Metabolites

Methanol was added to the crude mycelium extract. The insoluble material was filtered off and identified as D-mannitol (**1**, 9.2 g). The methanol soluble portion was subjected to flash chromatography, eluting with benzene followed by benzene-ether (9:1). This afforded methyl linoleate (**3**), a triglyceride (**5**), ergosterol (**7**), and linoleic acid (**4**) (Scheme 19). Methanol was added to the crude ethyl acetate mycelium extract. D-mannitol (**1**, 1.5 g) was filtered off and the methanol soluble portion evaporated to dryness (200 mg). It was dissolved in a water-methanol solution (90:10, 100 mL) and extracted with n-hexane (3 x 100 mL), dichloromethane (3 x 100 mL), and ethyl acetate (3 x 100 mL). Each of the extracts was dried over anhydrous sodium sulfate, filtered, and the solvents were removed under reduced pressure to give the hexane extract (170 mg), dichloromethane extract (12 mg), and the ethyl acetate extract (18 mg) (Scheme 20). The most abundant hexane extract was subjected to flash chromatography, eluting with Skellysolve B-acetone (93:7). This afforded the triglyceride (**5**), ergosterol (**7**), as well as a diglyceride (**6**) (Scheme 21). As shown in Scheme 22, the hexane portion of the ethyl acetate broth extract was subjected to flash chromatography, eluting with Skelly

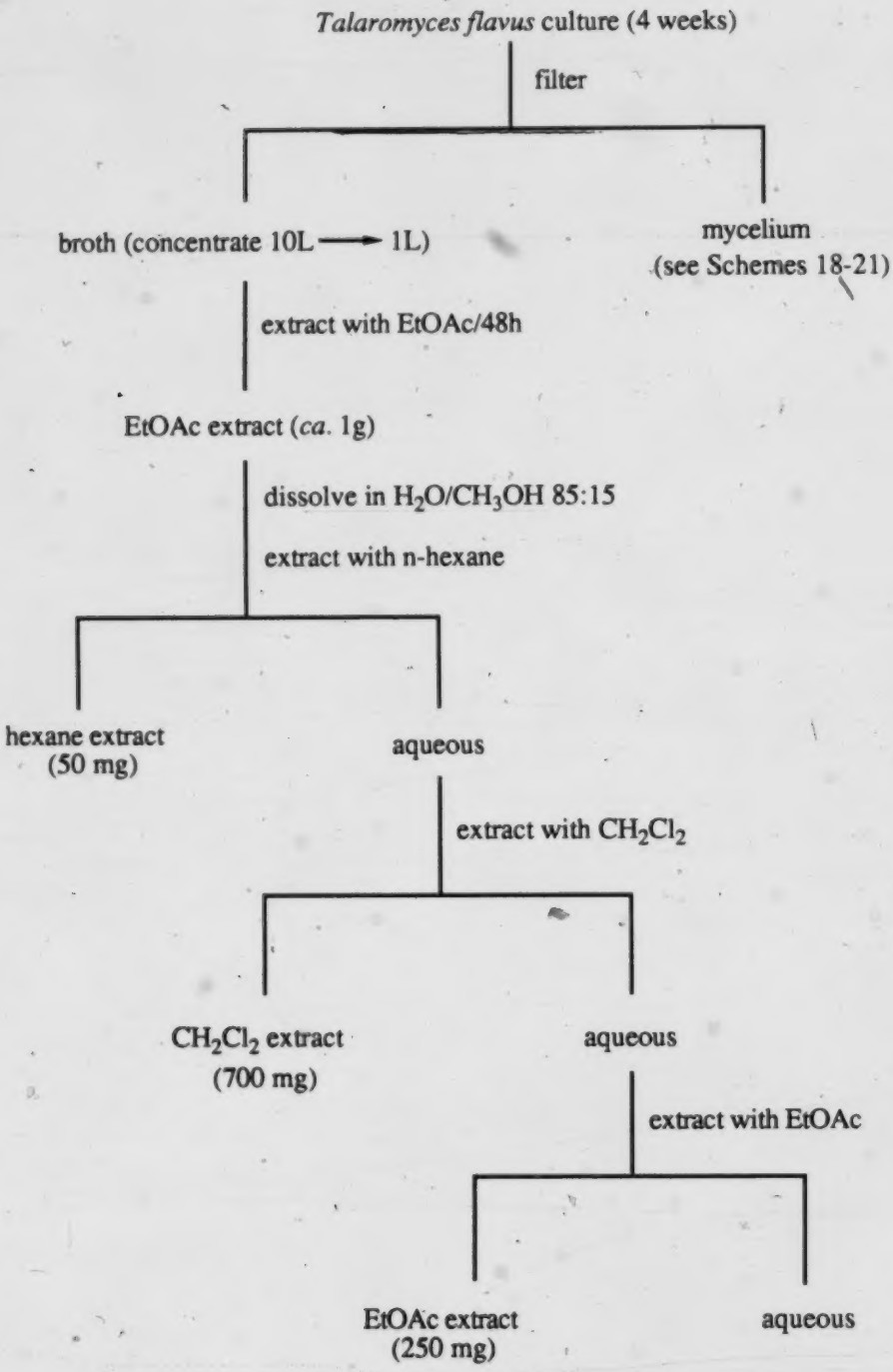

Scheme 17. Extraction of *Talaromyces flavus* broth

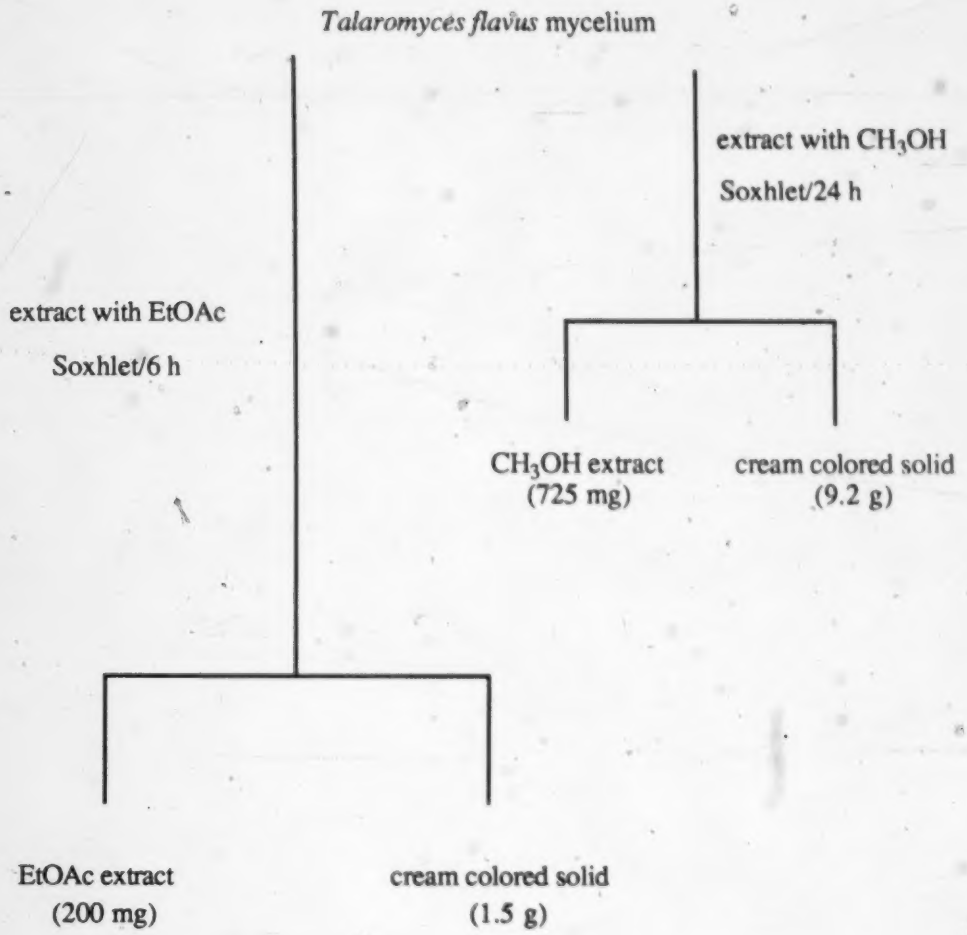

Scheme 18. Extraction of *Talaromyces flavus* mycelium

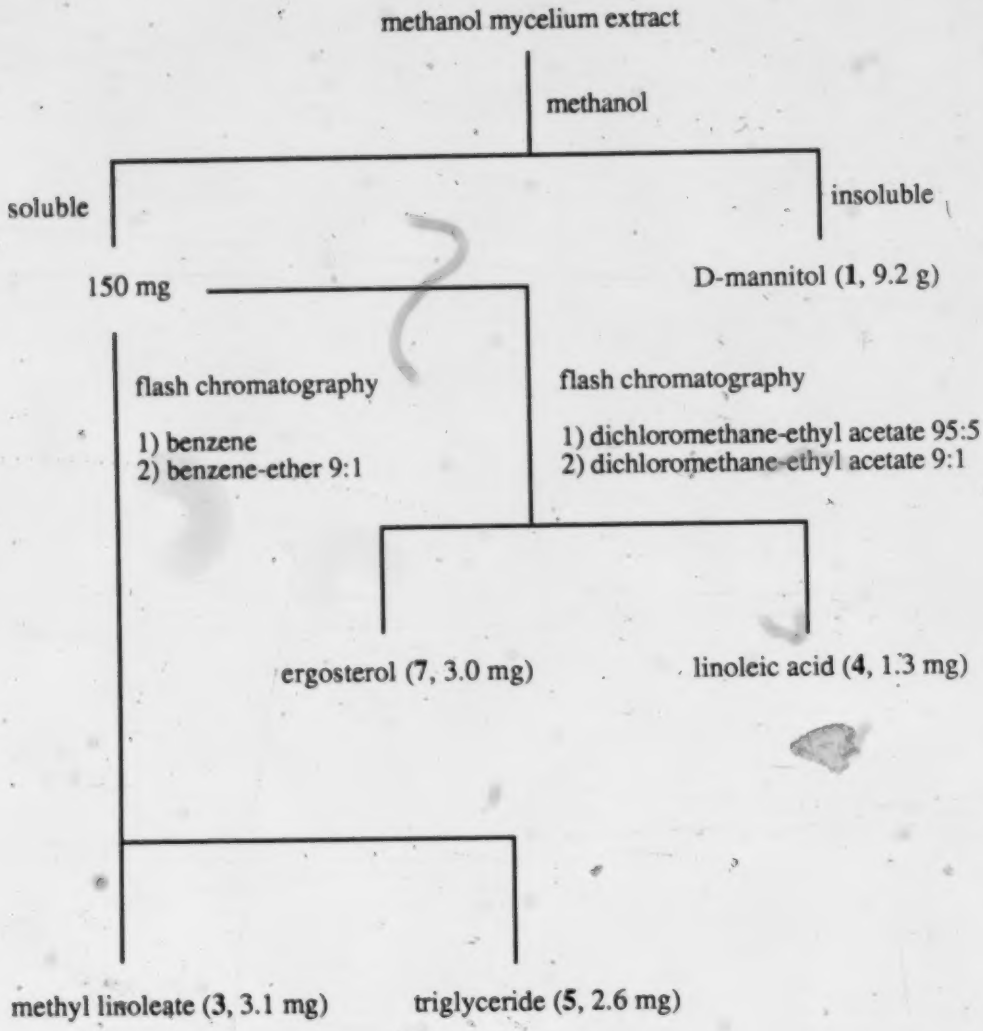

Scheme 19. Isolation of metabolites from the methanol mycelium extract

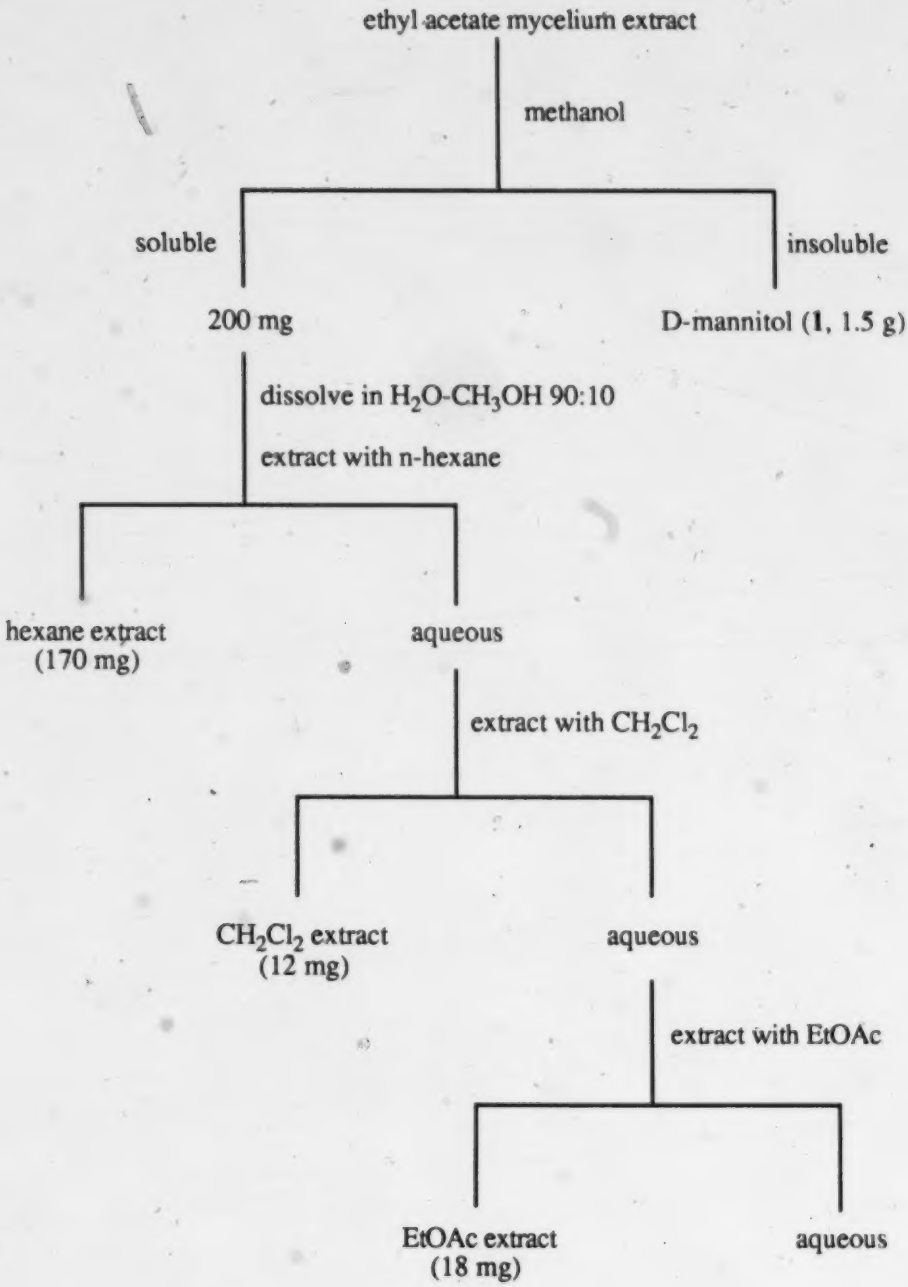

Scheme 20. Partition extraction of the ethyl acetate mycelium extract

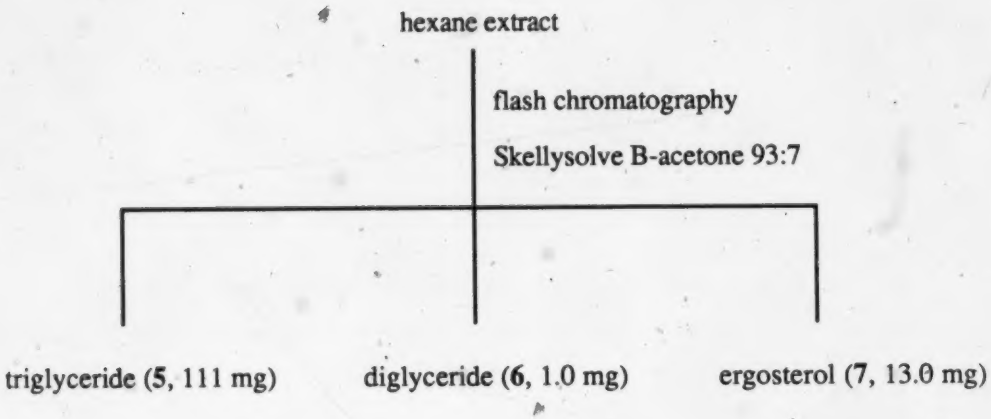

Scheme 21. Metabolites isolated by chromatography of the hexane portion of the ethyl acetate mycelium extract

hexane extract

flash chromatography

Skellysolve B-ether 7:1

triglyceride (**5**)
(5.3 mg)

ethyl acetate extract

flash chromatography

toluene-acetone-acetic acid
35:65:1

D-glucono-1,4-lactone (**8**)
(124 mg)

dichloromethane extract

flash chromatography

dichloromethane-methanol 97:3

27 (3.0 mg)	**17** (1.2 mg)	**21, 22** (1.0 mg)	**13** (3.4 mg)	**10** (4.8 mg)	**28** (3.8 mg)
19, 20 (0.6 mg)	**15** (2.8 mg)	**12** (7.5 mg)	**23** (3.0 mg)	**18** (5.0 mg)	

Scheme 22. Isolation of metabolites from the partition extracts of the ethyl acetate broth extract

solve B-ether (7:1). The major metabolite isolated was the triglyceride (**5**), identical with that reported from the mycelium extracts. The major metabolite isolated from flash chromatography of the ethyl acetate extract was D-glucono-1,4-lactone (**8**). The remaining metabolites were isolated from the dichloromethane portion of the ethyl acetate broth extract. Initial separation was achieved by flash chromatography, eluting with dichloromethane-methanol (97:3). Subsequent purifications of individual metabolites are described under their appropriate headings.

D-Mannitol (**1**)

D-Mannitol (**1**) precipitated from the ethyl acetate and methanol extracts of the mycelium on cooling. After removal of the solvent under reduced pressure, methanol was added to the extract and the solid was filtered off. Recrystallization from methanol afforded a white, granular solid (1.5 g and 9.2 g), mp = 170-172°C (168°C, lit.[25]); ir (KBr) ν_{max} cm^{-1}: 3318 (br), 2939, 1081, 1019; ^1H nmr (DMSO-d_6, 200 MHz): δ 4.40 (2H, d, J=6.0 Hz, CHOH), 4.31 (2H, t, J=6.0 Hz, CH_2OH), 4.12 (2H, d, J=7.5 Hz, CHOH), 3.63-3.35 (8H, m, CHOH); ^{13}C nmr (DMSO-d_6, 50 MHz): δ 71.3 (d, C-3, C-4), 69.7 (d, C-2, C-5), 63.8 (t, C-1, C-6); cims (NH_3): 183 (M^+ + 1, 63), 200 (M^+ + 18, 100).

Acetylation of D-mannitol (**1**)

Acetic anhydride (1.0 mL, 10.6 mmol) was added to a solution of D-mannitol (**1**, 11.5 mg, 0.063 mmol) in pyridine (1.0 mL, 12.4 mmol). The reaction mixture was allowed to stand at room temperature overnight. Toluene (5.0 mL) was added to the mixture and the solution was evaporated *in vacuo*. The crude acetylation product (28.7

mg) was dissolved in dichloromethane and passed through a small column of silica gel in a pipette to afford white flakes of D-mannitol hexaacetate (**2**, 18.5 mg, 0.043 mmol, 68% yield), mp = 123-125°C (126°C, lit.[25]); $[\alpha]_D$ +22.4° (c 6.2, $CHCl_3$); (+25.0° ($CHCl_3$), lit.[25]); ir ($CHCl_3$ cast) ν_{max} cm^{-1}: 2950, 1743, 1370, 1226, 1033; ^1H nmr ($CDCl_3$, 400 MHz): δ 5.43 (2H, d, J=9.0 Hz, H-3, H-4), 5.05 (2H, ddd, J=2.5, 5.0, 9.0 Hz, H-2, H-5), 4.20 (2H, dd, J=2.5, 12.5 Hz, H-1, H-6), 4.05 (2H, dd, J=5.0, 12.5 Hz, H-1', H-6'), 2.07 (6H, s, $OCOCH_3$), 2.05 (6H, s, $OCOCH_3$), 2.03 (6H, s, $OCOCH_3$); cims (NH_3): 452 (M^+ + 18, 100).

Methyl linoleate (**3**)

Methyl linoleate (**3**) was isolated by flash chromatography of the methanol mycelium extract, eluting with benzene (Scheme 19). It was obtained as a clear, colorless oil (3.1 mg), tlc: R_f = 0.56 (benzene); ir ($CHCl_3$ cast) ν_{max} cm^{-1}: 3000, 2925, 2584, 1745, 1460, 1430, 1375, 1360, 1195, 1170, 720; ^1H nmr ($CDCl_3$, 400 MHz): δ 5.43-5.28 (4H, m, $HC=CH$), 3.66 (3H, s, $COOCH_3$), 2.77 (2H, t, J=6.0 Hz, $C=CHCH_2CH=C$-), 2.30 (2H, t, J=8.0 -Hz, -CH_2COO), 2.08-1.97 (4H, m, -$C=CH-CH_2$), 1.62 (2H, br t, J=8.0 Hz, -CH_2CH_2COO), 1.40-1.23 (14H, m, CH_2), 0.89 (3H, m, CH_3); hrms m/z (relative intensity %) calc. for $C_{19}H_{34}O_2$ (M^+): 294.2560; found: 294.2553 (10), 263 (3), 220 (3), 143 (12), 97 (22), 87 (61), 74 (100); cims (NH_3): 312 (M^+ + 18, 100).

Linoleic acid (**4**)

Linoleic acid (**4**) was isolated by flash chromatography of the methanol mycelium extract, eluting with dichloromethane-ethyl acetate (9:1) (Scheme 19). It was obtained as

a clear, colorless oil (1.3 mg), tlc: R_f = 0.24 (dichloromethane-ethyl acetate 9:1); ir ($CHCl_3$ cast) ν_{max} cm^{-1}: 3460-2400 (br), 3000, 2954, 2925, 2854, 1710, 1460, 1410, 1280, 720; ^1H nmr ($CDCl_3$, 400 MHz): δ 5.42-5.29 (4H, m, HC=CH), 2.77 (2H, t, J=6.0 Hz, C=CH-CH_2-CH=C-), 2.36 (2H, br t, J= 6.0 Hz, CH_2COO), 2.08-1.97 (4H, m, -C=CH-CH_2), 1.63 (2H, br t, J=7.0 Hz, CH_2CH_2COO), 1.40-1.18 (14H, m, CH_2), 0.88 (3H, m, CH_3); hrms m/z (relative intensity %) calc. for $C_{18}H_{32}O_2$ (M^+): 280.2403; found: 280.2400 (2), 256 (23), 129 (17), 69 (74), 55 (100); cims (NH_3): 298 (M+ + 18, 71).

Triglyceride (5)

The triglyceride (5) was isolated by flash chromatography of the methanol and ethyl acetate mycelium extracts, eluting with benzene and Skellysolve B-acetone (93:7), respectively (Schemes 18, 19, 20, and 21). It was also obtained by flash chromatography of the hexane portion of the ethyl acetate broth extract, eluting with Skellysolve B-ether (7:1) (Schemes 17 and 22). The triglyceride (5) was obtained as a clear, colorless oil (2.6 mg, 111 mg, and 5.3 mg, respectively), tlc: R_f = 0.33 (benzene), 0.48 (Skellysolve B-acetone 93:7), 0.29 (Skellysolve B-ether 7:1); ir ($CHCl_3$ cast) ν_{max} cm^{-1}: 3000, 2925, 2854, 1746, 1460, 1160, 720; ^1H nmr ($CDCl_3$, 400 MHz): δ 5.43-5.29 (10H, m), 5.25 (1H, m), 4.29 (2H, dd, J=5.0, 12.0 Hz), 4.14 (2H, dd, J= 6.0, 12.0 Hz), 2.77 (6H, dt, J=1.0, 6.0 Hz), 2.31 (6H, dt, J=2.0, 6.0 Hz), 2.04 (8H, m), 1.60 (6H, m), 1.38-1.22 (50H, m), 0.88 (9H, m); lrms m/z (relative intensity %): 856 (12), 601 (15), 577 (53), 575 (93), 313 (21), 264 (31), 263 (35), 262 (100), 239 (16); hrms m/z (relative intensity %): 601 (14), 577 (36), 575 (26), 313 (20), 264 (19), 263 (24), 262 (69), 239 (14).

Diglyceride (6)

The diglyceride was isolated by flash chromatography of the ethyl acetate mycelium extract, eluting with Skellysolve B-acetone (93:7) (Schemes 18, 20, and 21). It was obtained as a clear, colorless oil (1.0 mg), tlc: R_f = 0.30 (Skellysolve B-acetone 93:7); ir ($CHCl_3$ cast) ν_{max} cm^{-1}: 3460 (br), 3000, 2925, 2854, 1745, 1465, 1377, 1165, 720; ^1H nmr ($CDCl_3$, 400 MHz): δ 5.32 (4H, m), 5.23 (1H, m), 4.27 (2H, dd, J=4.0, 12.0 Hz), 4.12 (2H, dd, J=6.0, 12.0 Hz), 2.75 (2H, t, J=6.0 Hz), 2.29 (4H, m), 2.00 (4H, m), 1.40-1.12 (43H, m), 0.86 (6H, m); lrms m/z (relative intensity %): M^+ not detected, 577 (10), 313 (28), 264 (14), 239 (20).

Ergosterol (7)

Ergosterol (7) was isolated by flash chromatography of the methanol and ethyl acetate mycelium extracts, eluting with dichloromethane-ethyl acetate (95:5) and Skellysolve B-acetone (93:7), respectively (Schemes 18, 19, 20, and 21). It was isolated as a cream colored solid (3.0 mg and 13.0 mg, respectively). Recrystallization from 95% ethanol gave ergosterol (7) as white plates, mp = 163-165°C (168°C, lit.[82]); tlc: R_f = 0.32 (dichloromethane-ethyl acetate 95:5), 0.10 (Skellysolve B-acetone 93:7); uv (ether, 4.0 mg/100mL) λ_{max} nm (log ε): 262 (3.81), 271 (3.91), 281 (3.92), 293 (3.70); ir ($CHCl_3$ cast) ν_{max} cm^{-1}: 3390 (br), 2954, 2870, 1459, 1382, 1369, 1060, 1026, 968, 832, 801; ^1H nmr ($CDCl_3$, 400 MHz): δ 5.57 (1H, dd, J=3.0, 6.0 Hz, H-C=C), 5.38 (1H, m, H-C=C), 5.20 (2H, m, H-C=C), 3.65 (1H, m, H-C-O), 2.46 (1H, dq, J=14.0, 2.5 Hz), 2.33 (1H, t, J=8.0 Hz), 2.09-1.33 (19H, m), 1.04 (3H, d, J=7.0 Hz), 0.94 (3H, s), 0.91 (3H, d, J=7.0 Hz), 0.85 (3H, d, J=7.0 Hz), 0.83 (3H, d, J=6.0 Hz), 0.63 (3H, s); hrms m/z (relative intensity %) calc. for $C_{28}H_{44}O$ (M^+): 396.3394; found:

396.3398 (100), 363 (71), 337 (31), 271 (15), 253 (29); cims (NH_3): 379 ($M^+ - H_2O$ + 1, 100).

D-Glucono-1,4-lactone (**8**)

D-Glucono-1,4-lactone (**8**) was isolated from the ethyl acetate portion of the broth extract (Schemes 17 and 22) by flash chromatography, eluting with toluene-acetone-acetic acid (35:65:1). It crystallized after evaporation of the solvents. Recrystallization from acetic acid gave D-glucono-1,4-lactone (**8**) as a white powder (124 mg), mp = 127-129°C (132-135°C, lit.[38]); tlc: R_f = 0.29 (toluene-acetone-acetic acid 35:65:1); ir (acetone cast) ν_{max} cm^{-1}: 3300 (br), 1776, 1182, 1100, 985; ^1H nmr (methanol-d_4, 400 MHz): δ 4.54 (1H, dd, J=4.8, 6.5 Hz, H-4), 4.35 (1H, dd J=4.7, 6.5 Hz, H-3), 4.24 (1H, d, J=4.7 Hz, H-2), 3.97 (1H, ddd, J=3.9, 4.8, 5.7 Hz, H-5), 3.77 (1H, dd, J=3.9, 11.7 Hz, H-6), 3.69 (1H, dd, J=5.7, 11.7 Hz, H-6'); ^{13}C nmr (CD_3OD-D_2O 1:1, 100 MHz): δ 177.5 (s, C-1), 81.0 (d, C-4), 74.4, 74.2, 71.4 (3 x d, C-2, C-3, C-5), 63.8 (t, C-6); hrms m/z (relative intensity %) calc. for $C_6H_{10}O_6$ (M^+): 178.0477; found: M^+ not detected, 160 (21), 142 (4), 103 (24), 73 (100); cims (NH_3): 196 (M^+ + 18, 100).

Acetylation of D-glucono-1,4-lactone (**8**)

Pyridine (1.0 mL, 12.4 mmol) was added to a solution of D-glucono-1,4-lactone (**8**, 9.0 mg, 0.051 mmol) in acetic anhydride (1.0 mL, 10.6 mmol). The reaction was allowed to stand at room temperature for six hours. Toluene (5.0 mL) was added to the mixture and the solution was evaporated under reduced pressure. Flash chromatography of the crude reaction product, eluting with Skellysolve B-acetone (2.5:1), afforded D-

glucono-1,4-lactone tetraacetate (**9**) as white needles (15.6 mg, 0.045 mmol, 88% yield), mp = 101-102°C (103°C, lit.[38]); tlc: R_f = 0.29 (Skellysolve B-acetone 2.5:1); $[\alpha]_D$ +59° (c 1.0, acetone); (+60.3° (acetone), lit.[38]); ir (acetone cast) ν_{max} cm^{-1}: 1806, 1751, 1373, 1224, 1194, 1067, 1046; ^1H nmr ($CDCl_3$, 400 MHz): δ 5.62 (1H, dd, J=3.0, 5.5 Hz, H-3), 5.35 (1H, ddd, J=3.0, 5.0, 8.0 Hz, H-5), 5.23 (1H, d, J=3.0 Hz, H-2), 4.96 (1H, dd, J=5.5, 8.0 Hz, H-4), 4.58 (1H, dd, J=3.0, 12.0 Hz, H-6), 4.15 (1H, dd, J=5.0, 12.0 Hz, H-6'), 2.19 (3H, s, $OCOCH_3$), 2.12 (3H, s, $OCOCH_3$), 2.10 (3H, s, $OCOCH_3$), 2.05 (3H, s, $OCOCH_3$); ^{13}C nmr ($CDCl_3$, 100 MHz): δ 170.3 (s), 169.3 (s), 169.1 (s), 169.0 (s), 168.7 (s), 76.9 (d), 72.0 (d), 71.0 (d), 67.6 (d), 62.1 (t), 20.6 (2C, q), 20.4 (q), 20.2 (q); hrms m/z (relative intensity %) calc. for $C_{14}H_{18}O_{10}$ (M^+): 346.0899; found: M^+ not detected, 226 (15), 184 (100), 142 (90), 100 (76); cims (NH_3): 364 (M^+ + 18, 100).

4,6-Dihydroxy-5-methylphthalide (**10**) (4,6-Dihydroxy-5-methyl-1(3H)-isobenzofuranone)

4,6-Dihydroxy-5-methylphthalide (**10**) was isolated by flash chromatography of the dichloromethane portion of the ethyl acetate broth extract, eluting with dichloromethane-methanol (97:3) (Schemes 17 and 22). It crystallized from the solvents as colorless needles (4.8 mg), mp = 240-241°C (241-242°C, lit.[45]); tlc: R_f = 0.19 (dichloromethane-methanol 97:3); uv (methanol, 1.0 mg/100 mL) λ_{max} nm (log ε): 213 (4.50), 259 (3.92), 306 (3.58); 1 drop 0.1N NaOH: 232 (4.35), 278 (3.75), 328 (3.58); 1 drop 0.1N NaOH-1 drop 0.1N HCl: 212 (4.48), 259 (3.91), 307 (3.58); ir (acetone cast) ν_{max} cm^{-1}: 3360 (br), 1730, 1610, 1470, 1450, 1342, 1092, 1024, 770; ^1H nmr (acetone-d_6, 400 MHz): δ 8.92 (1H, br s, O**H**), 8.64 (1H, br s, O**H**), 6.84 (1H, s, H-7), 5.19 (2H, s, H-3), 2.18 (3H, s, C-5 CH_3); (methanol-d_4, 400 MHz): δ 6.77

(1H, s, H-7), 5.19 (2H, s, H-3), 2.14 (3H, s, C-5 $C\underline{H}_3$); ^{13}C nmr (acetone-d_6, 100 MHz): δ 171.6 (s, C-1), 158.5 (s, C-6), 151.2 (s, C-4), 126.1 (s, C-3a), 125.2 (s, C-7a), 119.3 (s, C-5), 102.6 (d, C-7), 68.5 (t, C-3), 9.2 (q, C-5 $\underline{C}H_3$); (methanol-d_4, 100 MHz): δ 174.2 (s, C-1), 159.1 (s, C-6), 151.5 (s, C-4), 126.3 (s, C-3a), 124.7 (s, C-7a), 120.5 (s, C-5), 102.1 (d, C-7), 69.7 (t, C-3), 9.2 (q, C-5 $\underline{C}H_3$); hrms m/z (relative intensity %) calc. for $C_9H_8O_4$ (M^+): 180.0422; found: 180.0421 (55), 179 (13), 151 (100), 123 (22); cims (NH_3): 198 (M^+ + 18, 100).

Methylation of 4,6-dihydroxy-5-methylphthalide (**10**)

A solution of 4,6-dihydroxy-5-methylphthalide (**10**, 4.2 mg, 0.023 mmol), potassium carbonate (30.0 mg, 0.22 mmol), and methyl iodide (0.1 mL, 0.16 mmol) in dry acetone (5.0 mL) was heated under reflux for 2.5 hours. The reaction mixture was filtered and the solvent was removed under reduced pressure, yielding a white solid which was taken up in dichloromethane (10.0 mL). The solution was stirred at room temperature for 0.5 hour. It was then filtered and the solvent was removed under reduced pressure yielding a pale yellow solid (6.3 mg) which was purified by flash chromatography, eluting with Skellysolve B-ethyl acetate (4:1). This afforded white flakes of 4,6-dimethoxy-5-methylphthalide (**11**, 3.5 mg, 0.017 mmol, 74% yield), mp = 162-162.5°C (162°C, lit.[45]); tlc: R_f = 0.27 (Skellysolve B-ethyl acetate 4:1); uv (methanol, 1.0 mg/100mL) λ_{max} nm (log ε): 214 (3.75), 255 (3.08), 304 (2.78); ir ($CHCl_3$ cast) ν_{max} cm^{-1}: 3000, 2970, 2950, 1765, 1740, 1616, 1466, 1417, 1152, 1127, 1045, 767; ^1H nmr (acetone-d_6, 400 MHz): δ 7.02 (1H, s, H-7), 5.51 (2H, s, H-3), 3.96 (3H, s, $OC\underline{H}_3$), 3.93 (3H, s, $OC\underline{H}_3$), 2.14 (3H, s, C-5 $C\underline{H}_3$); ^{13}C nmr (acetone-d_6, 100 MHz): δ 171.1 (s, C-1), 160.8 (s, C-6), 154.0 (s, C-4), 128.9 (s, C-3a), 126.1 (s, C-5), 124.8 (s, C-7a), 100.9 (d, C-7), 68.9 (t, C-3), 59.4 (q, $O\underline{C}H_3$),

56.6 (q, O<u>C</u>H$_3$), 9.6 (q, C-5 <u>C</u>H$_3$); hrms m/z (relative intensity %) calc. for $C_{11}H_{12}O_4$ (M^+): 208.0736; found: 208.0738 (61), 207 (7), 179 (100), 151 (9); cims (NH_3): 209 ($M^+ + 1$, 100), 226 ($M^+ + 18$, 68).

5-Hydroxymethylfurfural (**12**)

5-Hydroxymethylfurfural (**12**) was isolated by flash chromatography of the dichloromethane portion of the ethyl acetate broth extract, eluting with dichloromethane-methanol (97:3) (Schemes 17 and 22). Further purification was achieved by flash chromatography, eluting with Skellysolve B-ethyl acetate-acetic acid (60:40:1). This afforded 5-hydroxymethylfurfural (**12**) as a clear, pale yellow oil (7.5 mg), tlc: R_f = 0.33 (dichloromethane-methanol 97:3), 0.28 (Skellysolve B-ethyl acetate-acetic acid 60:40:1); uv (methanol, 1.0 mg/100mL) λ_{max} nm (log ε): 221 (3.43), 281 (3.49); ir (CH_2Cl_2-CH_3OH cast) ν_{max} cm^{-1}: 3370 (br), 2920, 2840, 2700, 1674, 1522, 1396, 1191, 1022; ^{1}H nmr ($CDCl_3$, 200 MHz): δ 9.58 (1H, s, C<u>H</u>O), 7.19 (1H, d, J=3.5 Hz, H-3), 6.50 (1H, d, J=3.5 Hz, H-4), 4.70 (2H, s, C<u>H</u>$_2$OH), 1.62 (1H, br s, O<u>H</u>); (acetone-d_6, 400 MHz): δ 9.57 (1H, s, C<u>H</u>O), 7.36 (1H, d, J=3.5 Hz, H-3), 6.56 (1H, d, J=3.5 Hz, H-4), 4.62 (2H, s, C<u>H</u>$_2$OH); ^{13}C nmr (acetone-d_6, 100 MHz): δ 178.1 (d, <u>C</u>HO), 163.0 (s, C-5), 153.7 (s, C-2), 123.3 (d, C-3), 110.2 (d, C-4), 57.6 (t, C-6); hrms m/z (relative intensity %) calc. for $C_6H_6O_3$ (M^+): 126.0317; found: 126.0321 (70), 125 (16), 97 (100); cims (NH_3): 144 ($M^+ + 18$, 100).

7-Hydroxy-2,5-dimethylchromone (**13**) (7-Hydroxy-2,5-dimethyl-4H-1-benzopyran-4-one)

7-Hydroxy-2,5-dimethylchromone (**13**) was isolated by flash chromatography of the dichloromethane portion of the ethyl acetate broth extract, eluting with dichloromethane-methanol (97:3) (Schemes 17 and 22). It crystallized from the solvents as white flakes (3.4 mg), mp = 200°C (subl.), (257-260°C, sublimes at 200°C, lit.[58]); tlc: R_f = 0.25 (dichloromethane-methanol 97:3); uv (methanol, 1.0 mg/100mL) λ_{max} nm (log ε): 241 (4.12), 249 (4.13), 288 (3.92); 1 drop 0.1N NaOH: 254 (4.19), 325 (3.95); 1 drop 0.1N NaOH-1 drop 0.1N HCl: 241 (4.12), 249 (4.13), 288 (3.92); ir (methanol cast) ν_{max} cm^{-1}: 3400-3000 (br), 1649, 1618, 1557, 1162; ^1H nmr (methanol-d_4, 400 MHz): δ 6.64 (1H, d, J=2.5 Hz, H-8), 6.62 (1H, dq, J=2.5, 1.0 Hz, H-6), 6.00 (1H, q, J=1.0 Hz, H-3), 2.70 (3H, bs, C-5 $C\underline{H}_3$), 2.31 (3H, d, J=1.0 Hz, C-2 $C\underline{H}_3$); ^{13}C nmr (methanol-d_4, 100 MHz): δ 182.0 (s, C-4), 166.6 (s, C-2), 163.1 (s, C-7 or C-9), 161.5 (s, C-7 or C-9), 143.7 (s, C-5), 118.0 (d, C-3), 115.7 (s, C-10), 111.4 (d, C-6), 101.7 (d, C-8), 23.0 (q, C-5 $\underline{C}H_3$), 19.8 (q, C-2 $\underline{C}H_3$); hrms m/z (relative intensity %) calc. for $C_{11}H_{10}O_3$ (M^+): 190.0630; found: 190.0632 (100), 162 (14), 150 (11), 122 (8), 94 (3); cims (NH_3): 191 (M^+ + 1, 100).

Methylation of 7-hydroxy-2,5-dimethylchromone (**13**)

An excess of diazomethane in ether was added to a solution of **13** (1.3 mg, 0.0068 mmol) in methanol (3 drops) and the reaction mixture was allowed to stand at 0°C for five hours. The solution was then warmed to room temperature and filtered to afford a cream colored solid which was taken up in chloroform (5.0 mL). Evaporation to dryness and recrystallization of the solid from ether gave white flakes of 7-methoxy-2,5-

dimethylchromone (**14**, 1.2 mg, 0.0059 mmol, 87% yield), mp = 115-117°C, (115-117°C, lit.[57]); tlc: R_f = 0.54 (dichloromethane-methanol 97:3); uv (methanol, 1.0 mg/100mL) λ_{max} nm (log ε): 248 (3.71), 280 (3.57); ir (CH_2Cl_2 cast) ν_{max} cm^{-1}: 1663, 1612, 1574, 1179, 1157; ^1H nmr ($CDCl_3$, 400 MHz): δ 6.66 (2H, bs, H-6, H-8), 6.01 (1H, q, J=0.6 Hz, H-3), 3.86 (3H, s, OCH_3), 2.80 (3H, bs, C-5 CH_3), 2.29 (3H, d, J=0.6 Hz, C-2 CH_3); ^{13}C nmr ($CDCl_3$, 100 MHz): δ 163.6, 162.3, 159.2, 142.6, 116.2, 116.0, 111.8, 98.5, 55.6, 23.0, 20.0; hrms m/z (relative intensity %) calc. for $C_{12}H_{12}O_3$ (M^+): 204.0787; found: 204.0783 (100), 176 (6), 164 (5), 161 (19), 136 (5); cims (NH_3): 205 (M^+ + 1, 100).

4-Carboxy-5-hydroxyphthalaldehydic acid methyl ester (**15**)

4-Carboxy-5-hydroxyphthalaldehydic acid methyl ester (**15**) was obtained by flash chromatography of the dichloromethane portion of the ethyl acetate broth extract, eluting with dichloromethane-methanol (97:3) (Schemes 17 and 22). It crystallized from the solvents as yellow granules (2.8 mg), mp = 190°C (dec.); tlc: R_f = 0.35 (dichloromethane-methanol 97:3); uv (methanol, 1.2 mg/100mL) λ_{max} nm (log ε): 225 (4.15), 293 (3.90), 428 (2.65); 1 drop 0.1N NaOH: 229 (4.19), 305 (3.95), 426 (2.90); 1 drop 0.1N NaOH-1 drop 0.1N HCl: 226 (4.14), 293 (3.90), 427 (2.64); ir (methanol cast) ν_{max} cm^{-1}: 3560-2400 (br), 1757 (m), 1655, 1635, 1440, 1351, 1281, 1243, 1102, 1080; ^1H nmr (methanol-d_4, 300 MHz): δ 10.42 (1H, s, C<u>H</u>O), 6.70 (1H, s, Ar<u>H</u>), 6.38 (1H, s, Ar<u>H</u>), 3.52 (3H, s, $COOCH_3$); (acetone-d_6, 400 MHz): δ 10.46 (1H, s, C<u>H</u>O), 6.79 (1H, s, Ar<u>H</u>), 6.45 (1H, s, Ar<u>H</u>), 3.53 (3H, s, $COOCH_3$); ^{13}C nmr (methanol-d_4, 100 MHz): δ 196.6 (d, <u>C</u>HO), 169.4 (s), 166.3 (s), 160.1 (s), 136.8 (s), 122.7 (s), 114.6 (s), 103.9 (d), 102.4 (d), 56.4 (q, COO<u>C</u>H_3); hrms m/z (relative intensity %) calc. for $C_{10}H_8O_6$ (M^+): 224.0320; found: 224.0317 (30), 193 (95), 192

(86), 164 (100), 136 (22), 108 (13); cims (NH_3): 225 ($M^+ + 1$, 100), 242 ($M^+ + 18$, 32).

Reduction of 4-carboxy-5-hydroxyphthalaldehydic acid methyl ester (**15**)

To a solution of 4-carboxy-5-hydroxyphthalaldehydic acid methyl ester (**15**, 2.0 mg, 0.0089 mmol) in methanol (1.0 mL) was added sodium borohydride (0.5 mg, 0.013 mmol). After 15 seconds the yellow color of the solution faded. After 10 minutes acetic acid (1N, 2 drops) was added and the solvent was removed *in vacuo* to afford a clear, pale yellow oil. Purification of the reduction product by elution with dichloromethane-methanol (96:4) through a small silica gel pipette column afforded the reduction product as a clear, pale yellow oil (**16**, 1.3 mg); tlc: R_f = 0.26 (dichloromethane-methanol 96:4); ir (methanol cast) ν_{max} cm^{-1}: 3240 (br), 2920, 2840, 1755, 1618, 1466, 1368, 1347, 1242, 1098, 1032; ^1H nmr (acetone-d_6, 400 MHz): δ 6.74 (1H, s, ArH), 6.35 (1H, s, ArH), 5.01 (2H, s, OCH_2).

3-Hydroxymethyl-6,8-dimethoxycoumarin (**17**) (3-Hydroxymethyl-6,8-dimethoxy-2H-1-benzopyran-2-one)

The coumarin (**17**) was obtained by flash chromatography of the dichloromethane portion of the ethyl acetate broth extract, eluting with dichloromethane-methanol (97:3) (Schemes 17 and 22). The crude metabolite was further purified by passage through a small silica gel pipette column, eluting with dichloromethane-methanol (98:2), and then through another column which was eluted with Skellysolve B-ethyl acetate-acetic acid (45:55:1). It was obtained as an amorphous solid (1.2 mg); tlc: R_f = 0.36 (dichloromethane-methanol 97:3), 0.23 (dichloromethane-methanol 98:2), 0.26

(Skellysolve B-ethyl acetate-acetic acid 45:55:1); uv (methanol, 1.2 mg/100mL) λ_{max} nm (log ε): 256 (4.11), 286 (4.17); 1 drop 0.1N NaOH: 255 (4.09), 284 (4.19); ir (CH_2Cl_2 cast) ν_{max} cm^{-1}: 3360 (br), 1760 (sh), 1711, 1657, 1592, 1205, 1162; ^1H nmr ($CDCl_3$-CD_3OD 4:1, 400 MHz): δ 7.70 (1H, t, J=1.4 Hz, H-4), 6.65 (1H, d, J=2.6 Hz, H-7), 6.48 (1H, d, J=2.6 Hz, H-5), 4.55 (2H, d, J=1.4 Hz, $C\underline{H}_2OH$), 3.90 (3H, s, $OC\underline{H}_3$), 3.81 (3H, s, $OC\underline{H}_3$); ^{13}C nmr ($CDCl_3$, 100 MHz): δ 148.1 (s, C-4a), 138.7 (d, C-4), 128.6 (s, C-1a), 103.0 (d, C-5 or C-7), 101.2 (d, C-5 or C-7), 61.3 (t, $\underline{C}H_2OH$), 56.3 (q, $O\underline{C}H_3$), 55.8 (q, $O\underline{C}H_3$); hrms m/z (relative intensity %) calc. for $C_{12}H_{12}O_5$ (M^+): 236.0685; found: 236.0691 (100), 235 (11), 207 (20), 191 (14); cims (NH_3): 237 (M^+ + 1, 100), 254 (M^+ + 18, 84).

Altenusin (**18**) (3,4',5'-Trihydroxy-5-methoxy-2'-methyl[1,1'-biphenyl]-2-carboxylic acid)

Altenusin (**18**) was obtained by flash chromatography of the dichloromethane portion of the ethyl acetate broth extract, eluting with dichloromethane-methanol (97:3) (Schemes 17 and 22). The crude metabolite was further purified by dry flash chromatography, eluting with toluene-acetone-acetic acid (50:50:1) and then passed through a small silica gel pipette column, eluting with Skellysolve B-ethyl acetate-acetic acid (45:55:1). Altenusin (**18**) crystallized from the solvent as white flakes (5.0 mg), mp = 194-196°C (195-198°C, lit.[64]); tlc: R_f = 0.30 (toluene-acetone-acetic acid 50:50:1), 0.29 (Skellysolve B-ethyl acetate-acetic acid 45:55:1); ir (CH_2Cl_2-CH_3OH cast) ν_{max} cm^{-1}: 3600-2800 (br), 1645 (w), 1610, 1582, 1518, 1270, 1204, 1158; ^1H nmr ($CDCl_3$-CD_3OD 1:1, 400 MHz): δ 6.47 (1H, s, H-3' or H-6'), 6.40 (1H, s, H-3' or H-6'), 6.27 (1H, d, J=2.6 Hz, H-4 or H-6), 6.04 (1H, d, J=2.6 Hz, H-4 or H-6), 3.65 (3H, s, $OC\underline{H}_3$), 1.77 (3H, s, C-2' $C\underline{H}_3$); ^{13}C nmr ($CDCl_3$-CD_3OD 1:1, 100 MHz): δ 172.8 (s,

$\underline{C}O_2H$), 164.1 (s, C-3 or C-5), 163.1 (s, C-3 or C-5), 146.2 (s, C-1), 143.0 (s, C-4' or C-5'), 141.3 (s, C-4' or C-5'), 133.9 (s, C-1'), 126.6 (s, C-2'), 115.9 (d, C-3' or C-6'), 115.2 (d, C-3' or C-6'), 110.1 (d, C-6), 105.9 (s, C-2), 99.5 (d, C-4), 55.0 (q, $O\underline{C}H_3$), 18.5 (q, C-2' $\underline{C}H_3$); hrms m/z (relative intensity %) calc. for $C_{15}H_{14}O_6$ (M^+): 290.0790; found: 290.0788 (56), 272 (26), 246 (100), 245 (32), 244 (52), 216 (13), 215 (26); cims (NH_3): 247 ($M^+ - CO_2 + 1$, 93).

Dehydroaltenusin (**19**)

Dehydroaltenusin (**19**) was obtained by flash chromatography of the dichloromethane portion of the ethyl acetate broth extract, eluting with dichloromethane-methanol (97:3) (Schemes 17 and 22). The crude metabolite was further purified by flash chromatography, eluting with dichloromethane-methanol (99:1), and then passed through a small silica gel pipette column, eluting with Skellysolve B-ethyl acetate-acetic acid (50:50:1). It was further chromatographed in the same manner with dichloromethane-methanol (98:2). This afforded dehydroaltenusin (**19**) which still contained some impurities, ^1H nmr ($CDCl_3$, 400 MHz): δ 11.30 (1H, s, C-3' O$\underline{H}$), 6.73 (1H, d, J=2.3 Hz, H-4' or H-6'), 6.69 (1H, s, H-5), 6.63 (1H, d, J=2.3 Hz, H-4' or H-6'), 6.28 (1H, s, H-2), 3.91 (3H,s, O$\underline{C}H_3$), 1.73 (3H, s, C-6 $\underline{C}H_3$). It was allowed to stand at room temperature for 24 hours with acetic anhydride (0.3 mL, 3.5 mmol) and pyridine (0.3 mL, 4.1 mmol). Ethyl acetate (5.0 mL) and toluene (1.0 mL) were added to the reaction mixture and the solvents were removed under reduced pressure. This afforded the crude diacetate (**20**) which was purified by passage through a small silica gel pipette column, eluting with Skellysolve B-acetone (2:1). Dehydroaltenusin diacetate (**20**) crystallized from the solvents as white flakes (0.6 mg), mp = 190-193°C (185°C, lit.[64]); tlc: R_f = 0.39 (Skellysolve B-acetone 2:1), ir (CH_2Cl_2 cast) ν_{max} cm^{-1}: 1776,

1732, 1688, 1664, 1617, 1370, 1192, 1144, 800; ^{1}H nmr ($CDCl_3$, 400 MHz): δ 6.77 (1H, d, J=1.9 Hz, H-4'), 6.60 (1H, d, J=1.9 Hz, H-6'), 6.36 (1H, s, H-2), 6.30 (1H, q, J=1.4 Hz, H-5), 3.86 (3H, s, OCH_3), 2.42 (3H, s, $ArOCOCH_3$), 2.29 (3H, s, C-4 $OCOCH_3$), 1.73 (3H, d, J=1.4 Hz, C-6 CH_3); hrms m/z (relative intensity %) calc. for $C_{19}H_{16}O_8$ (M^+): 372.0845; found: 372.0848 (10), 330 (59), 288 (63), 270 (10), 260 (24), 244 (38), 232 (17), 194 (73), 193 (10), 165 (100); cims (NH_3): 390 (M^+ + 18, 100).

Desmethyldehydroaltenusin (**21**)

Desmethyldehydroaltenusin (**21**) was obtained by flash chromatography of the dichloromethane portion of the ethyl acetate broth extract, eluting with dichloromethane-methanol (97:3) (Schemes 17 and 22). The crude metabolite was further purified by dry flash chromatography, eluting with Skellysolve B-ethyl acetate-acetic acid (50:50:1). It was then passed through a small silica gel pipette column, eluting with dichloromethane-methanol (98:2). This afforded desmethyldehydroaltenusin (**21**) which was still somewhat impure. It was allowed to stand at room temperature for 24 hours with acetic anhydride (0.3 mL, 3.5 mmol) and pyridine (0.3 mL, 4.1 mmol). Ethyl acetate (5.0 mL) and toluene (1.0 mL) were added to the reaction mixture and the solvents were removed *in vacuo*. This afforded the crude triacetate (**22**) which was purified by passage through a small silica gel pipette column, eluting with Skellysolve B-acetone (2:1). Desmethyldehydroaltenusin triacetate (**22**) was obtained as an amorphous solid (1.0 mg), mp = 88-90°C; tlc: R_f = 0.33 (Skellysolve B-acetone 2:1); ir (CH_2Cl_2 cast) ν_{max} cm^{-1}: 1777, 1680, 1660, 1610, 1365, 1190, 1150, 1122, 1015; ^{1}H nmr ($CDCl_3$, 400 MHz): δ 7.10 (1H, d, J=1.7 Hz, H-4' or H-6'), 6.97 (1H, d, J=1.7 Hz, H-4' or H-6'), 6.37 (1H, s, H-2), 6.31 (1H, q, J=1.5 Hz, H-5), 2.43 (3H, s, $ArOCOCH_3$), 2.31 (3H, s,

$OCOCH_3$), 2.29 (3H, s, $OCOCH_3$), 1.74 (3H, d, J=1.5 Hz, C-6 CH_3); hrms m/z (relative intensity %) calc. for $C_{20}H_{16}O_9$ (M^+): 400.0794; found: 400.0784 (3), 358 (100), 316 (63), 274 (89), 256 (29), 246 (31), 230 (62), 218 (16); cims (NH_3): 418 ($M^+ + 18$, 100).

Talaroflavone (**23**) (Spiro[5'-hydroxy-2'-methyl-cyclopent-2'-ene-4'-one-1',3-7-hydroxy-5-methoxy-1(3H)-isobenzofuranone])

Talaroflavone (**23**) was obtained by flash chromatography of the dichloromethane portion of the ethyl acetate broth extract, eluting with dichloromethane-methanol (97:3) (Schemes 17 and 22). The crude metabolite was further purified by passing it through a small silica gel pipette column, eluting with Skellysolve B-ethyl acetate-acetic acid (45:55:1). It crystallized from the solvents as white flakes (3.0 mg), mp = 230°C (dec.); tlc: R_f = 0.25 (dichloromethane-methanol 97:3), 0.28 (Skellysolve B-ethyl acetate-acetic acid 45:55:1); $[\alpha]_D$ +181° (c 0.74, methanol); uv (methanol, 1.8 mg/100 mL) λ_{max} nm (log ε): 217 (4.19), 257 (3.66), 296 (3.28); 1 drop 0.1N NaOH: 228 (4.19), 256 (3.58), 325 (3.41); 1 drop 0.1N NaOH-1 drop 0.1N HCl: 216 (4.20), 257 (3.71), 295 (3.34); ir (methanol cast) ν_{max} cm^{-1}: 3240 (br), 1748, 1723, 1617, 1204, 1162, 1152, 1004; ^1H nmr (methanol-d_4, 400 MHz): δ 6.44 (1H, d, J=2.0 Hz, H-4 or H-6), 6.34 (1H, q, J=1.5 Hz, H-3'), 6.05 (1H, d, J=2.0 Hz, H-4 or H-6), 4.74 (1H, s, H-5'), 3.80 (3H, s, OCH_3), 1.86 (3H, d, J=1.5 Hz, C-2' CH_3); ^{13}C nmr (methanol-d_4, 100 MHz): δ 202.0 (s, C-4'), 171.4, 170.2, 168.5, (3 x s, C-1, C-2', C-5), 159.9 (s, C-7), 150.8 (s, C-3a), 131.4 (d, C-3'), 106.5 (s, C-7a), 103.5 (d, C-4 or C-6), 101.0 (d, C-4 or C-6), 94.2 (s, C-1'), 79.7 (d, C-5'), 56.5 (q, OCH_3), 13.4 (q, C-2' CH_3); hrms m/z (relative intensity %) calc. for $C_{14}H_{12}O_6$ (M^+): 276.0634; found: 276.0633 (100), 258

(64), 248 (30), 247 (21), 230 (17), 220 (39), 219 (64), 191 (24); cims (NH_3): 277 (M^+ + 1, 44), 294 (M^+ + 18, 76).

Acetylation of talaroflavone (**23**)

Pyridine (0.5 mL, 6.2 mmol) was added to a solution of talaroflavone (**23**, 4.0 mg, 0.014 mmol) in acetic anhydride (0.5 mL, 5.3 mmol). The reaction mixture was allowed to stand at room temperature for 22 hours. Ethyl acetate (5.0 mL) and toluene (1.0 mL) were added to the mixture and the solution was evaporated under reduced pressure. The crude acetylation product was passed through a small silica gel pipette column, eluting with Skellysolve B-acetone (2.5:1) to afford talaroflavone diacetate (**24**) as a clear, colorless oil (3.0 mg, 0.0083 mmol, 60% yield), tlc: R_f = 0.21 (Skellysolve B-acetone 2.5:1); ord (methanol, 3.0 mg/4.0 mL): $[\alpha]_{265}$ = +33°; cd (methanol, 3.0 mg/4.0 mL): $\Delta\Sigma_{235}$ = 6.3 $Lmol^{-1}cm^{-1}$; $\Delta\Sigma_{325}$ = 0.27 $Lmol^{-1}cm^{-1}$; ir (CH_2Cl_2 cast) ν_{max} cm^{-1}: 3080, 2920, 2840, 1777, 1732, 1621, 1491, 1371, 1256, 1221, 1189, 1143; ^1H nmr ($CDCl_3$, 400 MHz): δ 6.76 (1H, d, J=2.0 Hz, H-4 or H-6), 6.42 (1H, d, J=2.0 Hz, H-4 or H-6), 6.35 (1H, q, J=1.5 Hz, H-3'), 5.84 (1H, s, H-5'), 3.85 (3H, s, OCH_3), 2.39 (3H, s, $ArOCOCH_3$), 1.87 (6H, br s, C-5' $OCOCH_3$, C-2' CH_3); (methanol-d_4, 400 MHz): δ 6.93 (1H, d, J=2.0 Hz, H-4 or H-6), 6.61 (1H, d, J=2.0 Hz, H-4 or H-6), 6.49 (1H, q, J=1.5 Hz, H-3'), 5.81 (1H, s, H-5'), 3.89 (3H, s, OCH_3), 2.35 (3H, s, $ArOCOCH_3$), 1.86 (3H, d, J=1.5 Hz, C-2' CH_3), 1.82 (3H, s, C-5' $OCOCH_3$); ^{13}C nmr ($CDCl_3$, 100 MHz): δ 195.3 (s), 170.8 (s), 169.0 (s), 168.4 (s), 166.1 (s), 165.3 (s), 150.1 (s), 147.9 (s), 131.5 (d), 111.3 (s), 110.9 (d), 104.9 (d), 90.7 (s), 76.9 (d), 56.4 (q), 20.7 (q), 20.1 (q), 13.7 (q); (methanol-d_4, 100 MHz): δ 197.1 (s), 172.0 (s), 170.8 (s), 170.0 (s), 168.1 (s), 167.2 (s), 151.5 (s), 149.5 (s), 133.2 (d), 112.4 (s), 112.1 (d), 106.7 (d), 92.7 (s), 78.1 (d), 57.2 (q), 20.4 (q), 19.8

(q), 13.3 (q); hrms m/z (relative intensity %) calc. for $C_{18}H_{16}O_8$ (M^+): 360.0845; found: 360.0850 (12), 318 (100), 276 (97), 258 (99), 248 (6), 247 (25), 230 (6), 220 (10), 219 (24), 191 (4).

Talaroflavone *mono-p*-nitro benzoate (**25**)

A solution of talaroflavone (**23**, 3.8 mg, 0.014 mmol), *p*-nitrobenzoyl chloride (3.0 mg, 0.016 mmol), and pyridine (0.5 mL, 6.2 mmol) was allowed to stand at room temperature for 60 hours. The reaction mixture was taken up in ethyl acetate (2.0 mL) and toluene (0.5 mL) was added. The solvents were removed under reduced pressure to afford a cream colored solid which was purified by chromatography through a small silica gel pipette column, eluting with Skellysolve B-acetone (2:1). This procedure was repeated and the *mono-p*-nitrobenzoate of talaroflavone (**25**) crystallized from Skellysolve B-acetone (0.8 mg), tlc: R_f = 0.21 (Skellysolve B-acetone 2:1); ir (CH_2Cl_2 cast) ν_{max} cm^{-1}: 3430 (br), 1751, 1727, 1620, 1530, 1350, 1261; ^1H nmr ($CDCl_3$, 400 MHz): δ 8.45 (2H, d, J=9.0 Hz, Ar<u>H</u>), 8.39 (2H, d, J=9.0 Hz, Ar<u>H</u>), 7.04 (1H, d, J=1.9 Hz, H-4 or H-6), 6.42 (1H, d, J=1.9 Hz, H-4 or H-6), 6.38 (1H, q, J=1.5 Hz, H-3'), 4.84 (1H, s, H-5'), 3.89 (3H, s, OC<u>H</u>$_3$), 1.94 (3H, d, J=1.5 Hz, C-2' C<u>H</u>$_3$); hrms m/z (relative intensity %) calc. for $C_{21}H_{15}NO_9$ (M^+): 425.0747; found: 425.0735 (6), 276 (62), 258 (66), 248 (17), 247 (15), 230 (23), 220 (29), 219 (43), 191 (13).

Talaroflavone *di-p*-nitrobenzoate (**26**)

A solution of talaroflavone (**23**, 4.5 mg, 0.016 mmol), *p*-nitrobenzoyl chloride (6.7 mg, 0.036 mmol), and pyridine (0.5 mL, 6.2 mmol) was allowed to stand at room temperature for 72 hours. The reaction mixture was taken up in ethyl acetate (2.0 mL)

and toluene (0.5 mL) was added. The solvents were removed under reduced pressure to afford a cream colored solid which was purified by chromatography through a small pipette column of silica gel, eluting with Skellysolve B-acetone (2:1). This purification was repeated and afforded talaroflavone *di-p*-nitrobenzoate (**26**) as a white solid (0.5 mg), tlc: R_f = 0.45 (Skellysolve B-acetone 2:1); ir (CH_2Cl_2 cast) ν_{max} cm^{-1}: 1776 (sh), 1750, 1619, 1609, 1530, 1370, 1349, 1262, 1226, 718; ^1H nmr ($CDCl_3$, 400 MHz): δ 8.42 (2H, d, J=9.0 Hz, ArH), 8.37 (2H, d, J=9.0 Hz, ArH), 8.22 (2H, d, J=9.0 Hz, ArH), 7.93 (2H, d, J=9.0 Hz, ArH), 7.04 (1H, d, J=2.0 Hz, H-4 or H-6), 6.60 (1H, d, J=2.0 Hz, H-4 or H-6), 6.49 (1H, q, J=1.5 Hz, H-3'), 6.11 (1H, s, H-5'), 3.89 (3H, s, OCH_3), 2.00 (3H, d, J=1.5 Hz, C-2' CH_3); hrms m/z (relative intensity %) calc. for $C_{28}H_{18}N_2O_{12}$ (M^+): 574.0859; found: 574.0844 (8), 425 (4), 258 (45), 230 (27).

Deoxytalaroflavone (**27**)

Deoxytalaroflavone (**27**) was obtained by flash chromatography of the dichloromethane portion of the ethyl acetate broth extract, eluting with dichloromethane-methanol (97:3) (Schemes 17 and 22). It was further purified by flash chromatography, eluting with dichloromethane-methanol (99:1). This afforded white flakes of deoxytalaroflavone (**27**, 3.0 mg), mp = 178-180°C; tlc: R_f = 0.35 (Skellysolve B-acetone 2:1); ir (CH_2Cl_2 cast) ν_{max} cm^{-1}: 3400-2800 (br), 1713, 1679, 1610, 1565, 1390, 1239, 1226, 1200, 1109, 797, 733, 691; ^1H nmr ($CDCl_3$, 400 MHz): δ 11.35 (1H, s, C-3 OH), 6.70 (1H, d, J=2.3 Hz, H-4 or H-6), 6.69 (1H, d, J=2.3 Hz, H-4 or H-6), 3.94 (3H, s, OCH_3), 3.43 (1H, ddd, J=1.3, 6.6, 6.9 Hz, H-9), 2.95 (1H, dd, J=6.6, 19.0 Hz, H-8), 2.31 (1H, dd, J=1.3, 19.0 Hz, H-8'), 1.46 (3H, d, J=6.9 Hz, C-9 CH_3); ^{13}C nmr ($CDCl_3$, 100 MHz): δ 134.6 (s), 115.3 (s), 103.3 (d), 103.1 (d), 56.1 (q), 42.9 (t), 28.4 (d), 21.1 (q); hrms m/z (relative intensity %) calc. for $C_{14}H_{12}O_5$

(M^+): 260.0685; found: 260.0688 (100), 245 (8), 232 (16), 217 (45), 204 (8), 189 (13), 161 (19); cims (NH_3): 261 (M^+ + 1, 17), 278 (M^+ + 18, 100).

Compound 45s (**28**)

Compound 45s (**28**) was obtained by flash chromatography of the dichloromethane portion of the ethyl acetate broth extract, eluting with dichloromethane-methanol (97:3) (Schemes 17 and 22). It was further purified by flash chromatography, eluting with toluene-acetone-acetic acid (50:50:1), and then passed through a small silica gel pipette column, eluting with Skellysolve B-ethyl acetate-acetic acid (45:55:1). Compound 45s (**28**) crystallized from the solvent as white flakes (3.8 mg), mp = 233°C (dec.); tlc: R_f = 0.21 (toluene-acetone-acetic acid 50:50:1), 0.11 (Skellysolve B-ethyl acetate-acetic acid 45:55:1); ir (CH_2Cl_2-CH_3OH cast) ν_{max} cm^{-1}: 3600-2800 (br), 1710 (w), 1648, 1612, 1413, 1377, 1246, 1223, 1172, 1026; ^1H nmr ($CDCl_3$-CD_3OD 1:1, 400 MHz): δ 7.04 (1H, s, Ar<u>H</u>), 6.66 (1H, s, Ar<u>H</u>), 6.38 (1H, s, Ar<u>H</u>), 3.85 (3H, s, O<u>CH</u>$_3$), 2.36 (3H, s, Ar<u>CH</u>$_3$); ^{13}C nmr ($CDCl_3$-CD_3OD 1:1, 100 MHz): δ 173.7 (s), 169.1 (s), 165.6 (s), 162.4 (s), 136.3 (s), 133.0 (s), 128.7 (s), 125.3 (d), 124.0 (s), 113.2 (s), 97.2 (d), 94.3 (d), 92.5 (s), 55.7 (q, O<u>C</u>H$_3$), 17.5 (q, Ar<u>C</u>H$_3$); hrms m/z (relative intensity %) calc. for $C_{15}H_{12}O_7$ (M^+): 304.0583; found: 304.0589 (11), 287 (6), 260 (40), 259 (9), 258 (17), 232 (56), 216 (17), 200 (49), 188 (22), 173 (13), 145 (16), 115 (35), 57 (100).

PART 2. BIOLOGICAL ACTIVITY OF AND BIOSYNTHETIC STUDIES OF *TALAROMYCES FLAVUS* METABOLITES

IV. INTRODUCTION

As discussed in Part 1 of the thesis, one of the notable features of *T. flavus* rests in its effectiveness as a biological control for Verticillium wilt of eggplant, a disease caused by the fungus *V. dahliae*.[15] This disease moves slowly through the plant, stunting its growth and reducing fruit size, rather than killing. Neither crop rotation nor soil fumigants have been found to be effective in reducing losses from the disease. Crop rotation is not effective in reducing losses because the pathogen may persist as microsclerotia in the soil in the absence of a known host for many years. Soil fumigants delay the onset of symptoms and are used to reduce disease severity; however, their possible adverse effects on the environment and high cost disfavor their use.

The Verticillium wilt organism is a widespread soil inhabitant which infects a wide range of herbaceous and woody plants. Contact between host and pathogen is largely a random process, although physical and chemical stimuli may aid attraction, especially with soil borne pathogens. Penetration, and thereby infection, starts as soon as the two organisms are sufficiently intimate for their metabolic activities to affect each other. The penetration process may occur mechanically, enzymically, or passively. With Verticillium wilt, penetration occurs through the root system and progress is primarily in the xylem elements. The disease develops slowly, beginning with a yellowing of the lower leaves, causing a stunting of growth, and vascular discoloration. Following invasion, the pathogen establishes either a compatible or a noncompatible association with the host. In the compatible situation the diseased state ensues with the development of metabolic changes and symptom expression. One such change occurs in water relations. The main effect of vascular pathogens is to disrupt the passage of water through the stem. This may be attributed to the physical presence of the pathogen mycelium, development of tyloses which block the xylem, and gummosis within the

vessels. It is suggested that these mechanisms lead to failure on the part of the xylem vessels to transport an adequate supply of water to the other aerial organs. On the other hand, it is suggested that tyloses and gums are resistance mechanisms whereby the host limits the spread of the pathogen and that wilting is a result of dysfunction in cell permeability caused by toxins. The presence of parasites like *Verticillium* in vessels cause a 4 to 60 fold increase in the resistance of the stem to water flow. Further xylem occlusion comes from high molecular weight polysaccharides produced by the pathogen or cleaved from the xylem walls by hydrolytic enzymes. These block the pit membranes, reducing lateral water flow, and occluding the small vessels in petioles and leaves.

On the other hand, the incompatible state occurs when host defence mechanisms are successful and further development of the pathogen is prevented. Such defence mechanisms may by physical or chemical. Physical defence may occur with the formation of lignitubers and/or tyloses. The former is a corky or gum-like substance deposited in or between cortical cells preventing further invasion by the fungus. The term lignituber describes the thickenings formed on these cell walls opposite the penetrating hyphae of the invading fungus. The chemical composition of lignitubers consists of an inner region of cellulose, deposited around the advancing hyphae, encased in an outer layer of lignin. This defence mechanism has been found to occur in some hosts of *Verticillium* species, including *V. dahliae*. The other defence mechanism found in hosts invaded by *Verticillium* species is the formation of tyloses. These are swellings of xylem parenchyma or medullary ray cells which protrude into the xylem vessels. Some think of them as resistance mechanisms for vascular wilt diseases; however, it seems more likely that they result from weakening of the xylem vessel walls due to enzymic action by the pathogen and, hence, indicate host susceptibility.[83,84]

Verticillium dahliae is the cause of a wilting disease in a wide variety of host organisms, most severely in eggplant, tomato, potato, and cotton and to a lesser extent in

olive, rose, American elm, maple, sugar maple, peanut, sesame, pistachio, almond, grape, apricot, watermelon, spearmint, sumac, pea, mum, strawberry, sweet pepper, cantaloupe, sugar beet, horseradish, mint, soybean, and flax. Among isolates of this species, there is considerable variation in morphology and pathogenicity. Generally, the pathogenicity of isolates of *V. dahliae* is nonspecific, although some isolates have restricted or unique host ranges.[85,86] Some species have been classified into races, race one and race two, depending on their pathogenicity.[87] A much broader classification of isolates of *V. dahliae* is based on heterokaryon incompatibility. *Verticillium dahliae* is an imperfect fungus. Strains of *V. dahliae* may exchange genetic information through heterokaryosis and parasexuality. As the fungus has no known sexual cycle, these processes may be its only means of gene exchange. If two isolates can not form heterokaryons they are, in effect, genetically isolated. Such isolates are viewed as belonging to distinct populations, termed vegetative compatibility groups, within the species. Recently, 96 strains of *V. dahliae* isolated from 38 different host-plant species in 15 countries were tested for the ability to form heterokaryons with each other.[86] The strains were classified into vegetative compatible groups. Strains within a vegetative compatible group formed heterokaryons with each other but not with strains from a different group. It is suggested that this species may be viewed in two ways: as a single population of strains that can readily alter their virulence patterns so that they may attack any host plant or as a collection of morphologically similar strains that are partitioned into a finite number of genetically isolated groups, each with specific virulence capabilities. The data favor the latter view in that not every strain of *V. dahliae* has the same potential for virulence and host range. We were initially working with a *V. dahliae* strain isolated from tomato. This strain gave us problems in developing a reliable bioassay to follow the antifungal activity of *T. flavus* against *V. dahliae*. After discovering that there is such a diversity in the pathogenicity of strains of *V. dahliae*, we obtained a strain of *V. dahliae*

isolated from eggplant with which we were able to develop a reliable bioassay to follow the antifungal activity.

Five polyketide metabolites are reported to have been isolated from *V. dahliae*.[88,89] These are (-) vermelone, (+) scytalone, *cis*-4-hydroxyscytalone, juglone, and flaviolin (Figure 19),

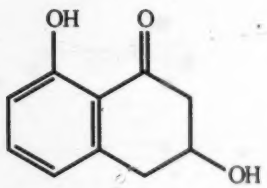

(-) vermelone

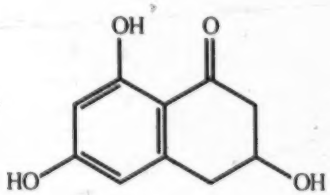

(+) scytalone

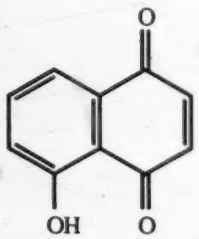

juglone

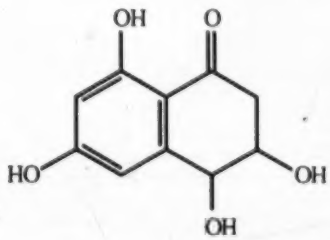

cis-4-hydroxyscytalone

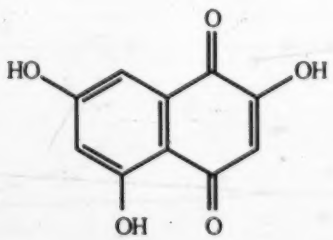

flaviolin

Figure 19. Metabolites isolated from *Verticillium dahliae*

In attempting to determine the mode of action of *T. flavus* against *V. dahliae*, a plug to plug bioassay was performed. The two fungi are inoculated parallel to one another on the same plate *ca.* 5 cm apart. After *ca.* two weeks growth, there is a definite area between the fungi which shows no growth; however, there are no obvious signs of intermingling or broken hyphae. Thus, there seems to be no antagonism of *V. dahliae* by *T. flavus* as such.[19] Although the mechanism of biological control of *V. dahliae* by *T. flavus* is not clearly understood, we engaged in an investigation of the water soluble metabolites of the *T. flavus* fungal broth with the hope that one or more of them would possess the antifungal activity displayed by *T. flavus*.

V. RESULTS AND DISCUSSION

Biological Activity and the *Talaromyces flavus* Broth

Talaromyces flavus proves to be a source of a number of organic secondary metabolites as discussed in the first part of this thesis. Interest in investigating the aqueous broth of *T. flavus* arises from the report[15] of utilizing *T. flavus* as a biological control agent for Verticillium wilt of eggplant, a disease caused by the fungus *V. dahliae*. Initially, a bioassay was developed to observe the antifungal activity of *T. flavus* against *V. dahliae* (Plate 1). This involves seeding an agar plate with *V. dahliae* and then injecting 100μL of the *T. flavus* broth into a small stainless steel vessel placed in the center of the plate. This sample diffuses into the medium and after 7-10 days the bioassay results are noted. An interesting effect in the growth of *V. dahliae* is observed. This fungus produces two types of spores; white conidial spores and black chlamydospores. These black chlamydospores are part of the microsclerotia and are the means by which *V. dahliae* survives in the soil. The microsclerotia store many nutrients and, thus, germinate easily. On the other hand, the white conidial spores do not survive as long as they store fewer nutrients. In this bioassay, a large zone of inhibition by the *T. flavus* aqueous broth is observed toward the production of microsclerotia by *V. dahliae* (Plate 1). It seems that by controlling *V. dahliae* microsclerotia production *T. flavus* controls Verticillium wilt of eggplant.

A number of aqueous separation techniques were utilized in an attempt to isolate the metabolite(s) responsible for this antifungal activity. In all experiments, this bioassay procedure described above was used to follow the biological activity. One of the more notable characteristics of the *T. flavus* broth is its pH. After four weeks growth, the pH of the broth is *ca.* 2.5 - 3.0. It is also found that this pH is obtained after *ca.* five days growth. The initial pH is 5.8 at t = 0 days and after just five days, the pH has fallen to

THE QUALITY OF THIS MICROFICHE IS HEAVILY DEPENDENT UPON THE QUALITY OF THE THESIS SUBMITTED FOR MICROFILMING.

UNFORTUNATELY THE COLOURED ILLUSTRATIONS OF THIS THESIS CAN ONLY YIELD DIFFERENT TONES OF GREY.

LA QUALITE DE CETTE MICROFICHE DEPEND GRANDEMENT DE LA QUALITE DE LA THESE SOUMISE AU MICROFILMAGE.

MALHEUREUSEMENT, LES DIFFERENTES ILLUSTRATIONS EN COULEURS DE CETTE THESE NE PEUVENT DONNER QUE DES TEINTES DE GRIS.

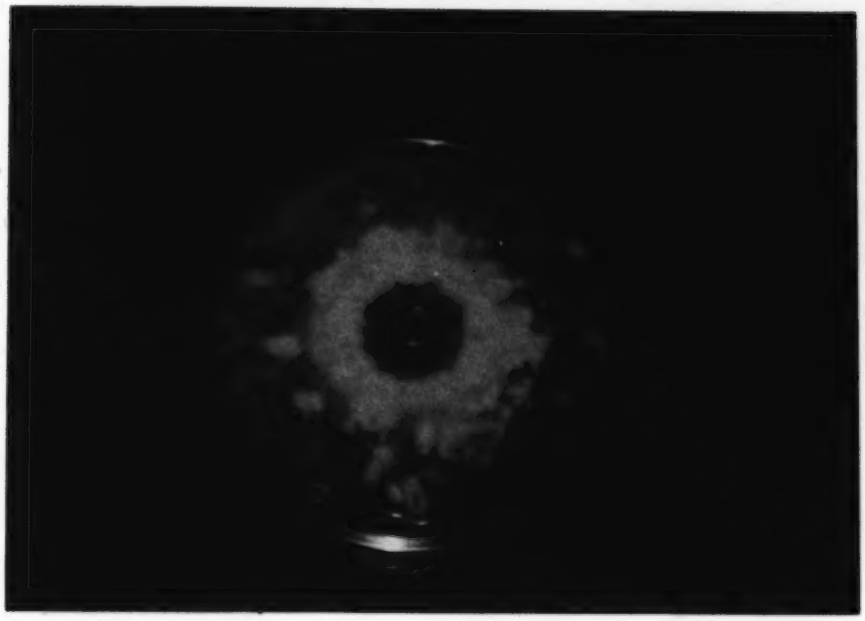

Plate 1. The antifungal bioassay. *Talaromyces flavus versus Verticillium dahliae*

ca. 2.8. A pH study, in which the antifungal bioassay was performed at pH's 3, 4, and 5, revealed that the clear zone in the center of the plate (Plate 1) decreased in size with increasing pH; however, at all three pH's the microsclerotia did not form. Thinking that an acid may be responsible for this activity, a 5% calcium chloride solution was added to a portion of the broth in an attempt to precipitate oxalic acid. This attempt failed. Ion exchange chromatography was then performed, using cation and anion exchange columns. Attempting to trap the active component on the column and then wash it off or have it pass straight through failed to result in any purification. The activity was lost as the bioassay results were negative. In an attempt to methylate the acid and, perhaps, render it water insoluble, a portion of the broth was treated with diazomethane. Again, this failed to produce positive results. Steam distillation was attempted in an effort to remove the active component if it were volatile. This did not succeed as the fungal broth gave a positive bioassay result after the distillation, while the distillate showed no inhibition of microsclerotia production. A small sample of the broth was passed through small Sep-Pak cartridges (C_{18} and amino) to see if any separation could be achieved; however, the activity was lost. Iron (II) sulfate and iron (III) nitrate were added individually to see if there existed an active metabolite capable of chelation with iron. No chelate extracted into organic solvent and the fungal broth retained its activity. The ^1H nmr spectrum (methanol-d_4-D_2O) of the fungal broth consists of resonances between 3 and 5 ppm. This suggests that all of the components in the aqueous broth are sugars or related oxygenated compounds. Attempts to remove the sugars by chromatography over charcoal and Celite resulted in the loss of biological activity. Reverse phase chromatography showed some promise initially; however, no solvent system could be found which would give both good chromatographic separation and be miscible with the aqueous broth. With this difficulty in continually losing the antifungal activity, a portion of the broth was autoclaved to determine if a heat sensitive compound - an enzyme or a

protein, for example - was responsible for this biological activity. Only a slight loss in activity was observed. In addition, a dialysis was performed with tubing of molecular weight cut off (MWCO) 1,000. After 24 hours, the contents of the dialysis bag (the fungal broth) had lost its activity, implying that the molecular weight of the active compound(s) was less than 1,000. Only chromatography over Sephadex G-50, eluting with water, or Bio-Gel P-2, eluting with water-ethanol (90:10) gave positive bioassay results. The latter active fractions from the column were pooled. Further chromatography over Sephadex LH-20 resulted in loss of activity. The active fractions from Sephadex G-50 (or Bio-Gel P-2) chromatographies were subjected to acetylation (acetic anhydride/pyridine). This afforded two spots by tlc, which were separated by flash chromatography. The major fraction (*ca.* 66%) appears to be, from its ^1H nmr spectrum, a mixture of acetylated sugars; however, the spectrum of the minor portion (*ca.* 33%) suggests that this fraction contains more than one compound. It is shown by gas chromatographic analysis to be a mixture of three compounds. Gas chromatographic mass spectral separation shows that these acetates have molecular weights of 226, 286, and 346. Despite the fact that hydrolysis of these acetates, with potassium carbonate in methanol or triethylamine in methanol, reveals that none shows antifungal activity, their identification was pursued. These three acetates appear as one spot by tlc; however, with repeated chromatography they are isolated in pure form. The acetate **30** of the first metabolite (**29**), has a molecular weight of 226 and a molecular formula of $C_{10}H_{10}O_6$, as determined by hrms. This compound (**30**) is a diacetate, as evidenced by its loss of two molecules of ketene (m/z 184 (66), 142 (100)) in the mass spectrum. The base peak at m/z 142 corresponds to the molecular formula of the alcohol **29**, $C_6H_6O_4$. The ir spectrum of **30** shows acetate absorptions at 1780 and 1741 cm^{-1}. Bands at 1656 and 1585 cm^{-1} are consistent with those of a γ-pyrone.[52] The uv spectrum of **30** (λ_{max} 292 nm) is consistent with a γ-pyrone chromophore.[90] This absorption band shows no

bathochromic shift on addition of base. The ^{1}H nmr spectrum shows vinylic hydrogens at 7.06 and 6.24 ppm (each a doublet, J = 7.0 Hz), an acetylated methylene group at 4.83 ppm, and acetate methyl signals at 2.30 and 2.12 ppm. The carbons of these acetates are seen at 170.0 (s), 167.9 (s), 20.6 (q), and 20.4 (q) ppm in the ^{13}C nmr spectrum, together with singlet carbons at 157.1, 155.6, and 137.0 ppm, doublet carbons at 130.5 and 103.8 ppm, and a methylene carbon at 61.3 ppm. These data are consistent with the diacetate of the γ-pyrone, hydroxymethylmaltol (**29**). Compound **29** is an isomer of kojic acid, a known antibiotic produced by a variety of microorganisms.[91] The ^{1}H and

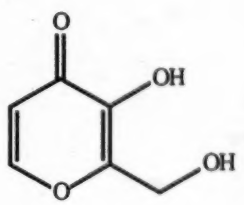

29

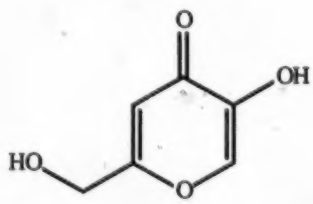

kojic acid

^{13}C nmr assignments are shown in Figure 20. The carbonyl carbon at 157.1 ppm shows a long range three bond coupling ($^{3}J_{CH}$) of 8 Hz with the C-6 hydrogen at 7.06 ppm. This agrees with the size of the coupling constant expected for this system.[92]

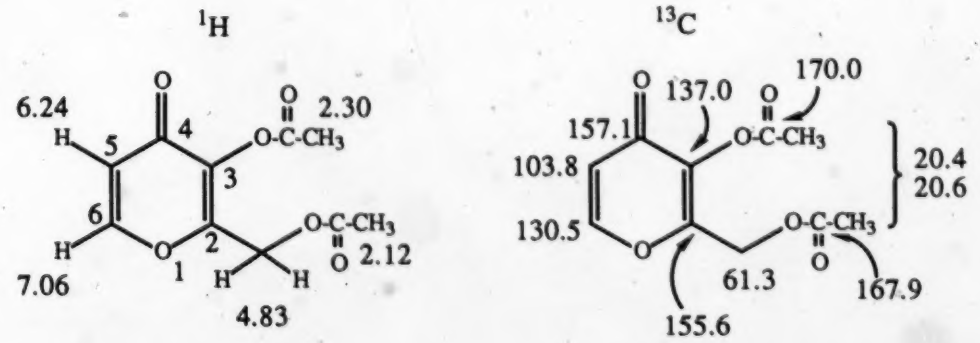

Figure 20. The ^{1}H and ^{13}C nmr assignments for hydroxymethylmaltol diacetate (**30**)

The isolation of hydroxymethylmaltol (**29**) (as its acetate **30**) is not surprising as the medium on which the fungus grows is a malt extract one.

The second of the three acetates isolated is a triacetate (**32**) as acetate methyl signals are seen in the ^{1}H nmr spectrum at 2.25, 2.11, and 2.08 ppm, together with ^{13}C nmr signals at 170.3 (s), 169.6 (s), 168.0 (s), 20.6 (q), 20.5 (q), and 20.2 (q) ppm. One acetate is lost as acetic acid and the other two acetates as ketene to afford the base peak at m/z 142. The mass spectral fragmentation is summarized in Scheme 23. The

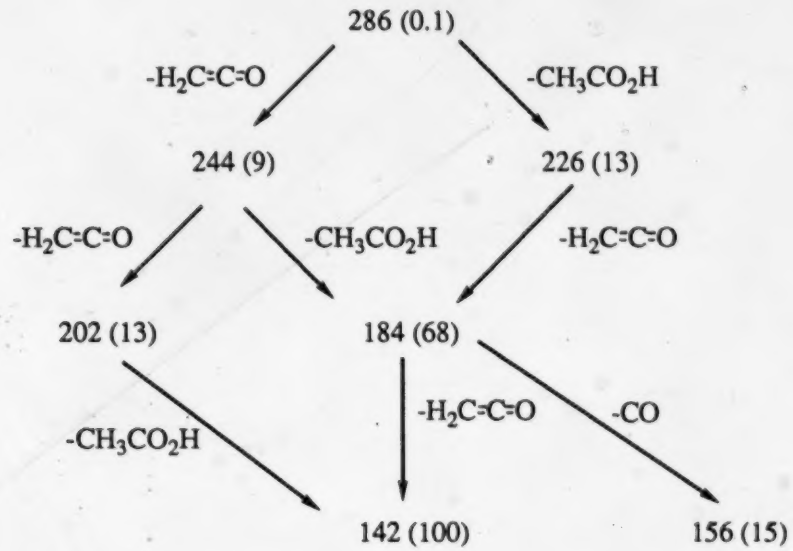

Scheme 23. The mass spectral fragmentation of acetate **32**

parent ion at m/z 286 corresponds to a molecular formula of $C_{12}H_{14}O_8$. This is confirmed by cims (304, $M^+ + 18$, 100). The ir spectrum shows acetate carbonyl bands at 1778 and 1750 cm^{-1}, together with double bond absorptions at 1665, 1655, and 1580 cm^{-1}. The ^{1}H nmr spectrum shows, in addition to the three acetate methyl groups, the spin system illustrated in Figure 21. The ^{13}C nmr spectrum consists of six carbons, in

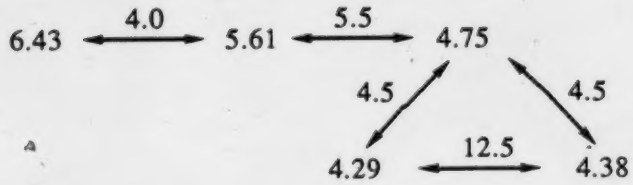

Figure 21. The ^{1}H-^{1}H couplings of acetate **32**

addition to those of the acetates, at 157.1 (s), 139.8 (s), 125.9 (d), 77.9 (d), 64.3 (d), and 62.0 (t) ppm. These data are consistent with the five- and six-membered ring enol acetates shown below.

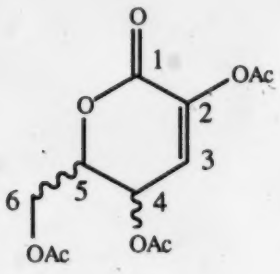

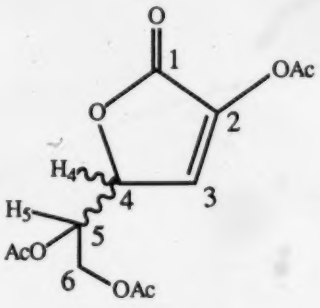

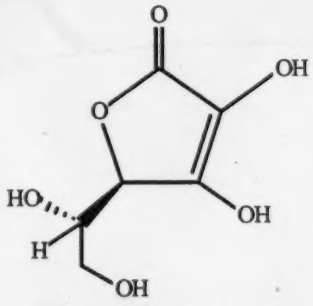

ascorbic acid

The coupling constant between H-4 and H-5 is 5.5 Hz. In ascorbic acid and derivatives of it, the coupling constant between H-4 and H-5 is 1.5 Hz.[93] Thus, it seems that the six-membered ring structure is more probable. The proposed structure for **32** is the triacetate of 3-deoxy-*threo*-1,5-lact-2-ene-1-one (**31**). Although the stereochemistry of compound **31** was not determined, it seems probable that it is derived from D-glucose as this sugar is a component of the medium. The ^{1}H and ^{13}C nmr assignments are shown in Figure 22.

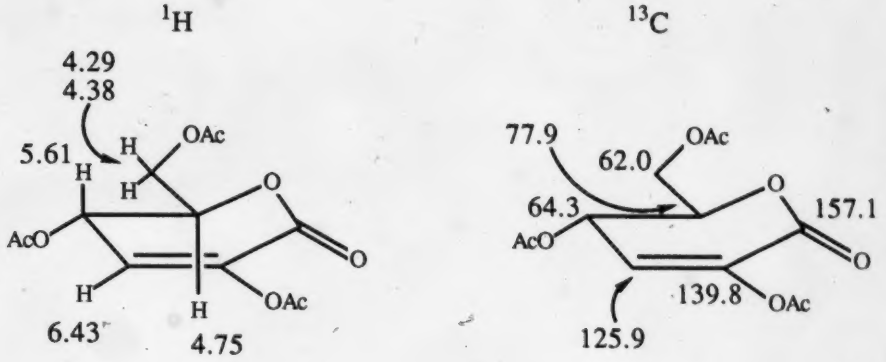

Figure 22. The ^{1}H and ^{13}C nmr assignments for acetate **32**

This unsaturated lactone (**31**) may form by dehydration of D-glucono-1,5-lactone (Scheme 24).

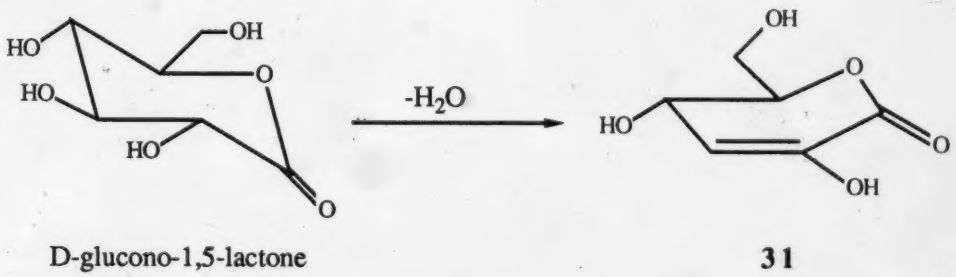

Scheme 24. Possible pathway for the formation of compound **31**

The origin of D-glucono-1,5-lactone in the fungal broth is related to the isolation of the acetate **9** of metabolite **8**. The spectral data of acetate **9** was familiar as the hydroxy compound **8** was isolated from the fungal broth extract (Part 1 of this thesis). Compound **9** is the tetraacetate of D-glucono-1,4-lactone (**8**). As mentioned in the first part of the thesis, D-glucono-1,4-lactone (**8**) is one of the three most abundant metabolites produced by the fungus. A clue as to the mechanism of biological control of *V. dahliae* by *T. flavus* rests with metabolite **8**. Although this metabolite shows some antibacterial activity (Table 27), it possesses no antifungal activity against *V. dahliae*. It

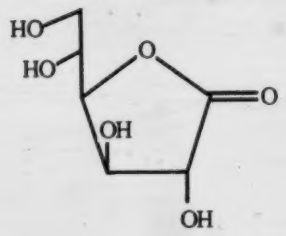

D-glucono-1,4-lactone (**8**)

is one of two products produced in the oxidation of D-glucose by glucose oxidase. The isolation of this enzyme from *T. flavus* is reported[94] this year. This enzyme is an oxidoreductase, oxidizing D-glucose to D-gluconic acid.[95] (Figure 23). Glucose oxidase is highly specific for β-D-glucose.[96] Its anomer, α-D-glucose, is oxidized 150 times more slowly. Although the kinetics and mechanism of the action of glucose oxidase have been studied,[97] no report discusses the structure of the oxidized product, other than to mention that it is the acid or one of the lactones. The primary products of the oxidation of an aldose could be the aldonic acid, the γ-, or the δ-lactone.[36] These are interconverted fairly readily in aqueous solution and the proportions of each depend on the pH. The δ-lactone has been shown, by means of optical rotation studies, to be the predominate kinetically controlled product of the oxidation of both forms of glucose. Hydrolysis of the δ-lactone followed by relactonization affords the thermodynamically more stable γ-lactone (**8**). The greater rate of hydrolysis of the δ-lactone compared to the γ-lactone is usually ascribed to relief of the unfavorable eclipsing interaction between the carbonyl group and the equatorial substituent at C-2 on going to the transition state.

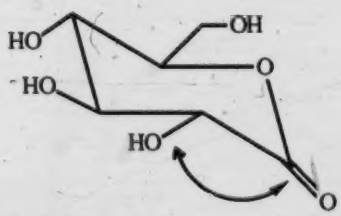

D-glucono-1,5-lactone

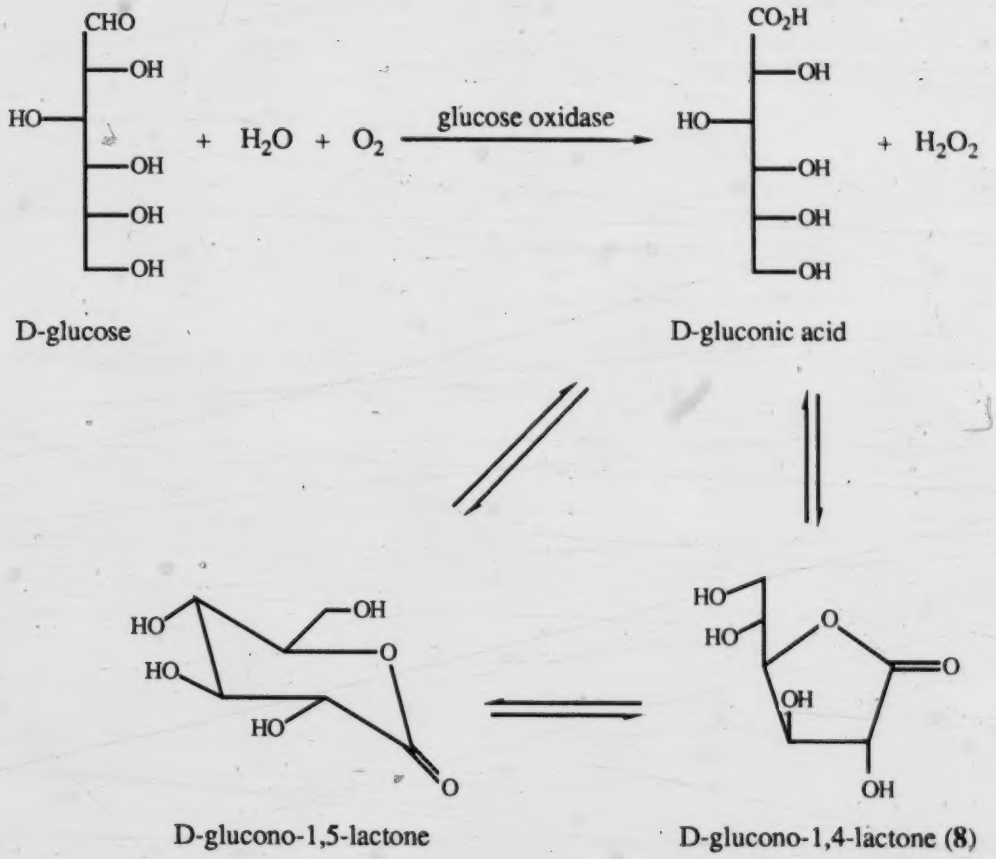

Figure 23. Oxidation of D-glucose by glucose oxidase

D-Glucono-1,5-lactone was not itself isolated from the broth; however, it may have been the major product of the oxidation reaction which then undergoes either dehydration to compound **31** or hydrolysis to the thermodynamically more stable[98,99] γ-lactone (**8**).

The other product of this enzyme oxidation is hydrogen peroxide. This peroxide inhibits microsclerotia production by *V. dahliae* as illustrated in Plate 2. This photograph shows three different concentrations of hydrogen peroxide, 2.7, 3.6, and 7.5 μL/mL. As the concentration of peroxide is increased, microsclerotia production by *V. dahliae* is reduced. The plate in the top left hand corner shows that microsclerotia production is

Plate 2. The effect of hydrogen peroxide on *Verticillium dahliae* chlamydiospore production: [H_2O_2] a) 2.7 µL/mL, b) 3.6 µL/mL, c) 7.5 µL/mL; d) *Talaromyces flavus* broth + catalase

restored after catalase[100] has been added to the broth. This enzyme breaks down hydrogen peroxide according to the equation illustrated in Figure 24.

$$2\,H_2O_2 \xrightarrow{\text{catalase}} 2\,H_2O + O_2$$

Figure 24. Action of catalase

Paper chromatography was utilized in an attempt to detect hydrogen peroxide in the broth by spraying with a ferrous cyanate reagent;[101,102] however, no coloration was observed. As it has been reported that the concentration of peroxide in the *T. flavus* broth is low (12μg/mL),[94] a more sensitive test for detecting hydrogen peroxide was employed.[103] This test determines the concentration of a peroxide solution and is based upon the reaction illustrated in Figure 25. The first reaction (1) is catalyzed by horseradish peroxidase (HRP).[100] In the presence of excess iodide, the iodine formed in (1) reacts

$$H_2O_2 + 2\,H^+ + 2\,I^- \xrightarrow[\text{peroxidase (HRP)}]{\text{horseradish}} I_2 + 2\,H_2O \quad (1)$$

in excess iodide

$$I_2 + I^- \rightleftharpoons I_3^- \quad (2)$$

triiodide ion $\varepsilon_{353} = 2.55 \times 10^4\ M^{-1}cm^{-1}$

Figure 25. The triiodide ion peroxide assay

with iodide and exists in equilibrium with the triiodide ion (2). This ion has an extinction coefficient (ε) at 353 nm of $2.55 \times 10^4\ M^{-1}cm^{-1}$. The change in absorbance at 353 nm is measured after completion of the reaction and, from this, the concentration of peroxide may be obtained. This experiment was performed using a 1 μL sample of the fungal broth; however, a very small change in the absorbance at 353 nm was seen. A 100 mL

aliquot of the broth ([1L] concentrated from the 10L batch grown) was concentrated to 10 mL. The enzyme assay resulted in a $\Delta A_{353} = 0.0357$ (see Appendix). It is known for this procedure that 0.1 M hydrogen peroxide gives $\Delta A_{353} = 0.255$.[104] From this, it is determined that the concentration of hydrogen peroxide in the broth per litre is *ca.* 50 mg or 50 μg/mL. The concentrations of hydrogen peroxide utilized in the bioassay to see inhibition of the growth of microsclerotia (Plate 1) are in the range of 100-120 μg/mL. This is a higher concentration than that determined from the ultraviolet study; however, the latter was performed a few months after the former. Perhaps some of the hydrogen peroxide had decomposed. Although this ultraviolet experiment for determining the concentration of a peroxide is not specific for hydrogen peroxide, the fact that addition of catalase to the fungal broth destroys the inhibitory effect *T. flavus* has on the production of microsclerotia by *V. dahliae* strongly supports the proposal that hydrogen peroxide is the causative agent of the antifungal activity. *Tert*-butylhydroperoxide was also tested for antifungal activity; however, it displayed little inhibition of microsclerotia production by *V. dahliae*.

If the concentration of hydrogen peroxide in the broth is as low as 50 μg/mL, there could be more than 2.5 g of oxidized glucose products (acid and lactone) produced. Only *ca.* 200 mg of the lactone (**8**) was isolated; however, this does not represent the maximum amount of **8** that may have been produced. Although the proportion of acid:δ-lactone:γ-lactone in the fungal broth is not known, there may be a significant proportion of acid (pK_a 3.81) present which contributes to the acidic pH of the broth.

Talaromyces flavus and *V. dahliae* are soil fungi and the antifungal activity between them occurs in the soil. Our studies, which involve growing *T. flavus* in still culture and utilizing the bioassay developed for use on an agar plate, would appear to mimic nature well.

Biosynthetic Studies of *Talaromyces flavus* Metabolites

As discussed in Part 1 of this thesis, a few of the metabolites isolated from *T. flavus*, previously unreported from nature, were thought to be biosynthetically interesting. The metabolites from the broth extract whose biosyntheses we were most interested in studying are 4,6-dihydroxy-5-methylphthalide (**10**), 4-carboxy-5-hydroxyphthalaldehydic acid methyl ester (**15**), and the spiro metabolite, talaroflavone (**23**). These three metabolites, along with the remainder of those isolated from *T. flavus*, have a polyketide biogenesis and, thus, [1-^{13}C] labelled sodium acetate was chosen as the precursor for the biosynthetic studies. This precursor was fed to the fungus after 9, 16, and 23 days growth and the fungus was harvested after 30 days. [1-^{13}C] Labelled sodium acetate was fed in 3-10.0 mmol batches (1.0 mmol/L fungus). The advantage of multiple over single-dose feeding lies in the opportunity it affords to maintain a steady precursor concentration while avoiding the toxic effects due to excessively high concentrations.[105]

In order to follow the labelling pattern of ^{13}C enriched metabolites, it is first necessary to assign the chemical shifts of the carbons in the ^{13}C nmr spectrum to the carbons of the metabolite. The assignment of the chemical shifts of the carbon atoms of 4,6-dihydroxy-5-methylphthalide (**10**) was discussed in Part 1 of the thesis. Table 24 depicts the ^{13}C nmr assignment for this metabolite (**10**).

The biosynthesis of phthalide metabolites is interesting as two phthalide backbones are known in nature: one in which the hydroxyl group is *peri*- to the carbonyl and the other in which the aromatic hydrogen is *peri*- to the carbonyl. Representative examples of the two regioisomeric groups are illustrated in Figure 26. The biogenesis of both regioisomers may be envisaged by cyclization of a tetraketide precursor and methylation by S-adenosylmethionine (SAM) to afford the known metabolite, 3-methyl-

Table 24. The ^{13}C nmr assignment of 4,6-dihydroxy-5-methylphthalide (**10**)

	δ_C (ppm, methanol-d_4)
C-1	174.2
C-3	69.7
C-3a	126.3
C-4	151.5
C-5	120.5
C-6	159.1
C-7	102.1
C-7a	124.7
C-5 $\underline{C}H_3$	9.2

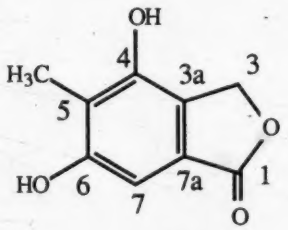

10

orsellinic acid[106,107] (Scheme 25). Oxidation of the methyl group (left path) affords the hydroxy acid, which may then cyclize to 5,7-dihydroxy-6-methylphthalide, a known natural product,[45,108] and other metabolites with this phthalide backbone, like nidulol (Figure 26). 5,7-Dihydroxy-4-methylphthalide (Figure 26) possesses the same backbone as its isomer, the 6-methyl metabolite; however, it is methylated at a different carbon. On the other hand, formation of the phthalide **10** isolated from *T. flavus*, and its O-methylated derivatives (Figure 26), is more interesting as it seems to involve a reduction of the acid moiety, in addition to the oxidation of the methyl group. This reduction of the acid is a transformation not commonly encountered in the biosynthesis of polyketides. Possible intermediates of differing oxidation states along the pathway include 3,5-dihydroxy-4-methylphthalaldehydic acid, a known natural product,[60] which has been implicated as a precursor in the formation of metabolite **15**. Reduction of the aldehyde to the alcohol and lactonization affords the regioisomer 4,6-dihydroxy-5-methylphthalide

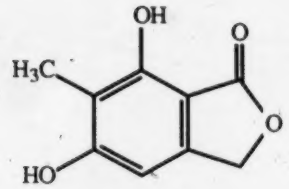

5,7-dihydroxy-6-methylphthalide
Alectoria nigricans[108]
Aspergillus duricaulis[45]

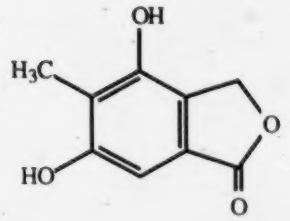

4,6-dihydroxy-5-methylphthalide (**10**)
Talaromyces flavus

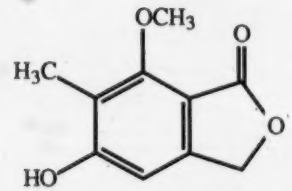

5-hydroxy-7-methoxy-6-methylphthalide
(nidulol)
Aspergillus silvaticus[47]
Aspergillus duricaulis[45]

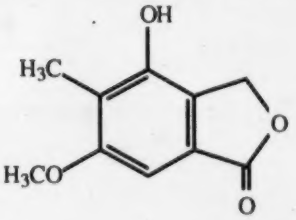

4-hydroxy-6-methoxy-5-methylphthalide
Aspergillus duricaulis[45]

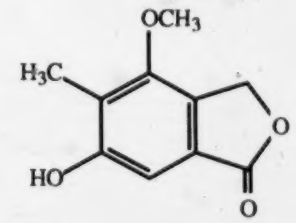

6-hydroxy-4-methoxy-5-methylphthalide
(silvaticol)
Aspergillus silvaticus[47]

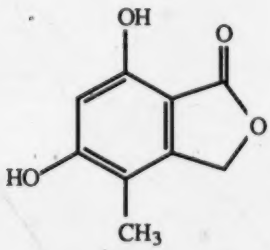

5,7-dihydroxy-4-methylphthalide
Aspergillus flavus[109]

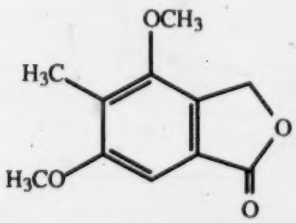

4,6-dimethoxy-5-methylphthalide
(Q-methylsilvaticol)
Aspergillus silvaticus[47]

Figure 26. Examples of the two regioisomeric phthalide backbones

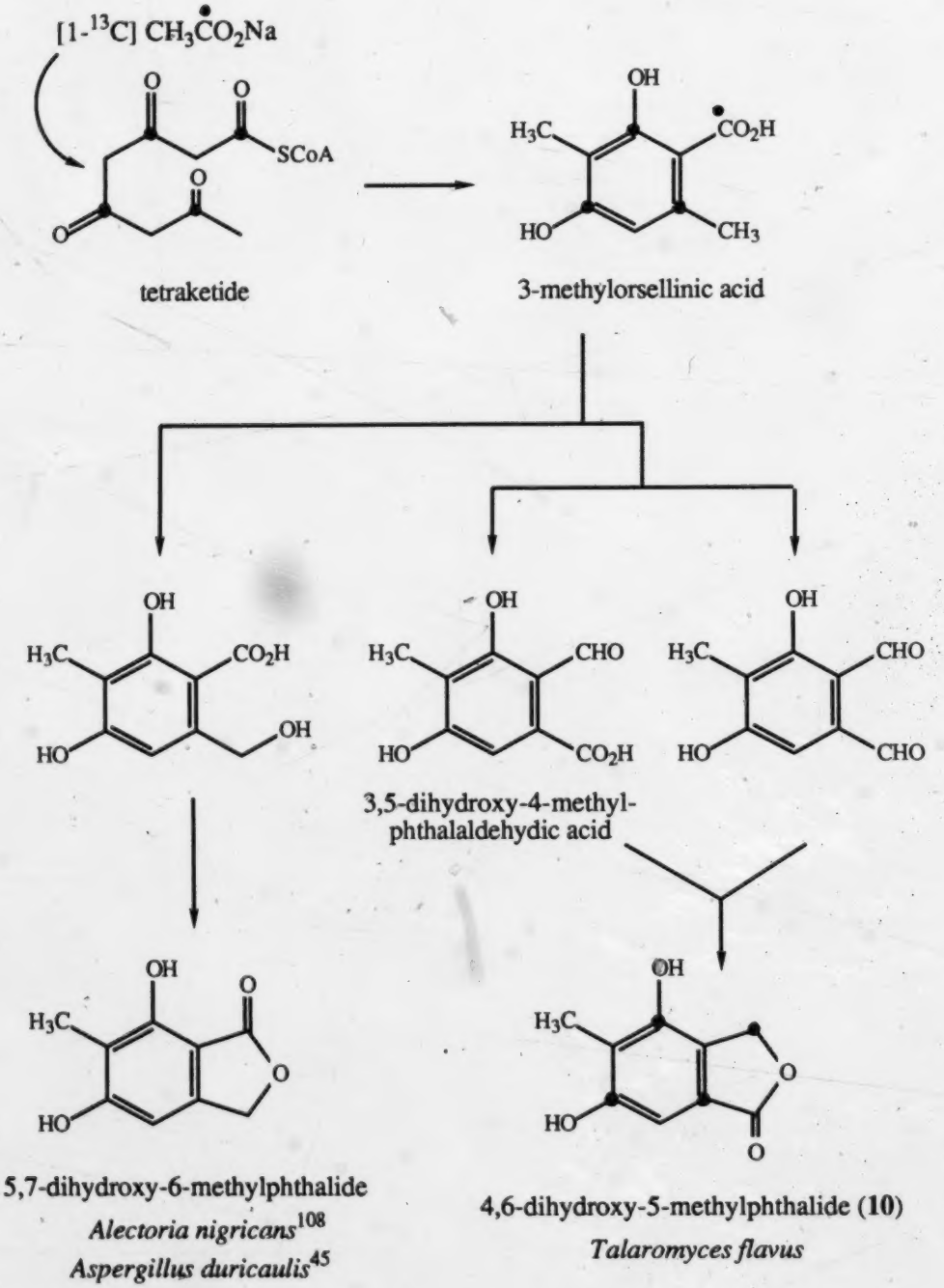

Scheme 25. Proposed biosynthetic pathway to the regioisomeric phthalide skeletons

(**10**). Another possible intermediate is the dialdehyde shown, which by means of a biological Cannizzaro reaction, would result in the regioselective formation of the natural product **10**. This reaction is known for the *mono*-O-methyl derivative, quadrilineatin, a natural product from *Aspergillus quadrilineatus*[110] (Figure 27).

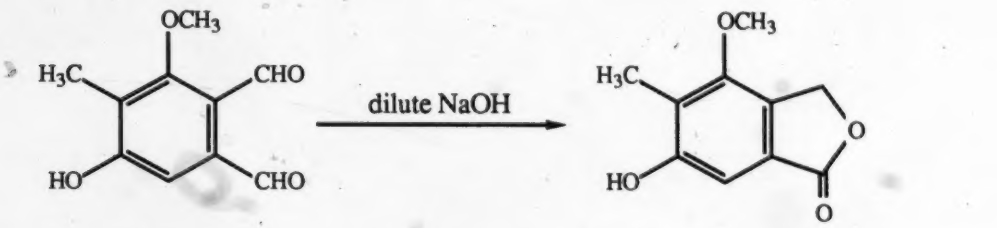

quadrilineatin
Aspergillus quadrilineatus[110]

6-hydroxy-4-methoxy-5-methylphthalide
(silvaticol)
Aspergillus silvaticus[47]

Figure 27. Cannizzaro reaction of quadrilineatin

Treatment of quadrilineatin with dilute sodium hydroxide affords, exclusively, 6-hydroxy-4-methoxy-5-methylphthalide, a metabolite isolated from *A. silvaticus*[47] and given the name silvaticol.

Feeding [1-^{13}C] labelled sodium acetate labels the tetraketide as shown in Scheme 25. Its incorporation into 3-methylorsellinic acid is at the four centers depicted. If the oxidation-reduction sequence of the methyl and acid groups, respectively, is occurring, then the methylene carbon of **10**, which arises from C-1 of acetate, should be labelled, while the carbonyl carbon, originating from C-2, should not show enrichment. Figure 28 shows the results of this labelling study. The ^{13}C nmr spectrum of the labelled phthalide compared to that at natural abundance shows label has been incorporated at four carbons. These enhanced signals include the phenolic carbons at 159.1 and 151.5 ppm, the quaternary ring junction carbon at 124.7 ppm, and an intense signal for the methylene carbon at 69.7 ppm. These are the four carbons that are expected to have incorporated

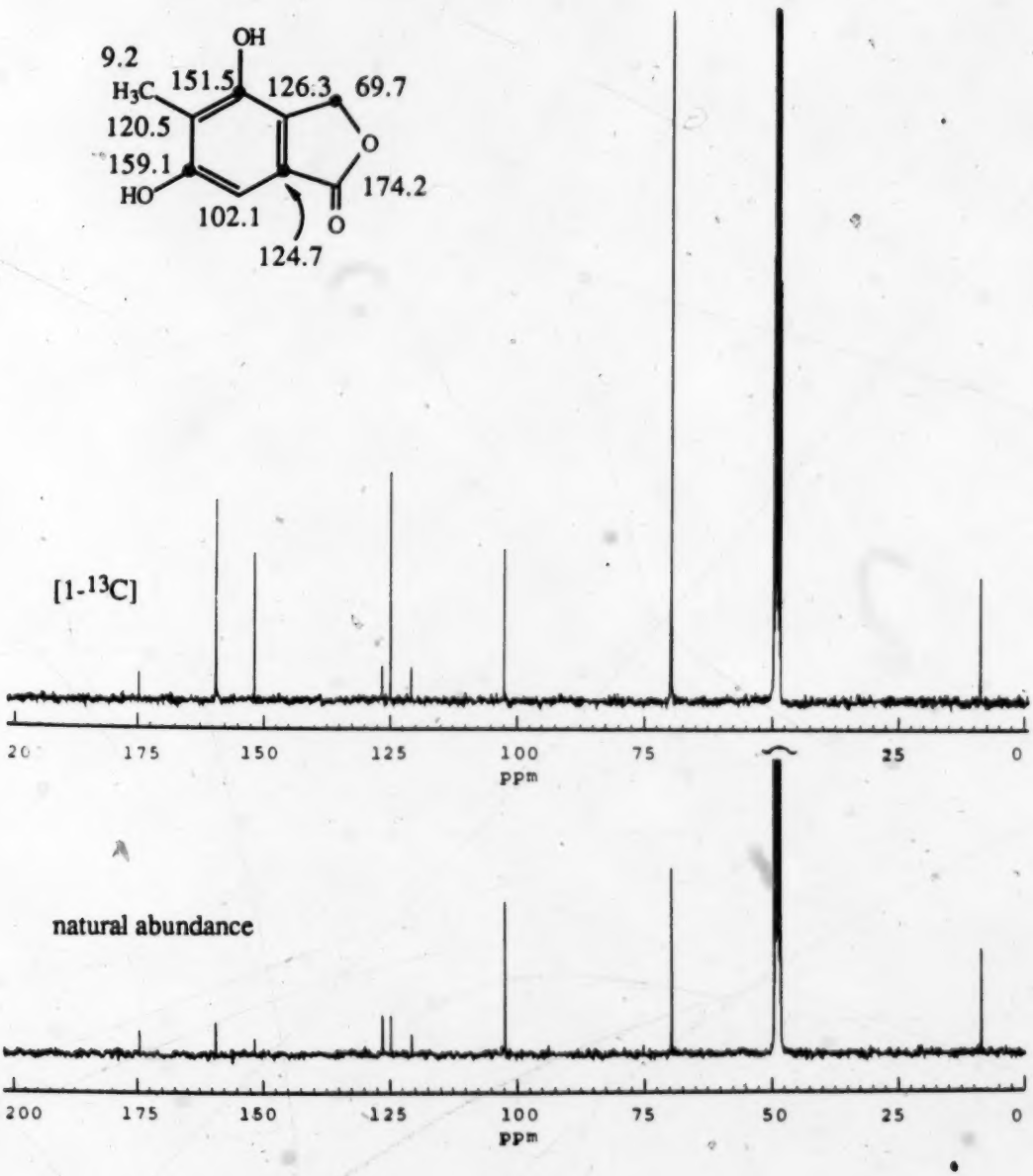

Figure 28. [1-^{13}C] $CH_3\overset{\bullet}{C}O_2Na$ labelling study of 4,6-dihydroxy-5-methylphthalide (**10**)

(broadband decoupled, methanol-d_4)

[1-^{13}C] labelled sodium acetate if this biosynthetic pathway is correct. The incorporation of labelled acetate into **10** is *ca.* 6%. In addition to the intense methylene signal, the carbonyl carbon at 174.2 ppm shows no enhancement in the labelled spectrum, thus confirming both its origin from C-2 of acetate as well as this unusual oxidation-reduction sequence along the pathway to 4,6-dihydroxy-5-methylphthalide (**10**).

Not only have metabolites constructed from the two phthalide backbones been isolated from nature but compounds having the two different backbones have been isolated from the same source. Nidulol (5-hydroxy-7-methoxy-6-methylphthalide), silvaticol (6-hydroxy-4-methoxy-5-methylphthalide), and O-methylsilvaticol (4,6-dimethoxy-5-methylphthalide) (Figure 26) are reported from *A. silvaticus*,[47] suggesting that some organisms have the capability to produce metabolites constructed from either phthalide backbone.

As discussed in the biosynthesis of 4,6-dihydroxy-5-methylphthalide (**10**), one of the possible intermediates along the pathway is 3,5-dihydroxy-4-methylphthal-aldehydic acid. This natural product may form by oxidation of the methyl group and reduction of the acid moiety of 3-methylorsellinic acid. [1-^{13}C] Labelled sodium acetate would be incorporated at four centers as shown in Scheme 26. The pathway from the acid to the proposed structure of metabolite **15** involves an oxidation of the methyl group, methylation of the acid to afford the ester, and a reduction of the hydroxyl bearing carbon, C-3. This reduction may occur before aromatization as this reaction would be chemically easier. The ^{13}C nmr assignments for metabolite **15** are shown in Table 25. The ^{13}C nmr spectrum of the labelled metabolite compared to that at natural abundance shows label has been incorporated at four carbons (Figure 29). These enhanced signals include the aldehyde carbon at 196.6 ppm, a downfield carbon at 166.3 ppm, a quaternary carbon at 136.8 ppm, and an aromatic methine at 103.9 ppm. The enrichment level is *ca.* 6%. The enriched carbons are consistent with those expected to be labelled if

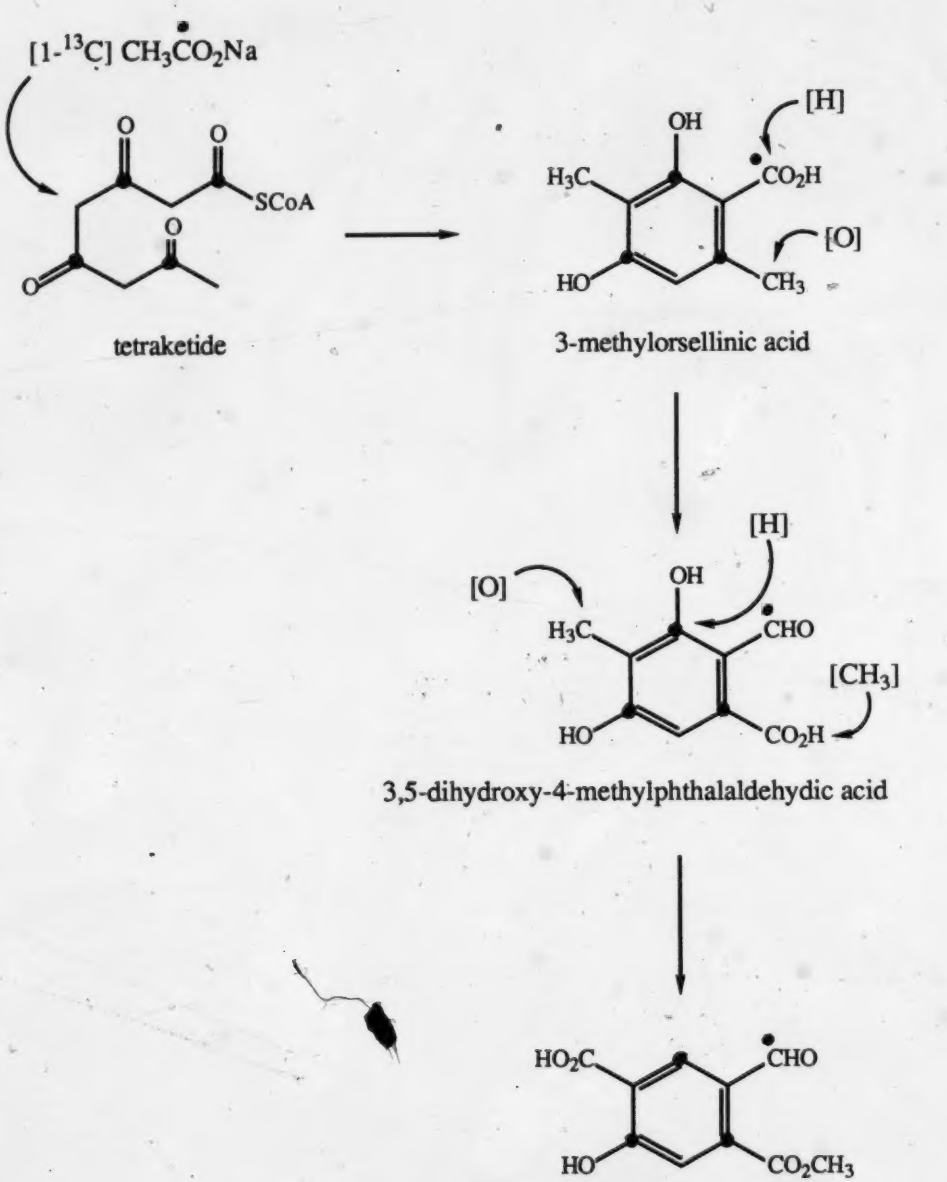

Scheme 26. Proposed biosynthetic pathway to metabolite **15**

Table 25. The ^{13}C nmr assignment of 4-carboxy-5-hydroxyphthalaldehydic acid methyl ester (**15**)

	δ_C (ppm, methanol-d_4)
C-1	136.8
C-2	114.6
C-3	103.9
C-4	122.7
C-5	166.3
C-6	102.4
$\underline{C}O_2CH_3$	160.1
$CO_2\underline{C}H_3$	56.4
$\underline{C}HO$	196.6
$\underline{C}O_2H$	169.4

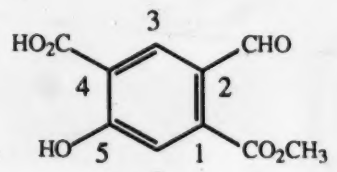

15

metabolite **15** arises from the precursor acid as illustrated in Scheme 26. The hydroxyl carbon has been assigned as the signal at 166.3 ppm on the basis of it being enriched. Its calculated shift is 162.5 ppm. As a result, the ester carbonyl, unlabelled and arising from C-2 of acetate, is assigned as 160.1 ppm. The C-3 methine carbon shows incorporation of [1-^{13}C] labelled acetate. It must arise from a carbon which, along the pathway, bore some type of oxygen functionality. This supports the proposal that there has been a reduction along the route. Although it is not possible to be completely confident of the structure and biosynthesis of metabolite **15**, it seems to be related to 3,5-dihydroxy-4-methylphthalaldehydic acid, a metabolite tied in to the biosynthesis of 4,6-dihydroxy-5-methylphthalide (**10**). It is interesting to note that the methyl ester of the acid, as well as metabolite **10**, are reported to promote the root growth of Chinese cabbage seedlings at

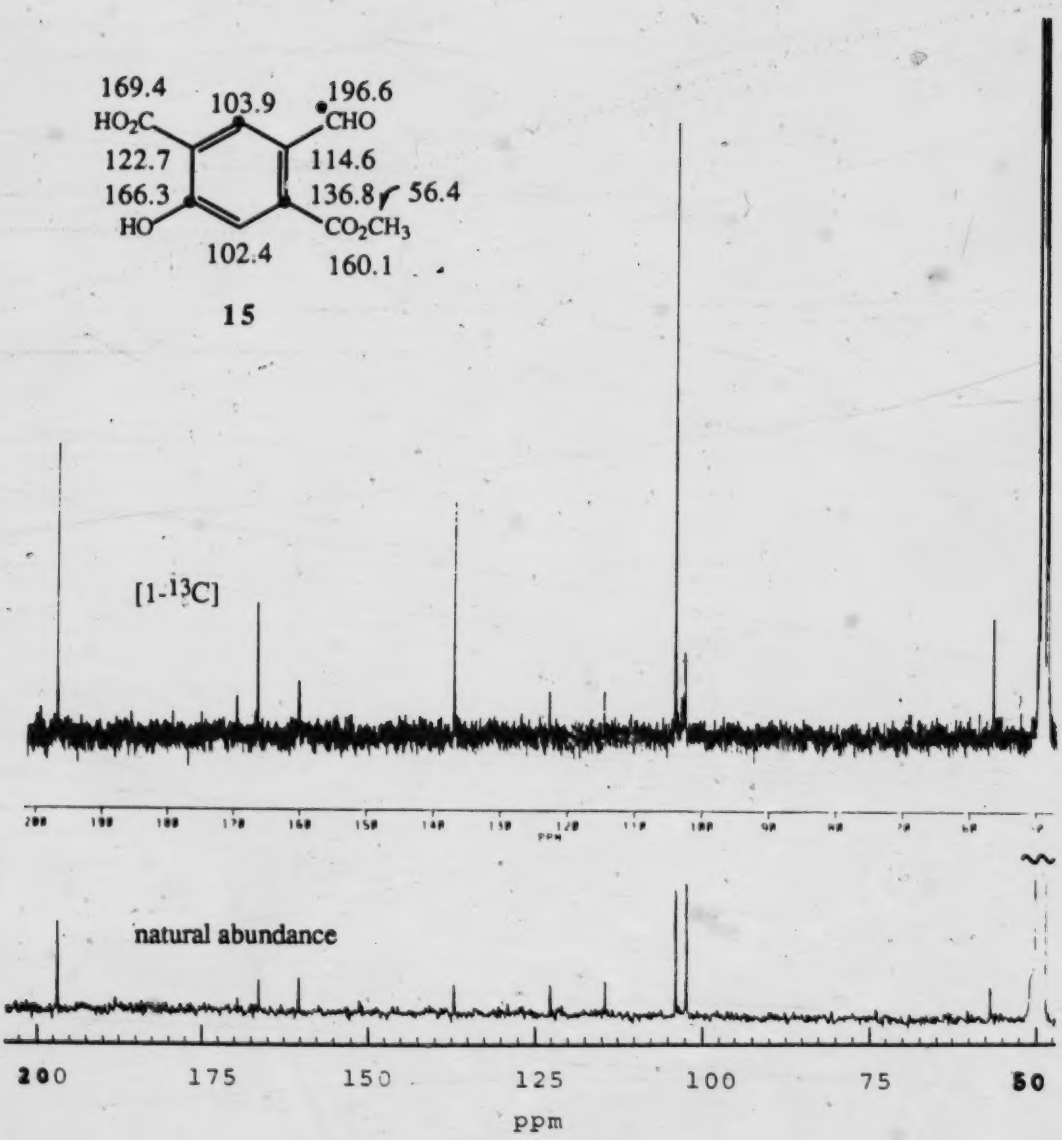

Figure 29. [1-^{13}C] $CH_3\overset{\bullet}{C}O_2Na$ labelling study of metabolite (**15**)

(broadband decoupled, methanol-d_4)

concentrations of 50 ppm; however, the acid itself shows no activity in this regard.[60]

The origin of the structurally and biosynthetically interesting spiro metabolite, talaroflavone (**23**), arises from a higher order polyketide, a heptaketide. As discussed in the first part of the thesis, talaroflavone (**23**) is thought to originate from the same heptaketide biphenyl derivative as that which gives rise to altenusin (**18**), dehydroaltenusin (**19**), and desmethyldehydroaltenusin (**21**). Feeding [1-^{13}C] labelled sodium acetate to *T. flavus* results in the incorporation of label at six carbon centers of **23**. Comparison of the intensity of the signals in the labelled spectrum with those at natural abundance (Figure 30) indicates that the six labelled carbons are the ones furthest downfield, at 202.0, 171.4, 170.2, 168.5, 159.9, and 150.8 ppm. The enrichment level is *ca.* 2.5%. The ^{13}C nmr assignment for talaroflavone (**23**) is shown in the figure. Although Table 26 indicates that some carbon assignments may be interchanged (C-1 (170.2) with C-5 (168.5) and C-2' (171.4)) and (C-4 (103.5) with C-6 (101.0)), this is of no consequence as the former three carbons are all labelled and the latter two carbons are not labelled. A biosynthetic pathway which accounts for the six most downfield carbons being labelled, as well as the bond joining the two unlabelled centers, C-3 and C-5', originating from the heptaketide biphenyl derivative seen before, is illustrated in Scheme 27. Oxidation of this biphenyl intermediate affords the dihydroarene oxide shown, whose intermediacy in the enzyme catalyzed hydroxylation of arenes is known.[111] Hydrolysis of the ketone, tautomerization of the enol, and oxidation of the benzylic alcohol provides the keto acid. Cyclization of an anion generated α- to the acid, followed by decarboxylation, provides the cyclopentadiene derivative. Lactonization and oxidation at the carbon α- to the ketone, probably *via* the enol, affords talaroflavone (**23**).

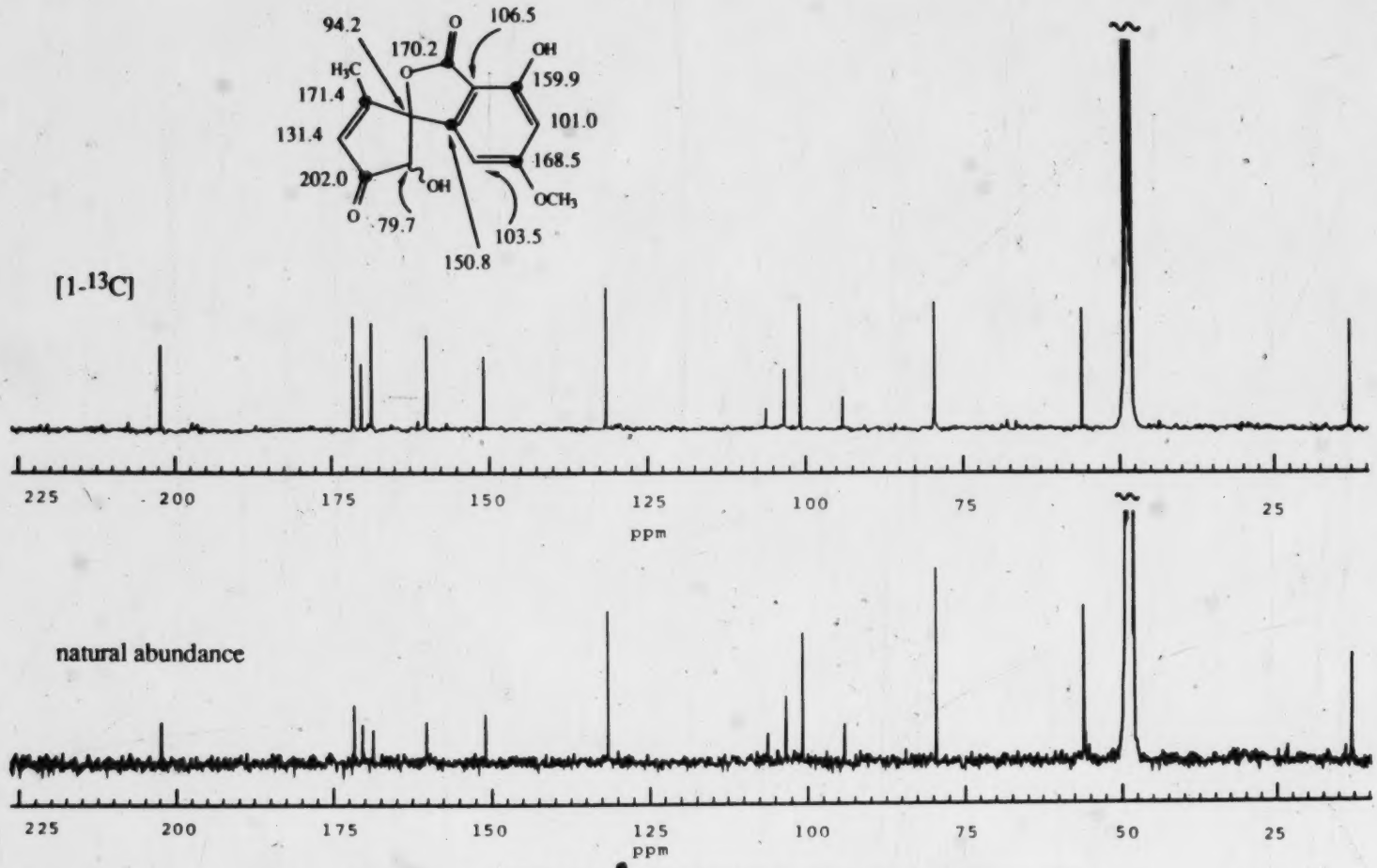

Figure 30. [1-^{13}C] $CH_3\overset{\bullet}{C}O_2Na$ labelling study of talaroflavone (**23**)

(broadband decoupled, methanol-d_4)

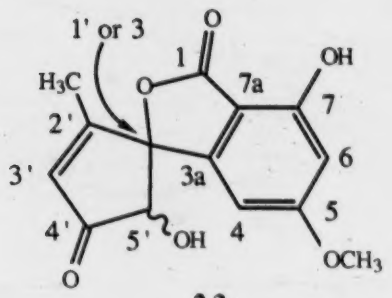

23

Table 26. ^{13}C nmr assignment of talaroflavone (23)

	chemical shift (ppm, multiplicity)
C-1	170.2[a] (s)
C-3 (C-1')	94.2 (s)
C-3a	150.8 (s)
C-4	103.5[b] (d)
C-5	168.5[a] (s)
C-6	101.0[b] (d)
C-7	159.9 (s)
C-7a	106.5 (s)
C-2'	171.4[a] (s)
C-3'	131.4 (d)
C-4'	202.0 (s)
C-5'	79.7 (d)
$\underline{C}H_3$	13.4 (q)
$O\underline{C}H_3$	56.5 (q)

a,b - assignments may be interchanged

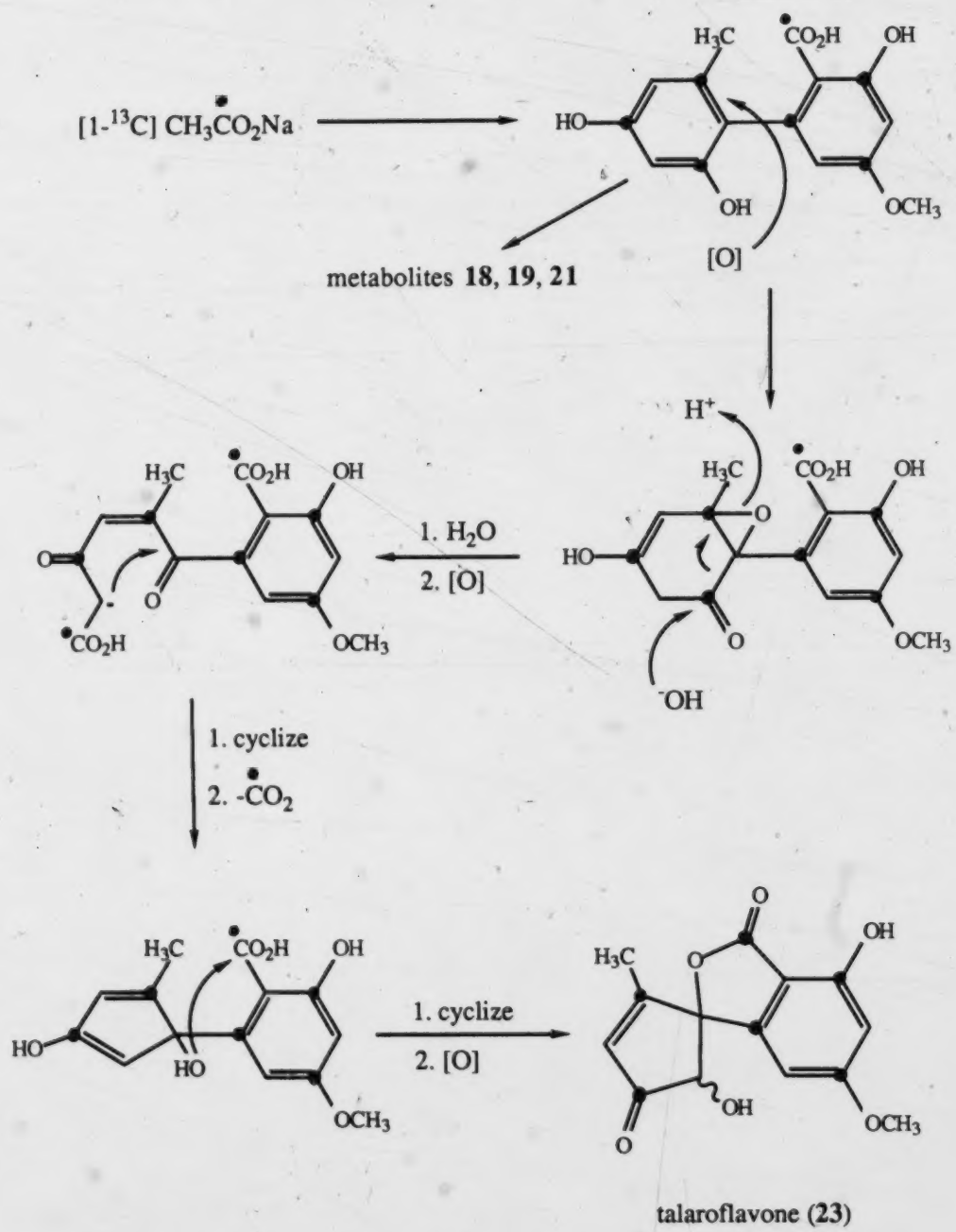

Scheme 27. Proposed biosynthetic pathway to talaroflavone (**23**)

VI. EXPERIMENTAL

Unless otherwise stated the following particulars apply. All solvents were distilled prior to use. Pyridine was distilled from CaH_2 and stored over KOH. Analytical thin layer chromatography (tlc) was carried out on aluminum sheets precoated (0.2 mm) with silica gel 60 F-254 (E. Merck, Darmstadt). Materials were detected by visualization under an ultraviolet (uv) lamp (254 or 350 nm), or by spraying with a solution of phosphomolybdic acid (5%) containing a trace of ceric sulfate in aqueous sulfuric acid (5%, v/v), or a solution of anisaldehyde (2%) in aqueous sulfuric acid (10%, v/v), followed by charring on a hot plate. Flash column chromatography[81] was performed with Merck Silica Gel 60 (40 - 63 μm). High resolution mass spectra (hrms) were recorded on an A.E.I. MS-50 mass spectrometer coupled to a Nova 4 computer. Chemical ionization mass spectra (cims) were recorded on an A.E.I. MS-12 mass spectrometer. Ammonia was used as the reagent gas. Data are reported as m/z (relative intensity). Unless diagnostically significant, peaks with intensities less than 10% of the base peak are omitted. Fourier transform infrared (ftir) spectra were recorded as CH_2Cl_2 or CH_3COCH_3 casts on a Nicolet 7199 FT interferometer. Ultraviolet (uv) spectra were obtained on a Hewlett Packard 8450A Diode Array spectrophotometer. ^1H nuclear magnetic resonance (^1H nmr) spectra were measured on a Bruker WH-400 or AM-400 spectrometer with an Aspect 2000 or 3000 computer system. Residual $C\underline{H}Cl_3$ in $CDCl_3$ or $C\underline{H}D_2OD$ in CD_3OD was employed as the internal standard (assigned as 7.26 and 3.30 ppm, respectively, downfield from tetramethylsilane (TMS)). Measurements are reported in ppm downfield from TMS (δ). ^{13}C nuclear magnetic resonance (^{13}C nmr) spectra were measured on a Bruker WH-400 or AM-400 spectrometer. $\underline{C}DCl_3$ was employed as the internal standard (assigned as 77.0 ppm, downfield from TMS (δ)). Gas chromatograms (gc) were obtained from a Hewlett Packard 5750 gas chromatograph

equipped with an OV-17 Chromosorb W/80-100 mesh column (6' x 3/16"). The injector and detector temperatures were 250°C and the column was heated to 150°C. Helium was used as the carrier gas. Gas chromatography-mass spectrometry (gc-ms) data were obtained from a Varian 1400 gas chromatogram linked with an A.E.I. MS-12 mass spectrometer. Detection was done by chemical ionization using ammonia as the carrier gas. The gas chromatogram was equipped with a 30m Supelco SPB 5 column. The column temperature was 50°C initially and then raised 10°C/min. to 250°C. Melting points were recorded on a Fisher-Johns or Leitz-Wetzlar melting point apparatus and are uncorrected.

Sephadex G-50 and LH-20 gels were obtained from Pharmacia Fine Chemicals, Uppsala, Sweden. Bio-Gel P-2 (100-200 mesh (wet), exclusion limit 1800 daltons) was obtained from Bio-Rad Laboratories, Richmond, California. Sep-Paks (C_{18} and amino) were obtained from Waters Associates, Milford, Massachusetts. Reverse phase thin layer chromatography (tlc) plates were obtained from Whatman Ltd. ($MKC_{18}F$ Reversed Phase TLC Plates, 200 μ thickness). C-18 reverse phase flash silica gel was obtained from Toronto Research Chemicals Inc., Downsview, Ontario. The cation exchange resin used was AGC-244 (Ionic Form H, Baker, strong acid, sulfonated polystyrene, 10% crosslinking, 30-80 mesh) and the anion exchange resin was Dowex-3 (weak base, primary and secondary amine, 20-50 mesh). Dialyses were performed with Spectrapor 6 dialysis tubing (MWCO 1,000, flat width 18 mm, diameter 11.5 mm). Sodium acetate [1-^{13}C] (91.8 atom % ^{13}C) was obtained from MSD Isotopes.

Growth of *Talaromyces flavus* and Isolation of the Aqueous Metabolites

Talaromyces flavus (ATCC 52201; UAMH 4890) was grown in liquid still

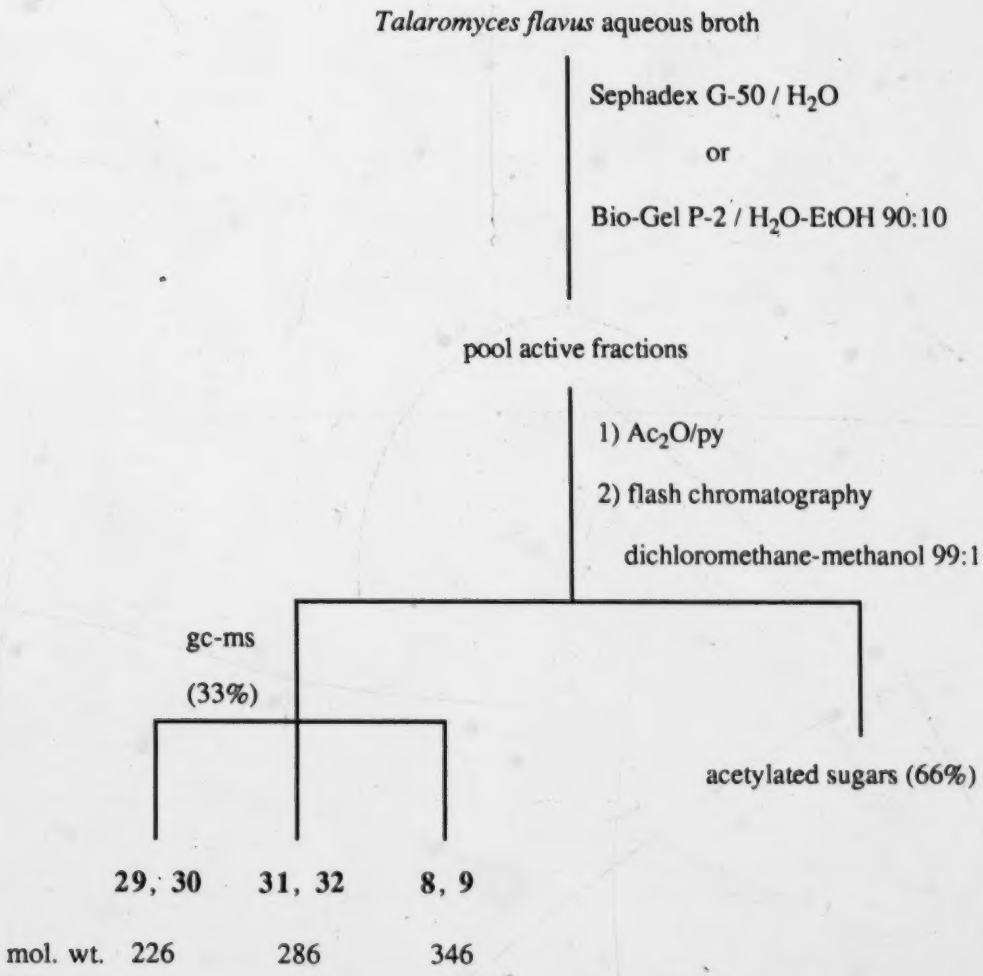

Scheme 28. Isolation of metabolites from *Talaromyces flavus* aqueous broth

culture in 10 L batches at room temperature as reported in the Experimental section of Part 1 of this series. After four weeks the mycelium was separated from the culture broth by filtration through cheesecloth. The broth was concentrated *in vacuo* to *ca.* one litre and continuously extracted with ethyl acetate for 48 hours. The fungal broth was concentrated to a syrup and passed over a column of Sephadex G-50, eluting with water, or a column of Bio-Gel P-2, eluting with water-95% ethanol (90:10). The active fractions were pooled and freeze-dried. The freeze-dried syrup was subjected to acetylation (acetic anhydride-pyridine) and then purified by flash chromatography, eluting with dichloromethane-methanol (99:1). A clear colorless oil (150 mg, 33%) appeared to be one spot by tlc; however, gc-ms analysis showed that there were three compounds present whose separation was possible with repeated chromatography (Scheme 28).

Hydroxymethylmaltol (**29**)

A portion of the active aqueous broth was freeze-dried and then allowed to stand with acetic anhydride (1.0 mL, 10.6 mmol) and pyridine (1.0 mL, 12.4 mmol) at room temperature for 24 hours. The reaction mixture was taken up in ethyl acetate (10.0 mL) and toluene (5.0 mL) and the solvents were removed under reduced pressure to afford a dark brown oil. This oil was purified by flash chromatography, eluting with dichloromethane-methanol (99:1). This procedure was repeated and afforded the diacetate of hydroxymethylmaltol (**29**) as a clear, colorless oil (**30**, 0.6 mg), tlc: R_f = 0.21 (dichloromethane-methanol 99:1); uv (methanol, 1.0 mg/100mL) λ_{max} nm (log ϵ): 292 (3.92); ir (CH_2Cl_2 cast) ν_{max} cm^{-1}: 1780 (m), 1741, 1656, 1585, 1370, 1222, 1195, 1175, 1101, 1065, 882, 759; ^1H nmr ($CDCl_3$, 400 MHz): δ 7.06 (1H, d, J=7.0 Hz, H-6), 6.24 (1H, d, J=7.0 Hz, H-5), 4.83 (2H, s, CH_2OCOCH_3), 2.30 (3H, s, C-3 $OCOCH_3$), 2.12 (3H, s, C-2 $OCOCH_3$); ^{13}C nmr ($CDCl_3$, 100 MHz): δ 170.0 (s,

$O\underline{C}OCH_3$), 167.9 (s, $O\underline{C}OCH_3$), 157.1 (s, C-4), 155.6 (s, C-2), 137.0 (s, C-3), 130.5 (d, C-6), 103.8 (d, C-5), 61.3 (t, $\underline{C}H_2$), 20.6 (q, $OCO\underline{C}H_3$), 20.4 (q, $OCO\underline{C}H_3$); hrms m/z (relative intensity %) calc. for $C_{10}H_{10}O_6$ (M^+): 226.0477; found: 226.0475 (14), 184 (66), 142 (100), 114 (4), 96 (26).

3-Deoxy-*threo*-1,5-lact-2-ene-1-one (**31**)

A portion of the active aqueous broth was freeze-dried and then allowed to stand with acetic anhydride (1.0 mL, 10.6 mmol) and pyridine (1.0 mL, 12.4 mmol) at room temperature for 24 hours. The reaction mixture was taken up in ethyl acetate (10.0 mL) and toluene (5.0 mL) and the solvents were removed under reduced pressure to afford a dark brown oil. This oil was purified by flash chromatography, eluting with dichloromethane-methanol (99:1). This procedure was repeated and afforded the triacetate of 3-deoxy-*threo*-1,5-lact-2-ene-1-one (**31**) as a clear, colorless oil (**32**, 0.6 mg), tlc: $R_f = 0.21$ (dichloromethane-methanol 99:1); ir (CH_2Cl_2 cast) ν_{max} cm^{-1}: 1778, 1750, 1665, 1655, 1580, 1425, 1372, 1227, 1198, 1136, 1047; ^1H nmr ($CDCl_3$, 400 MHz): δ 6.43 (1H, d, J=4.0 Hz, H-3), 5.61 (1H, dd, J=4.0, 5.5 Hz, H-4), 4.75 (1H, dt, J= 5.5, 4.5 Hz, H-5), 4.38 (1H, dd, J=4.5, 12.5 Hz, H-6), 4.29 (1H, dd, J=4.5, 12.5 Hz, H-6'), 2.25 (3H, s, $OCOC\underline{H}_3$), 2.11 (3H, s, $OCOC\underline{H}_3$), 2.08 (3H, s, $OCOC\underline{H}_3$); ^{13}C nmr ($CDCl_3$, 100 MHz): δ 170.3 (s, $O\underline{C}OCH_3$), 169.6 (s, $O\underline{C}OCH_3$), 168.0 (s, $O\underline{C}OCH_3$), 157.1 (s, C-1), 139.8 (s, C-2), 125.9 (d, C-3), 77.9 (d, C-5), 64.3 (d, C-4), 62.0 (t, C-6), 20.6 (q, $OCO\underline{C}H_3$), 20.5 (q, $OCO\underline{C}H_3$), 20.2 (q, $OCO\underline{C}H_3$); hrms m/z (relative intensity %) calc. for $C_{12}H_{14}O_8$ (M^+): 286.0688; found: 286.0694 (0.1), 244 (9), 226 (13), 202 (13), 184 (68), 156 (15), 142 (100); cims (NH_3): 304 ($M^+ + 18$, 100).

D-Glucono-1,4-lactone (**8**)

A portion of the active aqueous broth was freeze-dried and then allowed to stand with acetic anhydride (1.0 mL, 10.6 mmol) and pyridine (1.0 mL, 12.4 mmol) at room temperature for 24 hours. The reaction mixture was taken up in ethyl acetate (10.0 mL) and toluene (5.0 mL) and the solvents were removed under reduced pressure to afford a dark brown oil. This oil was purified by flash chromatography, eluting with dichloromethane-methanol (99:1). This procedure was repeated and afforded the tetraacetate of D-glucono-1,4-lactone (**8**) as a clear, colorless oil (**9**, 25.7 mg), tlc: R_f = 0.21 (dichloromethane-methanol 99:1); $[\alpha]_D$ +59° (c 1.0, acetone); (+60.3° (acetone), lit.[38]); ir (acetone cast) ν_{max} cm^{-1}: 1806, 1751, 1373, 1224, 1194, 1067, 1046; ^1H nmr ($CDCl_3$, 400 MHz): δ 5.62 (1H, dd, J=3.0, 5.5 Hz, H-3), 5.35 (1H, ddd, J=3.0, 5.0, 8.0 Hz, H-5), 5.23 (1H, d, J=3.0 Hz, H-2), 4.96 (1H, dd, J=5.5, 8.0 Hz, H-4), 4.58 (1H, dd, J=3.0, 12.0 Hz, H-6), 4.15 (1H, dd, J=5.0, 12.0 Hz, H-6'), 2.19 (3H, s, $OCOCH_3$), 2.12 (3H, s, $OCOCH_3$), 2.10 (3H, s, $OCOCH_3$), 2.05 (3H, s, $OCOCH_3$); ^{13}C nmr ($CDCl_3$, 100 MHz): δ 170.3 (s), 169.3 (s), 169.1 (s), 169.0 (s), 168.7 (s), 76.9 (d), 72.0 (d), 71.0 (d), 67.6 (d), 62.1 (t), 20.6 (2C, q), 20.4 (q), 20.2 (q); hrms m/z (relative intensity %) calc. for $C_{14}H_{18}O_{10}$ (M^+): 346.0899; found: M^+ not detected, 226 (15), 184 (100), 142 (90), 100 (76); cims (NH_3): 364 (M^+ + 18, 100).

Biosynthetic Studies of Metabolites Produced by *Talaromyces flavus*

Incorporation of [1-^{13}C] labelled acetate

Talaromyces flavus was grown in liquid still culture on sterile malt extract medium in ten 2 L Fernbach flasks (1 L of medium per flask) as described in the

Experimental section of Part 1 of this series. After nine days growth, a sterile solution of sodium [1-^{13}C] acetate (0.082 g, 1.0 mmol) in distilled water (5.0 mL) was injected into each flask. After a further 7 and then 14 days, an additional 1.0 mmol of labelled acetate was injected into each flask. After a total of four weeks growth, the mycelium was removed by filtration through cheesecloth, washed with methanol, and air dried. The fungal broth was concentrated *in vacuo* to *ca.* 1 L and subjected to continuous extraction with ethyl acetate for 48 hours. The crude extract was evaporated to dryness *in vacuo* and then dissolved in a water-methanol solution (85:15, 100 mL). This solution was extracted with n-hexane (3 x 100 mL) and then dichloromethane (3 x 100 mL). The organic extracts were dried over anhydrous sodium sulfate, filtered, and the solvents were removed under reduced pressure. The crude dichloromethane extract (*ca.* 1 g) was separated by flash chromatography over silica gel, eluting with dichloromethane-methanol (97:3). The fractions were further purified as indicated for the individual components, 4,6-dihydroxy-5-methylphthalide (**10**), 4-carboxy-5-hydroxyphthalaldehydic acid methyl ester (**15**), and talaroflavone (**23**).

[1-^{13}C] Acetate Labelled Metabolites

4,6-Dihydroxy-5-methylphthalide (**10**) (4,6-Dihydroxy-5-methyl-1-(3H)-isobenzofuranone)

4,6-Dihydroxy-5-methylphthalide (**10**, 4.2 mg, *ca.* 6% incorporation), ^{13}C nmr (methanol-d_4, 100 MHz) enriched signals: δ 159.1 (C-6), 151.5 (C-4), 124.7 (C-7a), 69.7 (C-3); natural abundance signals: δ 174.2 (C-1), 126.3 (C-3a), 120.5 (C-5), 102.1 (C-7), 9.2 (C-5 $\underline{C}H_3$).

4-Carboxy-5-hydroxyphthalaldehydic acid methyl ester (**15**)

4-Carboxy-5-hydroxyphthalaldehydic acid methyl ester (**15**, 4.0 mg, *ca.* 6% incorporation), ^{13}C nmr (methanol-d_4, 100 MHz) enriched signals: δ 196.6 (C-2 $\underline{C}HO$), 166.3 (C-5), 136.8 (C-1), 103.9 (C-3); natural abundance signals: δ 169.4 (C-4 $\underline{C}O_2H$, 160.1 (C-1 $\underline{C}O_2CH_3$), 122.7 (C-4), 114.6 (C-2), 102.4 (C-6), 56.4 (C-1 $CO_2\underline{C}H_3$).

Talaroflavone (**23**) (Spiro[5'-hydroxy-2'-methyl-cyclopent-2'-ene-4'-one-1',3-7-hydroxy-5-methoxy-1(3H)-isobenzofuranone])

Talaroflavone (**23**, 5.0 mg, *ca.* 2.5% incorporation), ^{13}C nmr (methanol-d_4, 100 MHz) enriched signals: δ 202.0 (C-4'), 171.4, 170.2, 168.5 (C-2', C-1, C-5), 159.9 (C-7), 150.8 (C-3a); natural abundance signals: δ 131.4 (C-3'), 106.5 (C-7a), 103.5, 101.0 (C-4, C-6), 94.2 (C-3), 79.7 (C-5'), 56.5 ($O\underline{C}H_3$), 13.4 (C-2' $\underline{C}H_3$).

Biological Studies of the Aqueous Broth, Organic Extracts, and Metabolites of *Talaromyces flavus*

Inhibition of *Verticillium dahliae* by *Talaromyces flavus*

The inhibition of growth of *Verticillium dahliae* by *Talaromyces flavus* was determined by agar diffusion using an aqueous test solution. Presterilized vessels (5/16" OD x 5/16" long cylinder cut from 304 stainless steel tubes) were placed onto Mueller Hinton agar plates which had been swabbed with *V. dahliae*. The *T. flavus* aqueous test solution (100 μL) was placed into the stainless steel vessel. The plates were incubated at 24°C. The solution diffused into the medium and after 10-14 days the growth of the microsclerotia of *V. dahliae* was noted.

The bioassay was carried out in the same manner as described above when testing hydrogen peroxide (Fisher, 30% by weight) and *tert*-butylhydroperoxide (Aldrich, 70% by weight). Test results were noted after 7-10 days.

Hydrogen peroxide detection

The catalase enzyme was obtained from bovine liver (Sigma, twice recrystallized) containing *ca.* 0.01 mg thymol/mL. The solution consists of 22 mg protein/mL (1,199,000 units/mL). The molecular weight of the enzyme is 250,000 g/mol so that the solution concentration is 88 μM. A 2 μM solution was utilized in which 2.0 μL (contains 50-55 units of enzyme) was added to the fungal broth (100 μL, *ca.* 0.3 μmol of H_2O_2). The bioassay was performed as described above.

In the ultraviolet study for the detection of peroxide, sodium iodide (0.75 g), citric acid (2.42 mL of a 0.5 M solution), and sodium hydroxide (1.0 mL of a 1.0 M solution) were combined to make up a 100 mL test solution of pH 3.8, in which the concentration of iodide ion is 0.05 M. To 10.0 mL of this solution was added 5.0 μL of horseradish peroxidase (*ca.* 1.0 μM). The absorbance of this solution at 353 nm was measured. The fungal broth (1.0 μL) was then added and the reaction was allowed to proceed for 20 minutes. The absorbance of the solution at 353 nm was measured once again and the change in absorbance was noted.

Antibacterial Studies

The biological activity of crude extracts of *T. flavus* (ethyl acetate and methanol mycelium extracts and ethyl acetate broth extract) was tested against several bacteria using the Kirby-Bauer agar diffusion assay. In this bioassay, filter paper discs soaked with the

crude extract solution (5.0 mg/mL in methanol) or the pure metabolites (2.0 mg/mL in methanol) were placed on the surface of an agar medium (Mueller-Hinton) containing a standardized suspension of bacteria. After 24 hours of incubation at 37°C the surface of the agar acquired a turbid appearance (a positive result was recorded when transparent haloes (inhibition zone) remained around the filter paper discs). A solvent blank and standard concentrations of an antibiotic (Penicillin G 10 units and Cephalothin 30 μg, Sensitivity Discs, Difco Laboratories) were used to compare the relative antibacterial activity of the crude extracts. The results are shown in Table 27. The inhibition zone diameters obtained with the crude extracts were somewhat smaller compared with those produced by Penicillin G (>22 mm) and Cephalothin (>18 mm). D-glucono-1,4-lactone (**8**) and 4,6-dihydroxy-5-methylphthalide (**10**) show inhibition zones half the size of those produced by the standard antibiotics.

Table 27. Bioactivity of crude extracts and metabolites **8** and **10** of *Talaromyces flavus*.

zone diameter (mm)

List of Cultures	broth extract	mycelium (EtOAc)	mycelium (CH_3OH)
Pseudomonas aeruginosa	16	-	-
Staphylococcus aureus	18	-	-
Streptococcus pyogenes	20	-	-

zone diameter (mm)

List of Cultures	D-glucono-1,4 lactone (**8**)	4,6-dihydroxy-5-methylphthalide (**10**)
Pseudomonas aeruginosa	12	-
Staphylococcus aureus	10	12
Streptococcus pyogenes	10	-

VII. BIBLIOGRAPHY

1. K.H. Domsch, W. Gams, and T.H. Anderson, Compendium of Soil Fungi. Volume 1. Academic Press, London, 1980, pp. 752-759.
2. A.C. Stolk and R.A. Samson, *Studies in Mycology*, **2**, 1 (1972).
3. M. Yamazaki and E. Okuyama, *Chem. Pharm. Bull.*, **28**, 3649 (1980).
4. S. Natori, F. Sato, and S. Udagawa, *Chem. Pharm. Bull.*, **13**, 385 (1965).
5. K. Mizuno, A. Yagi, M. Takada, K. Matsuura, K. Yamaguchi, and K. Asano, *J. Antibiot.*, **27**, 560 (1974).
6. G.W. van Eijk, *Experientia*, **29**, 522 (1973).
7. D.G. Lynn, N.J. Phillips, W.C. Hutton, J. Shabanowitz, D.I. Fennell, and R.J. Cole, *J. Am. Chem. Soc.*, **104**, 7319 (1982).
8. W.C. Hutton, N.J. Phillips, D.W. Graden, and D.G. Lynn, *J. Chem. Soc. Chem. Commun.*, 864 (1983).
9. N.J. Phillips, R.J. Cole, and D.G. Lynn, *Tetrahedron Lett.*, **28**, 1619 (1987).
10. J. Fuska, P. Nemec, and I. Kuhr, *J. Antibiot.*, **25**, 208 (1972).
11. R.K. Boeckman, Jr., J. Fayos, and J. Clardy, *J. Am. Chem. Soc.*, **96**, 5954 (1974).
12. J. Fuska, P. Nemec, and A. Fuskova, *J. Antibiot.*, **32**, 667 (1979).
13. J. Fuska, A. Fuskova, and P. Nemec, *Biologia*, **34**, 735 (1979).
14. J. Fuska, D. Uhrin, B. Proska, Z. Voticky, and J. Ruppeldt, *J. Antibiot.*, **39**, 1605 (1986).
15. J.J. Marois, S.A. Johnston, M.T. Dunn, and G.C. Papavizas, *Plant Dis.*, **66**, 1166 (1982).
16. D.L. McLaren, H.C. Huang, and S.R. Rimmer, *Can. J. Plant Pathol.*, **8**, 43 (1986).

17. M.G. Boosalis, *Phytopathology*, **46**, 473 (1956).

18. B.K. Dutta, *Plant and Soil*, **63**, 209 (1981).

19. J.P. Tewari, private communication.

20. J.J. Marois, D.R. Fravel, and G.C. Papavizas, *Soil Biol. Biochem.*, **16**, 387 (1984).

21. D.R. Fravel, J.J. Marois, M.T. Dunn, and G.C. Papavizas, *Soil Biol. Biochem.*, **17**, 163 (1985).

22. D.R. Fravel and J.J. Marois, *Phytopathology*, **76**, 643 (1986).

23. G.C. Papavizas, D.R. Fravel, and J.A. Lewis, *Phytopathology*, **77**, 131 (1987).

24. We thank Professor R.U. Lemieux for providing us with an authentic sample of D-mannitol.

25. Dictionary of Organic Compounds. Fifth Edition. Chapman and Hall, Toronto, 1982, p. 3629.

26. W.B. Turner and D.C. Aldridge, Fungal Metabolites II. Academic Press, London, 1983, p. 497.

27. C. Litchfield, Analysis of Triglycerides. Academic Press, New York, 1972, pp. 222-224.

28. L. Fieser and M. Fieser, Steroids. Reinhold Publishing Corporation, New York, 1959, p. 93.

29. K. Nakanishi and P.H. Solomon, Infrared Absorption Spectroscopy. Second Edition. Holden-Day Inc., Oakland, 1977, p. 41.

30. W.P. Aue, E. Bartholdi, and R.R. Ernst, *J. Chem. Phys.*, **64**, 2229 (1976).

31. K. Nagayama, A. Kumar, K. Wüthrich, and R.R. Ernst, *J. Magn. Res.*, **40**, 321 (1980).

32. Z. Walaszek and D. Horton, *Carbohydr. Res.*, **105**, 131 (1982).

33. K. Bock and C. Pedersen, *Adv. Carbohydr. Chem. Biochem.*, **41**, 27 (1983).

34. We thank Professor R.U. Lemieux for providing us with D-glucono-1,5-lactone.

35. H.S. Isbell and H.L. Frush, *U.S. Bur. Stand. J. Res.*, **11**, 649 (1933).

36. B. Capon, *Chem. Rev.*, **69**, 407 (1969).

37. R.M. Silverstein, G.C. Bassler, and T.C. Morrill, Spectrometric Identification of Organic Compounds. Fourth Edition. John Wiley and Sons, Inc., New York, 1981, p. 196.

38. Ref. 25, p. 2757.

39. A.I. Scott, Interpretation of the Ultraviolet Spectra of Natural Products. Pergamon Press, New York, 1964, pp. 91-96.

40. L.M. Jackman and S. Sternhell, Applications of NMR Spectroscopy in Organic Chemistry. Second Edition. Pergamon Press, New York, 1969, p. 31, p.314.

41. G.C. Levy, R.L. Lichter, and G.L. Nelson, Carbon-13 Nuclear Magnetic Resonance Spectroscopy. Second Edition. John Wiley and Sons, Inc., New York, 1980, pp. 102-135.

42. J.L. Marshall, Carbon-Carbon and Carbon-Proton NMR Couplings: Applications to Organic Stereochemistry and Conformational Analysis. Verlag Chemie International, Deerfield Beach, 1983, pp. 42-51.

43. H. Achenbach and A. Mühlenfeld, *Z. Naturforsch*, **40b**, 426 (1985).

44. Ref. 37, p. 22.

45. H. Achenbach, A. Mühlenfeld, and G.U. Brillinger, *Liebigs Ann. Chem.*, 1596 (1985).

46. We thank Professor H. Achenbach for providing us with the samples and spectra of 4,6-dihydroxy-5-methylphthalide and 4,6-dimethoxy-5-methylphthalide.

47. M. Fujita, M. Yamada, S. Nakajima, K. Kawai, and M. Nagai, *Chem. Pharm. Bull.*, **32**, 2622 (1984).

48. Ref. 39, pp. 135-136.

49. Ref. 37, p. 232.

50. M.T.W. Hearn, *Aust. J. Chem.*, **29**, 107 (1976).

51. J.C. Speck, Jr., *Advan. Carbohydr. Chem.*, **13**, 63 (1958).

52. Ref. 29, p. 47.

53. Y. Kimura, M. Kozawa, K. Baba, and K. Hata, *Planta Med.*, **48**, 164 (1983).

54. Y. Kashiwada, G. Nonaka, and I. Nishioka, *Chem. Pharm. Bull.*, **32**, 3493 (1984).

55. H. Budzikiewicz, C. Djerassi, and D.H. Williams, Structure Elucidation of Natural Products by Mass Spectrometry, Volume 2: Steroids, Terpenoids, Sugars, and Miscellaneous Classes. Holden-Day, Inc., San Francisco, 1964, pp. 261-266.

56. T. Suga and T. Hirata, *Bull. Chem. Soc. Jpn.*, **51**, 872 (1978).

57. P. Gramatica, M.P. Gianotti, G. Speranza, and P. Manitto, *Heterocycles*, **24**, 743 (1986).

58. K. Makino, A. Yagi, and I. Nishioka, *Chem. Pharm. Bull.*, **21**, 149 (1973).

59. H.O. House, Modern Synthetic Reactions. Second Edition. Benjamin/Cummings Publishing Co., Menlo Park, 1972, p. 71.

60. T. Sassa, M. Ikeda, and Y. Miura, *Agr. Biol. Chem.*, **37**, 2937 (1973).

61. F.H. Wehrli and T. Wirthlin, Interpretation of Carbon-13 NMR Spectra. Heyden and Son Ltd., London, 1976, p. 47.

62. Ref. 37, p. 230.

63. Ref. 55, pp. 254-260.

64. R.G. Coombe, J.J. Jacobs, and T.R. Watson, *Aust. J. Chem.*, **23**, 2343 (1970).

65. T. Rosett, R.H. Sankhala, C.E. Stickings, M.E.U. Taylor, and R. Thomas, *Biochem. J.*, **67**, 390 (1957).

66. K. Kameda and M. Namiki, *Chem. Lett.*, 265 (1974).

67. D.L. Pavia, G.M. Lampman, and G.S. Kriz, Jr., Introduction to Spectroscopy: A Guide for Students of Organic Chemistry. Saunders College Publishing, Philadelphia, 1979, pp. 97-98.

68. D. Rogers, D.J. Williams, and R. Thomas, *Chem. Commun.*, 393 (1971).

69. Ref. 29, pp. 38-39.

70. Ref. 39, p.119.

71. Ref. 39, p. 58.

72. J.B. Stothers, Carbon-13 NMR Spectroscopy. Academic Press, New York, 1972, p. 193, p. 290.

73. Ref. 29, p. 38.

74. J. Massicot, J.-P. Marthe, and S. Heitz, *Bull. Soc. Chim. Fr.*, 2712 (1963).

75. Ref. 37, p. 220.

76. A. Pelter, R.S. Ward, and T.I. Gray, *J. Chem. Soc. Perkin I*, 2475 (1976).

77. M.P. Lane, T.T. Nakashima, and J.C. Vederas, *J. Am. Chem. Soc.*, **104**, 913 (1982).

78. J.F. Grove, *Progress in the Chemistry of Organic Natural Products*, **22**, 203-264 (1964).

79. Ref. 29, p. 38, p. 47.

80. Ref. 37, p. 23.

81. W. C. Still, M. Kahn, and A. Mitra, *J. Org. Chem.*, **43**, 2923 (1978).

82. Ref. 25, p. 2469.

83. J.C. Walker, Diseases of Vegetable Crops. McGraw-Hill Book Co., Inc., New York, 1952, pp. 301-302, pp. 360-368, pp. 464-466.

84. G.R. Dixon, Vegetable Crop Diseases. Macmillan Publishers Ltd., Hong Kong, 1981, pp. 1-44.

85. J.E. Puhalla, *Phytopathology*, **69**, 1186 (1979).

86. J.E. Puhalla and M. Hummel, *Phytopathology*, **73**, 1305 (1983).

87. C.G. Bender and P.B. Shoemaker, *Plant Dis.*, **68**, 305 (1984).

88. Ref. 26, pp. 100-103.

89. A. Stoessl, in Toxins in Plant Disease. R.B. Durbin, Ed., Academic Press, New York, 1981, pp.140-141.

90. Ref. 39, p. 140, pp. 143-144.

91. T. Teitei, *Aust. J. Chem.*, **36**, 2307 (1983).

92. C.A. Kingsbury, M. Cliffton, and J.H. Looker, *J. Org. Chem.*, **41**, 2777 (1976).

93. J.A.J.M. Vekemans, R.G.M. de Bruyn, R.C.H.M. Caris, A.J.P.M. Kokx, J.J.H.G. Konings, E.F. Godefroi, and G.J.F. Chittenden, *J. Org. Chem.*, **52**, 1093 (1987).

94. K.K. Kim, D.R. Fravel, and G.C. Papavizas, *Phytopathology*, **77**, 616, 1720 (1987), and *Phytopathology*, **78**, 488 (1988).

95. G. Richter, in Industrial Enzymology. T. Godfrey and J. Reichelt, Eds., Nature Press, New York, 1983, pp. 428-436, pp. 491-492.

96. M. Dixon and E.C. Webb, Enzymes. Third Edition. Longman Group Ltd., London, 1979, pp. 243-244.

97. Q.H. Gibson, B.E.P. Swoboda, and V. Massey, *J. Biol. Chem.*, **239**, 3927 (1964).

98. H.C. Brown, J.H. Brewster, and H. Schechter, *J. Am. Chem. Soc.*, **76**, 467 (1954).

99. R.U. Lemieux, in Molecular Rearrangements. Part 2. P. de Mayo, Ed., Interscience Division of John Wiley and Sons, Inc., New York, 1964, p. 719.

100. We thank Professor H.B. Dunford for supplying us with the catalase enzyme (from bovine liver (Sigma)) as well as the horseradish peroxidase.

101. M.H. Abraham, A.G. Davies, D.R. Llewellyn, and E.M. Thain, *Anal. Chim.*

Acta, **17**, 499 (1957).

102. A. Zaffaroni, R.B. Burton, and E.H. Keutmann, *Science*, **111**, 6 (1950).

103. M.L. Cotton and H.B. Dunford, *Can. J. Chem.*, **51**, 582 (1973).

104. I.D. MacDonald, private communication.

105. A.G. McInnes, J.A. Walter, J.L.C. Wright, and L.C. Vining, in Topics in C-13 NMR Spectroscopy. Volume 2. G.C. Levy, Ed., John Wiley and Sons, New York, 1976, pp. 123-178.

106. S. Takenaka, N. Ojima, and S. Seto, *J. Chem. Soc. Chem. Commun.*, 391 (1972).

107. H. Verachtert and L. Hanssens, *Ann. Microbiol. (Paris)*, **126A**, 143 (1975).

108. Y. Solberg, *Acta Chem. Scand.*, **B29**, 145 (1975).

109. J.F. Grove, *J. Chem. Soc. Perkin I*, 2406 (1972).

110. J.H. Birkinshaw, P. Chaplen, and R. Lahoz-Oliver, *Biochem. J.*, **67**, 155 (1957).

111. B.J. Auret, S.K. Balani, D.R. Boyd, R.M.E. Greene, and G.A. Berchtold, *J. Chem. Soc. Perkin I*, 2659 (1984).

VIII. APPENDIX

Results of the ultraviolet study for the detection of a peroxide in the fungal broth of *Talaromyces flavus* - initial absorbance at t = 0 minutes

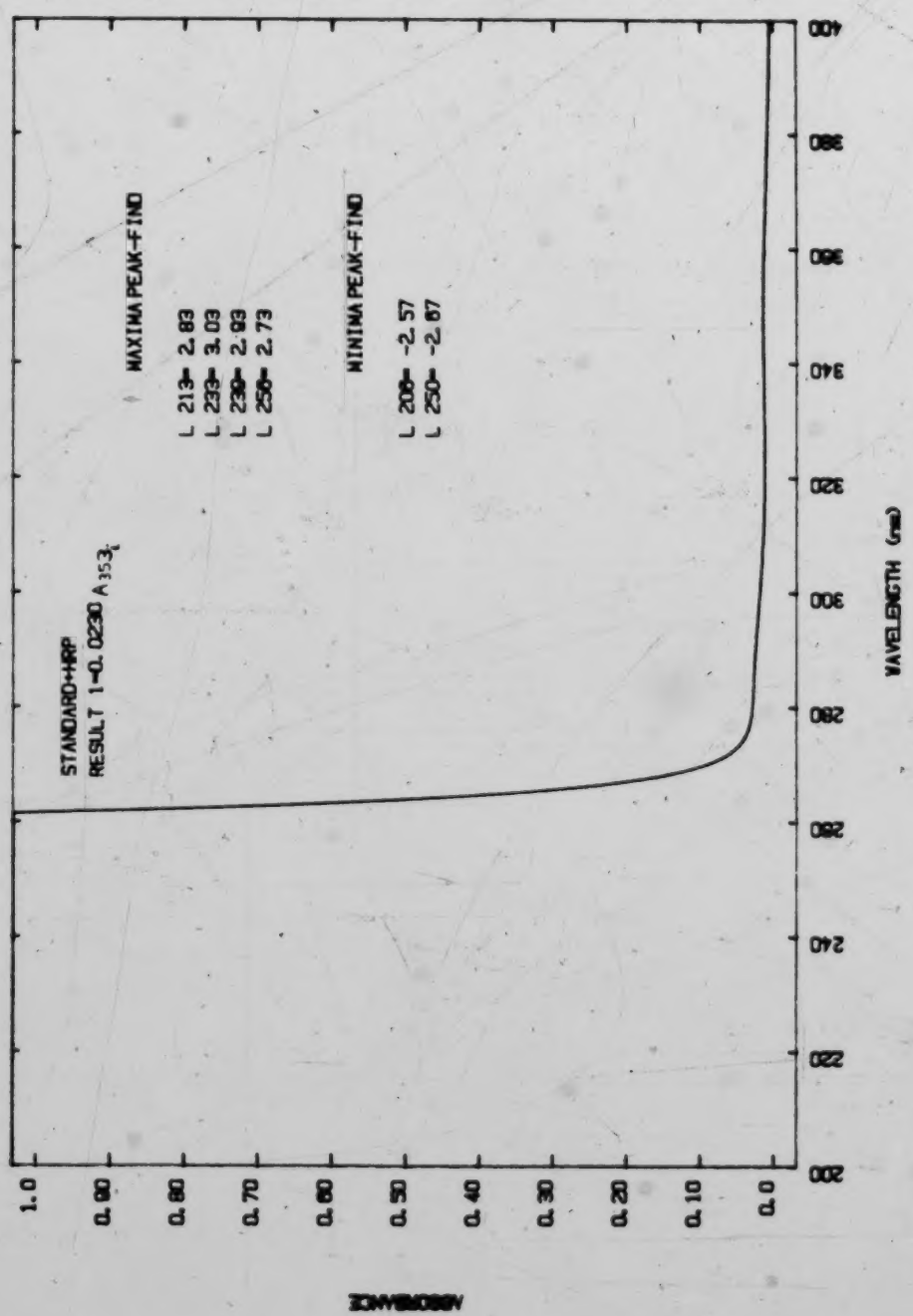
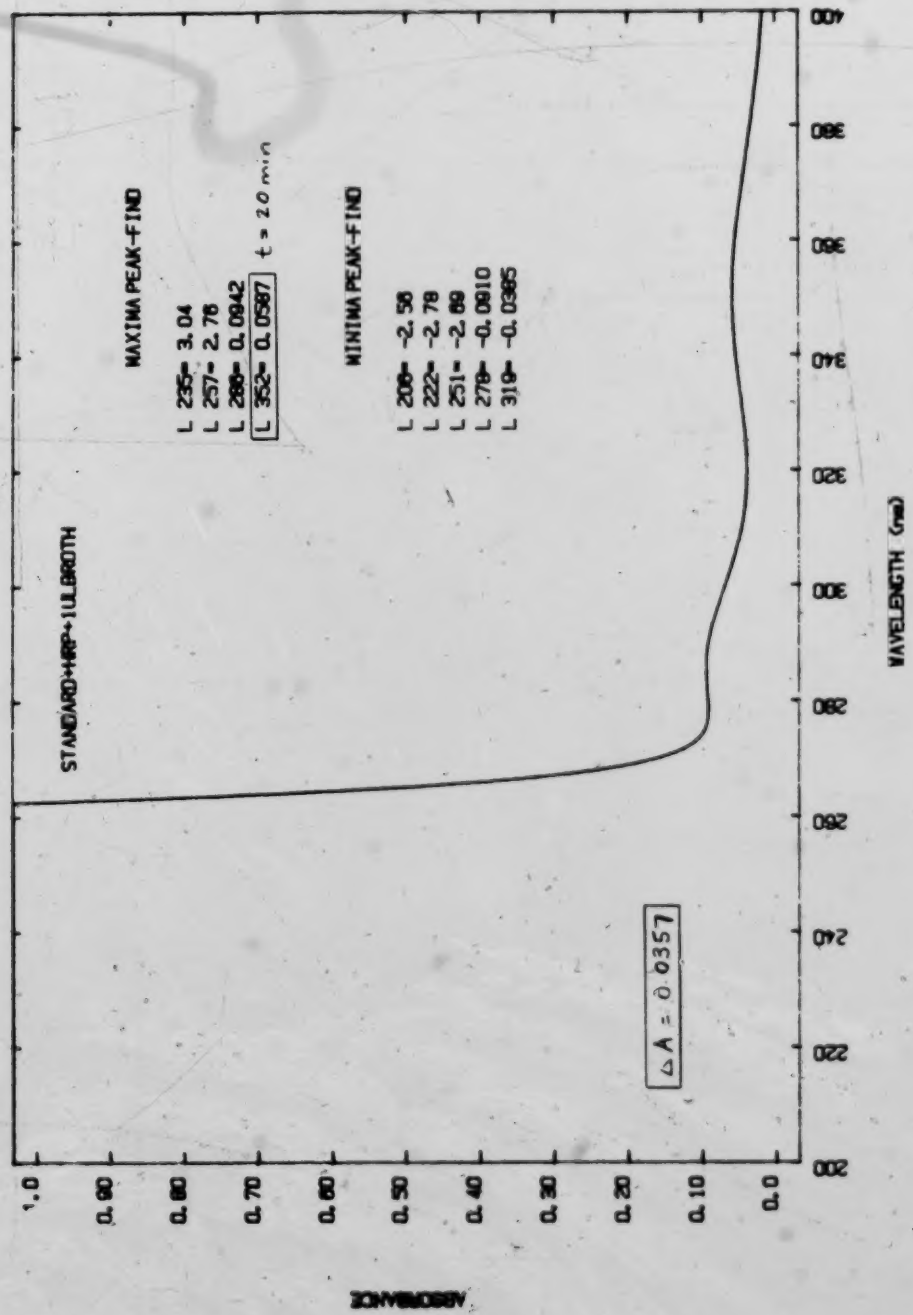
Results of the ultraviolet study for the detection of a peroxide in the fungal broth of *Talaromyces flavus* - final absorbance at t = 20 minutes